PULSE COMPRESSION using FREQUENCY or PHASE CODING

Frequency coding:

- Costas

Phase coding:

- Barker
- Frank
- P3 and P4
- P(n,k)
- Generalized Barker
- MPSL

Costas frequency coding

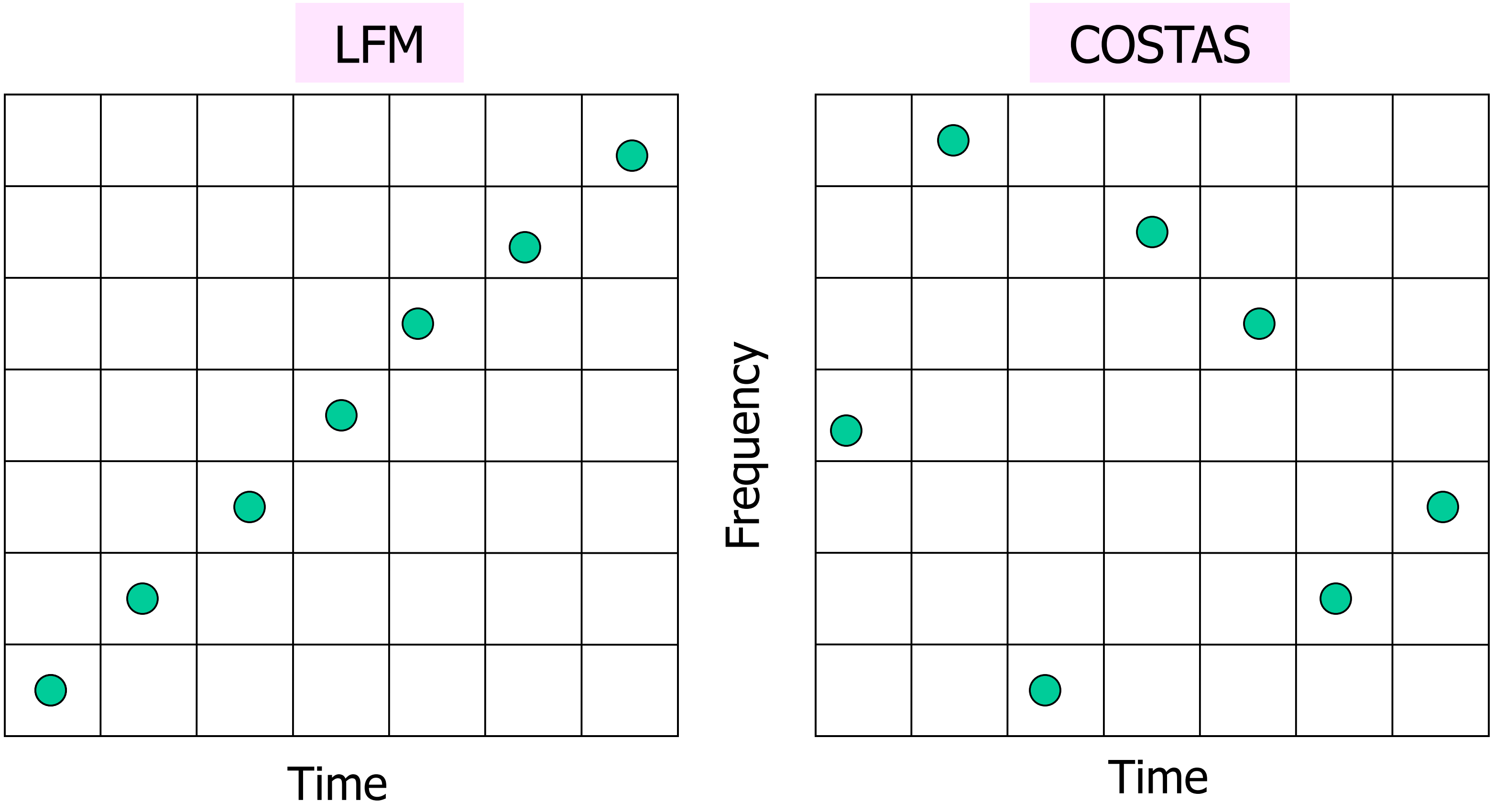

Ridge type of ambiguity function

Thumbtack ambiguity function

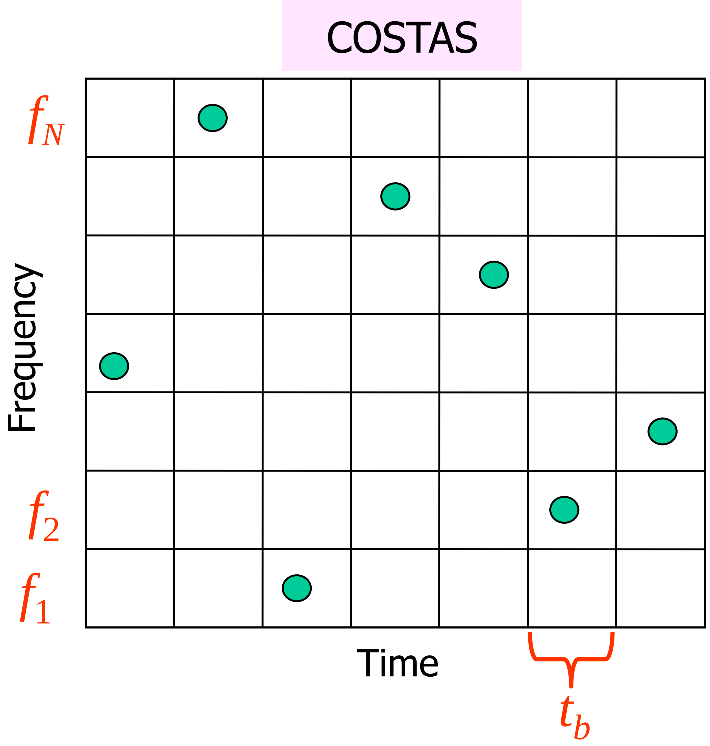

John P. Costas

“The world’s ugliest music” by Scott Rickards

https://youtu.be/RENk9PK06AQ

$$f_n - f_{n-1} = \frac{1}{t_b}$$

$\Rightarrow$ Orthogonality

A Costas signal can be described by an $N \times N$ binary matrix, with a single “1” (dot) at each raw and at each column, and a distinct vector differences between all pairs of dots. (Costas array)

The single dot at each raw and at each column implies a frequency hoping signal with:

- Only one carrier used at each time slot (bit).
- Each carrier is used only once.

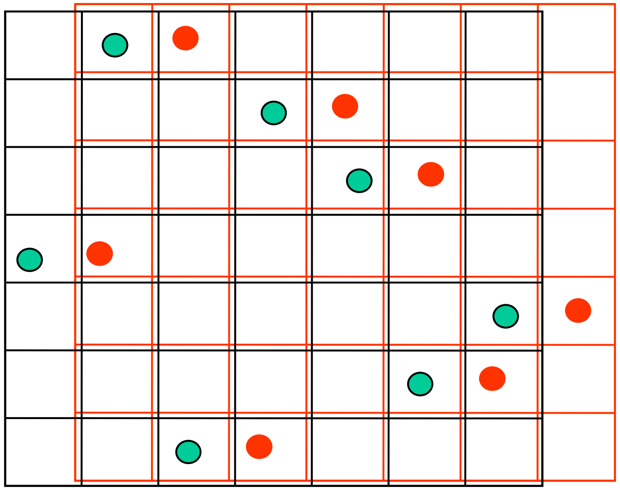

$\tau = 1, \quad \nu = 0 \quad \Rightarrow 0$ coincidence

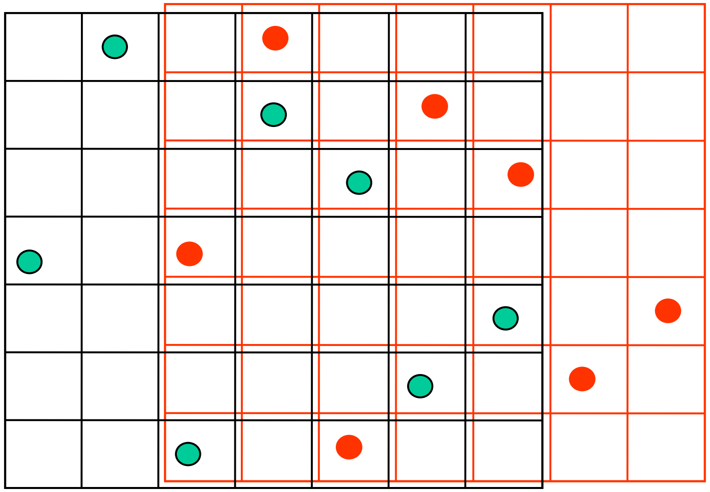

$\tau = 2, \quad \nu = 0 \quad \Rightarrow 0$ coincidence

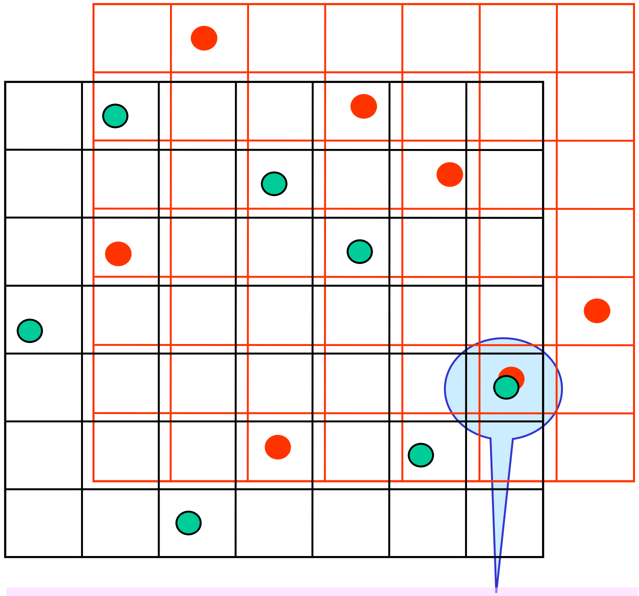

$\tau = 1, \quad \nu = 1 \quad \Rightarrow 1$ coincidence

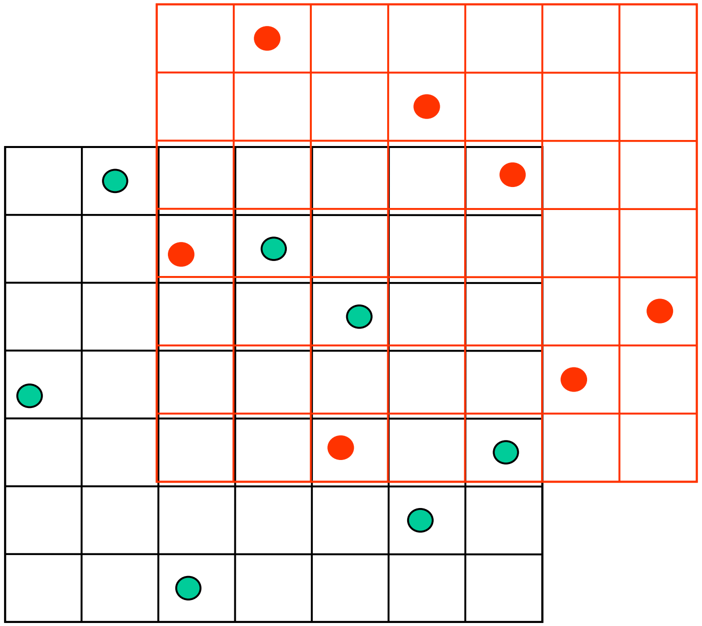

$\tau = 2, \quad \nu = 2 \quad \Rightarrow 0$ coincidence

A binary $N \times N$ array is "Costas" if the number of coincidences between dots in the array and in a shifted copy of it, is never larger than one, for any combination of horizontal (delay) and vertical (Doppler) integer shifts.

At $\tau = 0$ and $\nu = 0$ shifts, there are N coincidences

This are the reasons for the thumbtack shape

At all $\tau = 0$ xor $\nu = 0$ shifts, there are **0** coincidences

Costas J., "A study of a class of detection waveforms having nearly ideal range-doppler ambiguity properties", Proc. IEEE, vol. 72, Aug. 1984, pp. 996-1009.

Golomb, S.W. and Taylor, H., "Constructions and properties of Costas arrays", Proc. IEEE, vol. 72, Sept. 1984, pp. 1143-1163.

Beard, J. K., Russo, J. C., Erickson, K., Monteleone, M., and Wright, M., "Costas array generation and search methodology", IEEE Transactions on Aerospace and Electronic Systems, vol. 43, 2, April 2007, pp. 522-538.

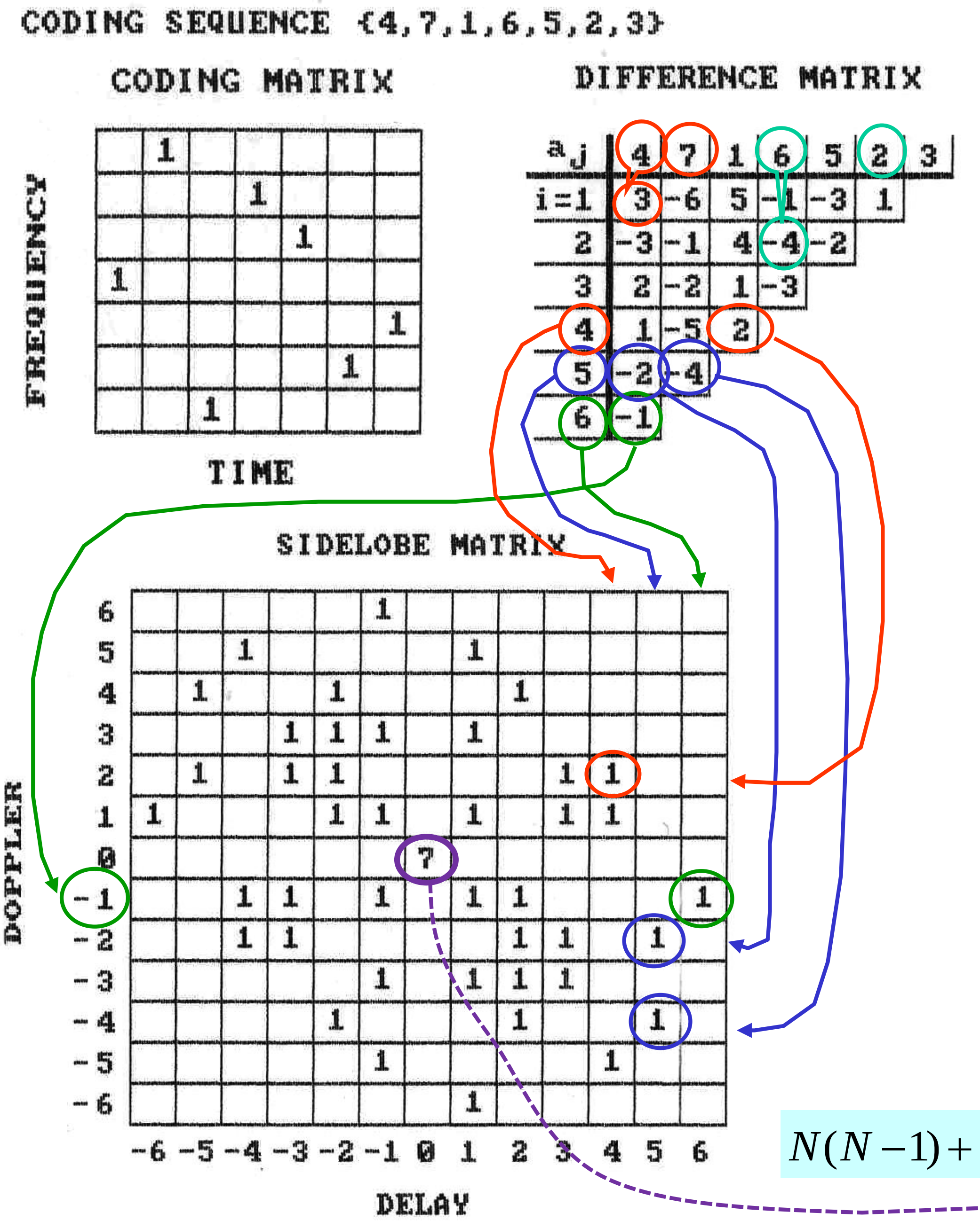

CODING SEQUENCE {4,7,1,6,5,2,3}

CODING MATRIX

	1					
			1			
				1		
1						
						1
					1	
		1				

DIFFERENCE MATRIX

a_j	4	7	1	6	5	2	3
i=1	3	-6	5	-1	-3	1	
2	-3	-1	4	-4	-2		
3	2	-2	1	-3			
4	1	-5	2				
5	-2	-4					
6	-1						

SIDELOBE MATRIX

	-6	-5	-4	-3	-2	-1	0	1	2	3	4	5	6
6						1							
5			1					1					
4		1			1				1				
3				1	1	1		1					
2		1		1	1					1	1		
1	1				1	1		1		1	1		
0							7						
-1			1	1		1		1	1				1
-2			1	1					1	1		1	
-3						1		1	1	1			
-4					1				1			1	
-5						1					1		
-6								1					

A sequence is a difference set if there are no repeats in any row of the difference matrix

The number of “1” in the sidelobe matrix = $N(N\text{-}1)$.

$$N = 7 \;\Rightarrow\; 7\cdot 6 = 42$$

The number of “0” in the sidelobe matrix = $3N(N\text{-}1)$.

$$N(N-1)+3N(N-1)+1=4N(N-1)+1=(2N-1)^2$$

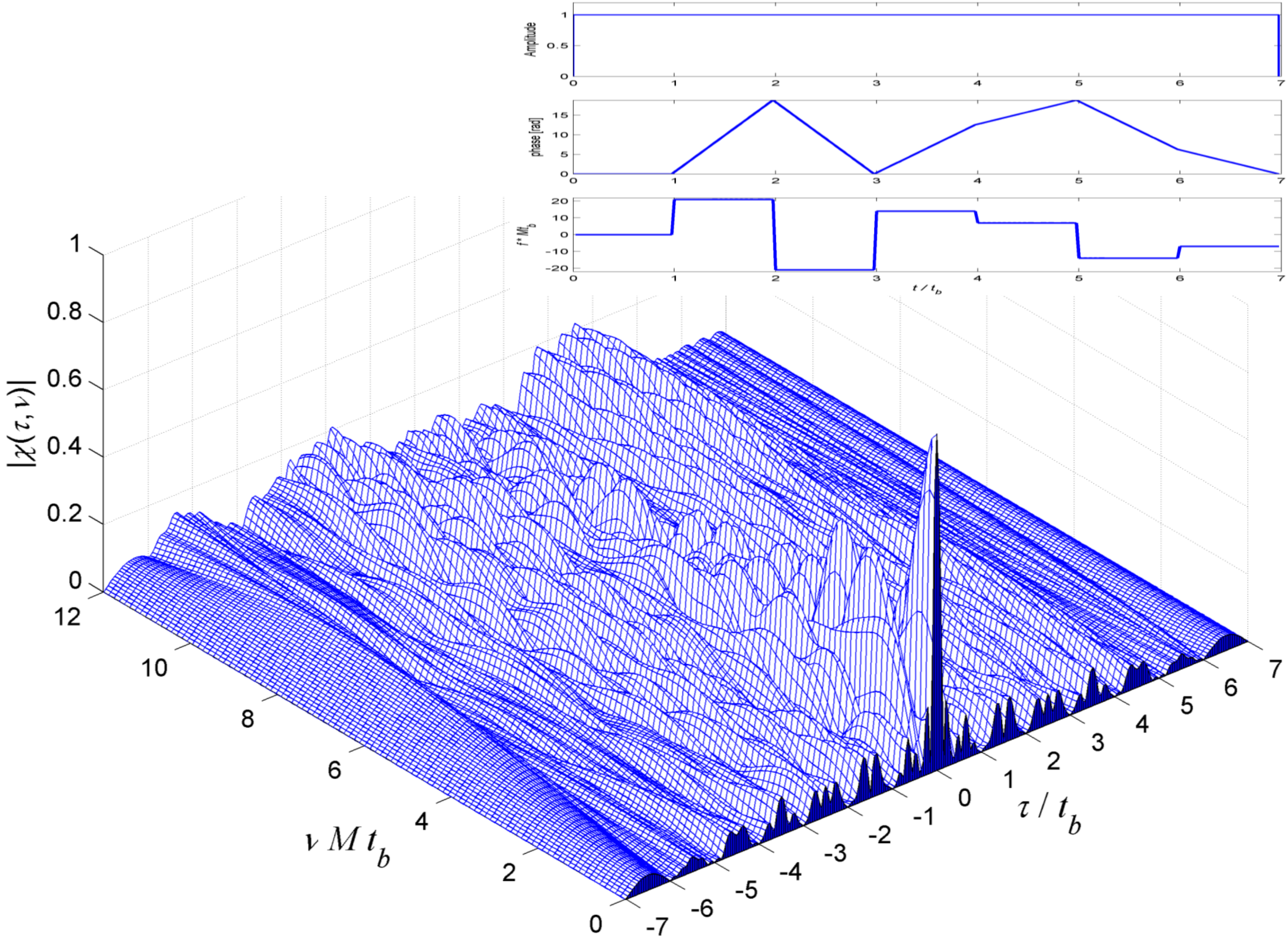
Amplitude
1
0.5
0
0 1 2 3 4 5 6 7
phase [rad]
15
10
5
0
f * Mt_b
20
10
0
-10
-20
t / t_b
|χ(τ,ν)|
1
0.8
0.6
0.4
0.2
0
12
10
8
6
4
2
0
ν M t_b
-7 -6 -5 -4 -3 -2 -1 0 1 2 3 4 5 6 7
τ / t_b

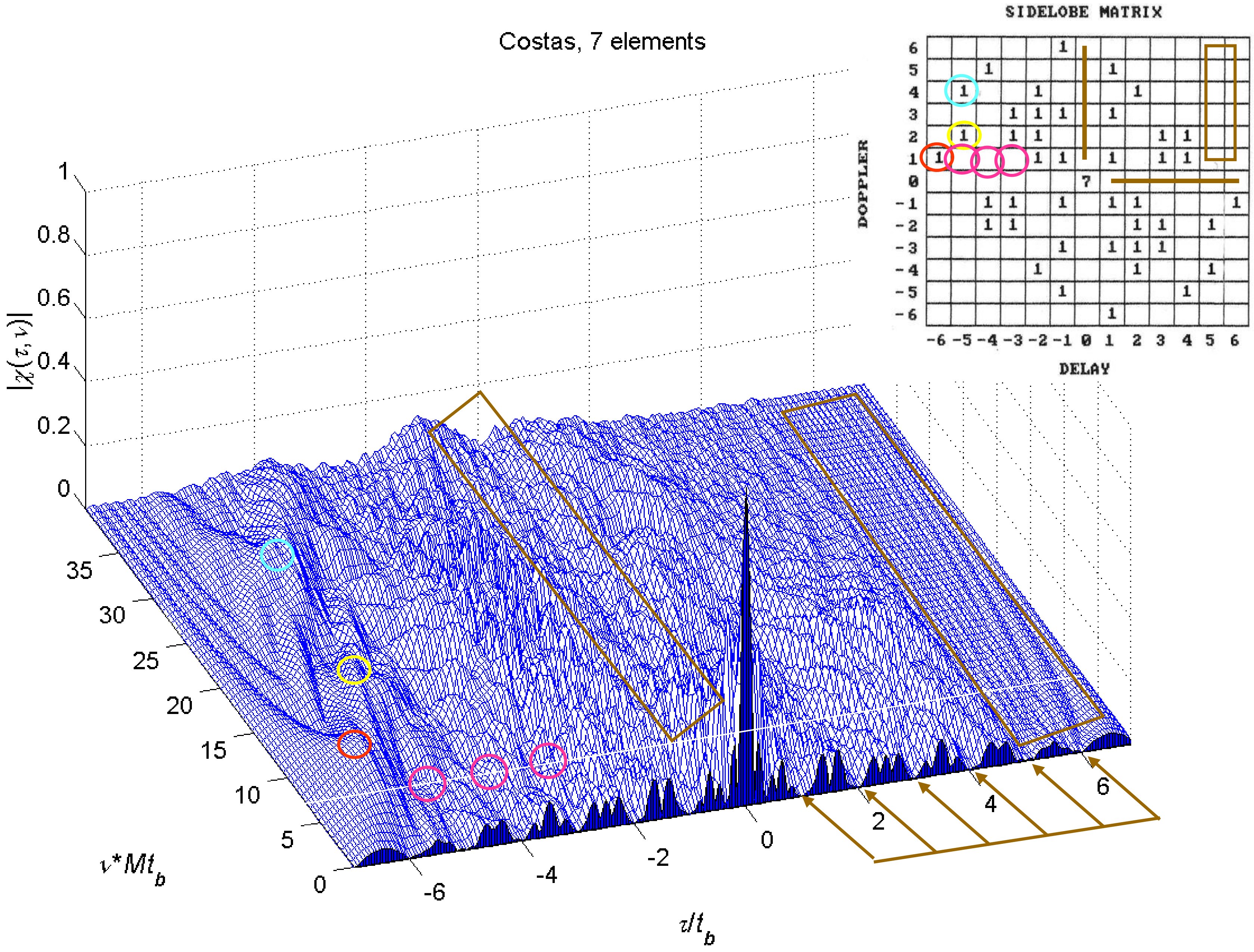

SIDELOBE MATRIX

DOPPLER

6						1							
5			1					1					
4		1			1				1				
3				1	1	1		1					
2		1		1	1					1	1		
1	1				1	1		1		1	1		
0							7						
-1			1	1		1		1	1				1
-2			1	1					1	1		1	
-3						1		1	1	1			
-4					1				1			1	
-5						1					1		
-6								1					
	-6	-5	-4	-3	-2	-1	0	1	2	3	4	5	6

DELAY

$$f_n - f_{n-1} = \frac{1}{t_b}$$

$\Rightarrow$ Orthogonality

Because of the orthogonality, the ambiguity function at the gird points

$$\left|\chi\left(mt_b, \frac{n}{t_b}\right)\right|$$

must agree with the values {0, 1 or N} of the sidelobe matrix

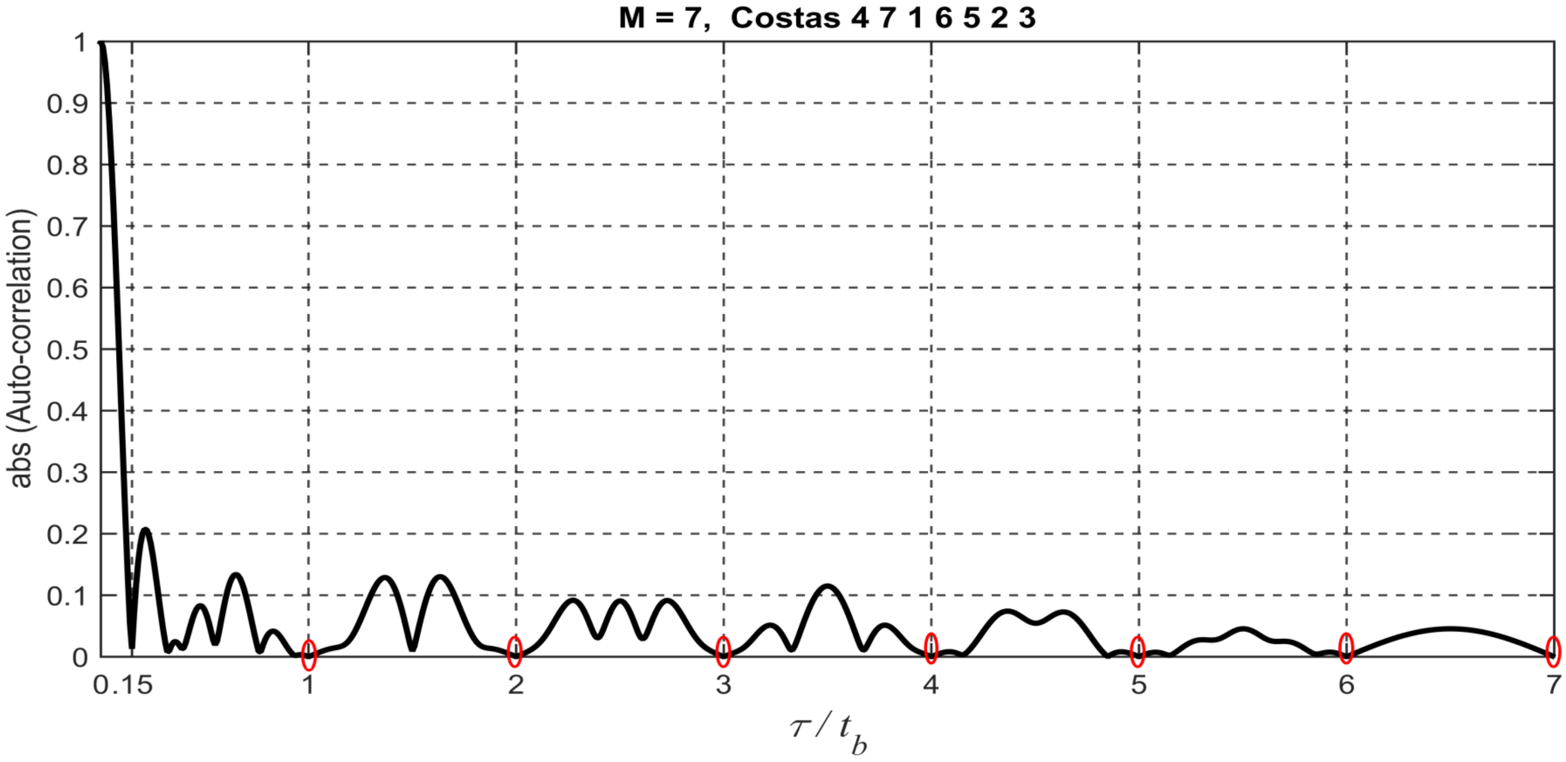

Because the signal spends equal time (t_b) at each carrier, the frequency spectrum of the envelope should be relatively flat over the frequency span:

$$-\frac{1}{2}\frac{M}{t_b} < f < \frac{1}{2}\frac{M}{t_b} \qquad \text{or} \qquad -\frac{M}{2} < f\, t_b < \frac{M}{2}$$

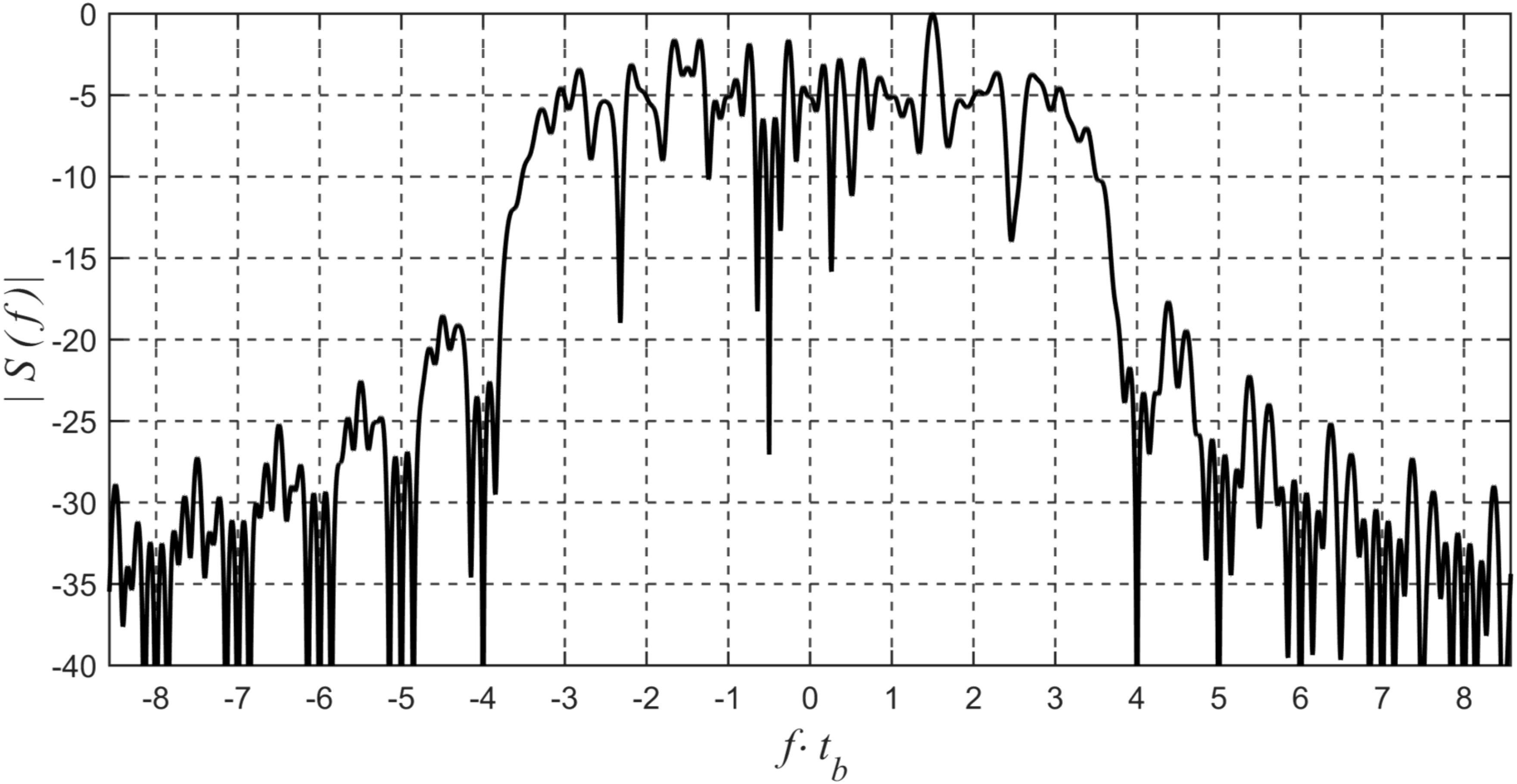

FREQUENCY CODED WAVEFORMS

An 8x8 Costas array

[1 8 3 6 2 7 5 4]

0	1	0	0	0	0	0	0
0	0	0	0	0	1	0	0
0	0	0	1	0	0	0	0
0	0	0	0	0	0	1	0
0	0	0	0	0	0	0	1
0	0	1	0	0	0	0	0
0	0	0	0	1	0	0	0
1	0	0	0	0	0	0	0

2-D autocorrelation of the array

0	**0**	**0**	**0**	**0**	**0**	**0**	**0**	**1**	**0**	**0**	**0**	**0**	**0**	**0**
0	**0**	**0**	**0**	**1**	**0**	**0**	**0**	**0**	**0**	**0**	**0**	**1**	**0**	**0**
0	**0**	**0**	**0**	**0**	**0**	**1**	**0**	**1**	**0**	**1**	**0**	**0**	**0**	**0**
0	**1**	**0**	**0**	**0**	**0**	**1**	**0**	**0**	**0**	**1**	**0**	**0**	**1**	**0**
0	**0**	**1**	**0**	**0**	**1**	**0**	**0**	**1**	**1**	**0**	**0**	**0**	**0**	**1**
0	**0**	**0**	**1**	**0**	**1**	**1**	**0**	**0**	**1**	**1**	**1**	**0**	**0**	**0**
0	**0**	**0**	**1**	**1**	**1**	**1**	**0**	**0**	**1**	**0**	**1**	**1**	**0**	**0**
0	**0**	**0**	**0**	**0**	**0**	**0**	8	**0**	**0**	**0**	**0**	**0**	**0**	**0**
0	0	1	1	0	1	0	0	1	1	1	1	0	0	0
0	0	0	1	1	1	0	0	1	1	0	1	0	0	0
1	0	0	0	0	1	1	0	0	1	0	0	1	0	0
0	1	0	0	1	0	0	0	1	0	0	0	0	1	0
0	0	0	0	1	0	1	0	1	0	0	0	0	0	0
0	0	1	0	0	0	0	0	0	0	1	0	0	0	0
0	0	0	0	0	0	1	0	0	0	0	0	0	0	0

AF of the 8 element Costas signal

0	0	0	0	0	0	0	0	1	0	0	0	0	0	0
0	0	0	0	1	0	0	0	0	0	0	0	1	0	0
0	0	0	0	0	0	1	0	1	0	1	0	0	0	0
0	1	0	0	0	0	1	0	0	0	1	0	0	1	0
0	0	1	0	0	1	0	0	1	1	0	0	0	0	1
0	0	0	1	0	1	1	0	0	1	1	1	0	0	0
0	0	0	1	1	1	1	0	0	1	0	1	1	0	0
0	0	0	0	0	0	0	8	0	0	0	0	0	0	0

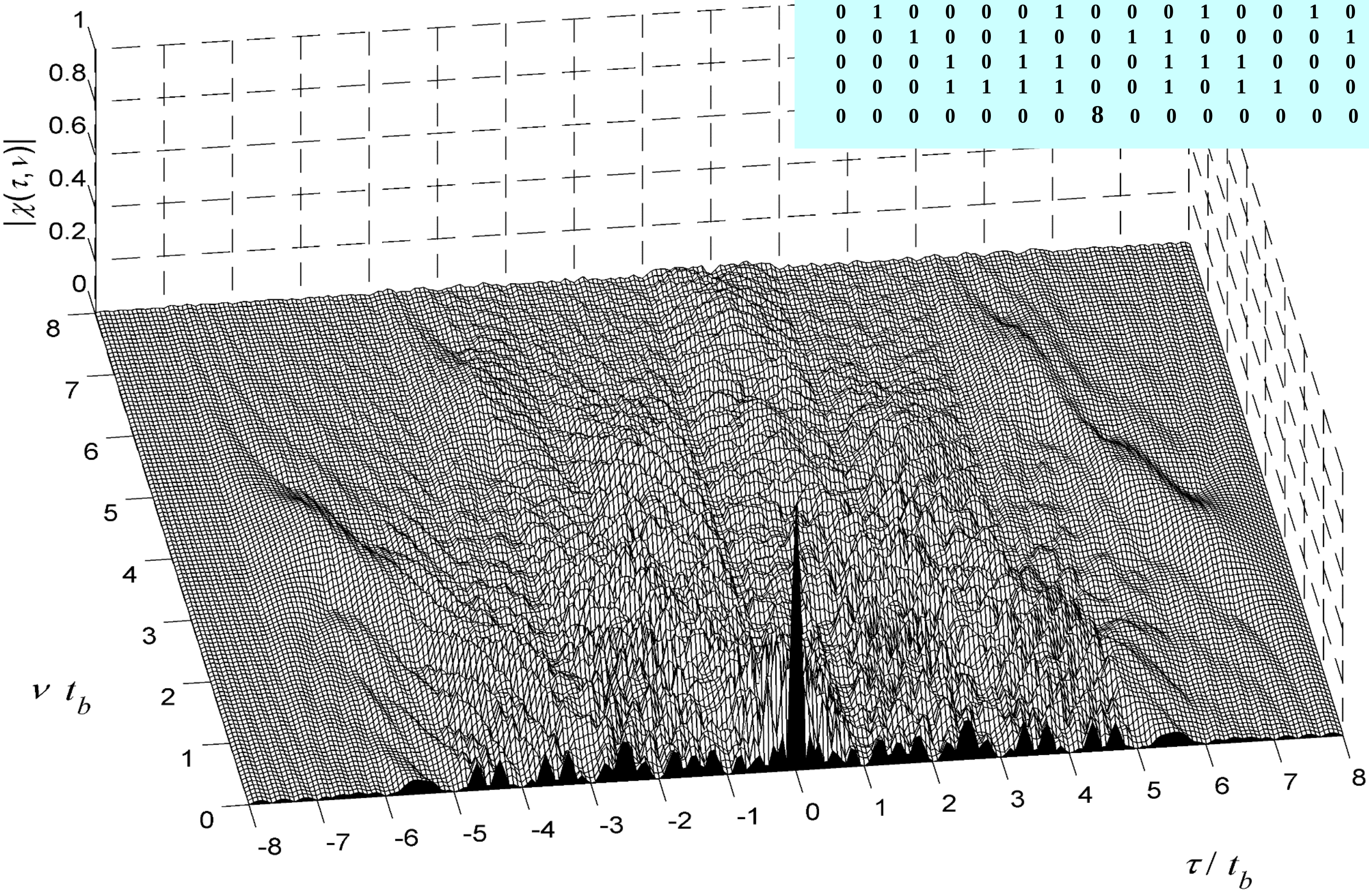

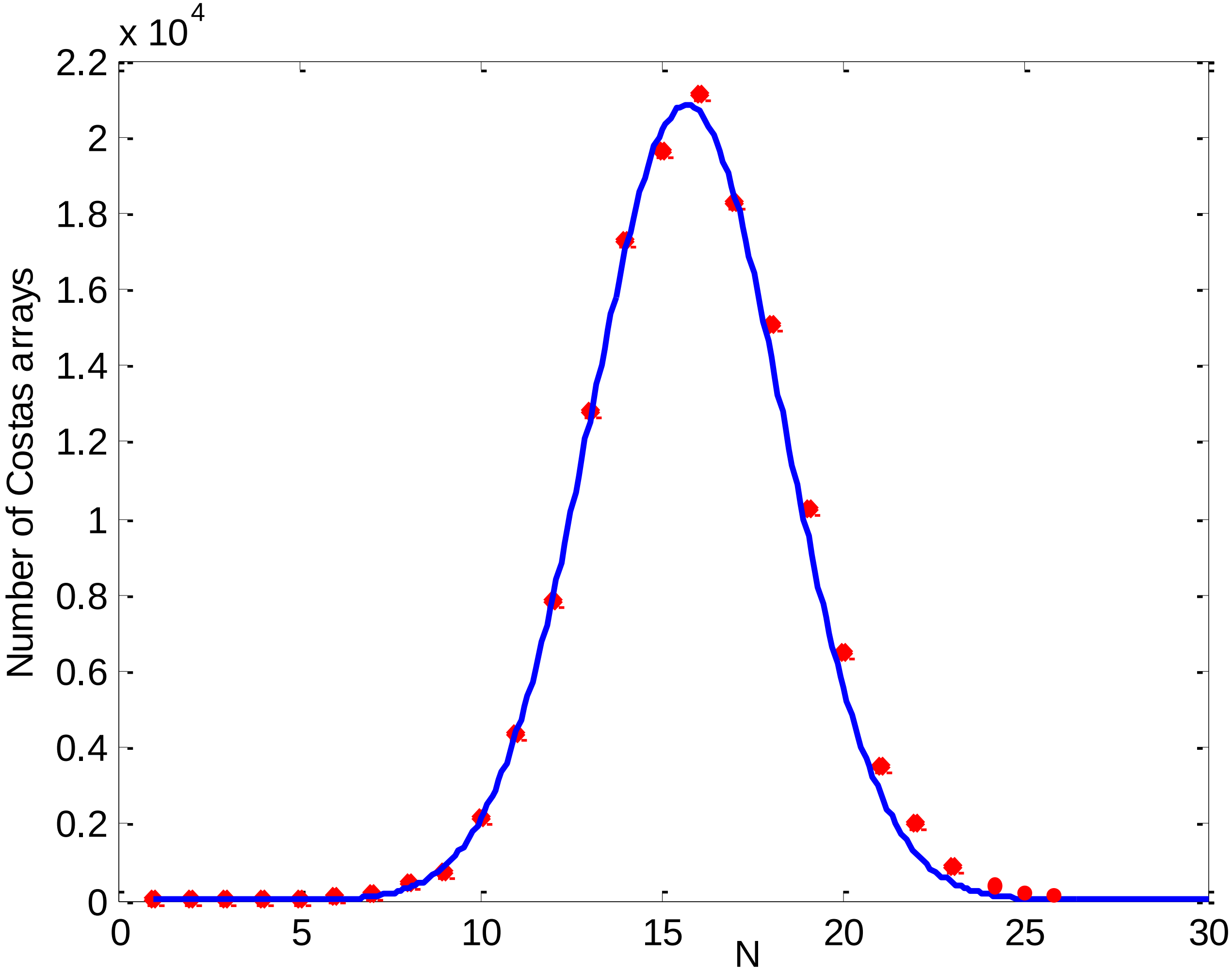

The number of Costas arrays

Silverman J., et al "On the number of Costas arrays as a function of array size", Proc. IEEE, Vol 76 (7), July 1988, pp. 851-853.

Beard J. K., et. al "Combinatoric collaboration on Costas arrays and radar applications", IEEE 2004 Radar Conf., Philadelphia, pp. 260-265.

Beard J. k., "Generating Costas arrays to order 200", CISS 2005.

Number of Costas arrays

N	C(*N*)	c(*N*)
1	1	1
2	2	1
3	4	1
4	12	2
5	40	6
6	116	17
7	200	30
8	444	60
9	760	100
10	2160	277
11	4368	555
12	7852	990
13	12828	1616
14	17252	2168
15	19612	2467
16	21104	2648
17	18276	2294
18	15096	1892
19	10240	1283
20	6464	810
21	3536	446
22	2052	259
23	872	114
24	200	25
25	88	12
26	56	8
27	204	29
28	712	89
29	164	23

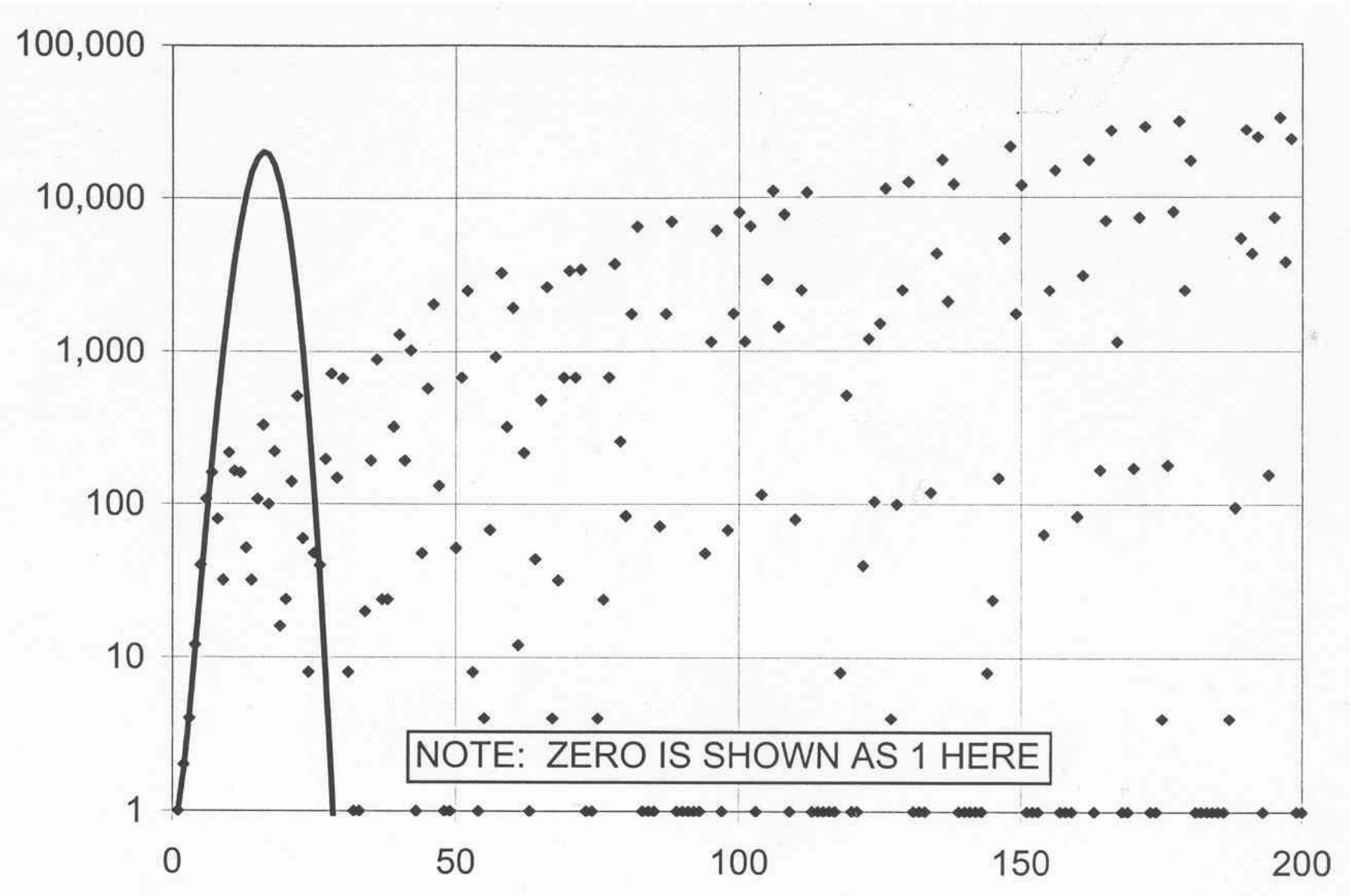

Beard J. K., et. al “Combinatoric collaboration on Costas arrays and radar applications”, IEEE 2004 Radar Conf., Philadelphia, pp. 260-265.

Welch 1 construction method for $N = (p - 1) = 4$, p = prime

$p=5$

$GF(5) = \{0\ 1\ 2\ 3\ 4\}$ 2 and 3 are primitive elements of $GF(5)$

Using $\alpha=2$:

$$j = 0\ ;\quad i = 2^0 = 1$$

$$j = 1\ ;\quad i = 2^1 = 2$$

$$j = 2;\quad i = 2^2 = 4$$

$$j = 3;\quad i = 2^3 = 8 \equiv 3 \bmod 5$$

➔ Coding sequence = {1 2 4 3}

Using $\alpha=3$:

$$j = 0\ ;\quad i = 3^0 = 1$$

$$j = 1\ ;\quad i = 3^1 = 3$$

$$j = 2;\quad i = 3^2 = 9 \equiv 4 \bmod 5$$

$$j = 3;\quad i = 3^3 = 27 \equiv 2 \bmod 5$$

➔ Coding sequence = {1 3 4 2}

$$\{\ 1\ \ 2\ \ 4\ \ 3\ \} - 1 = \cancel{0}\ \ 1\ \ 3\ \ 2 \xrightarrow{\textbf{Welch 2}} \{\ 1\ 3\ 2\ \}$$

All twelve Costas arrays of size 4

1000	0001	0010	0010	1000	0001
0010	1000	1000	0100	0001	0100
0001	0010	0100	0001	0100	1000
0100	0100	0001	1000	0010	0010

0100	0100	1000	0001	0100	0010
0010	0001	0100	0010	1000	0001
1000	0010	0001	1000	0010	0100
0001	1000	0010	0100	0001	1000

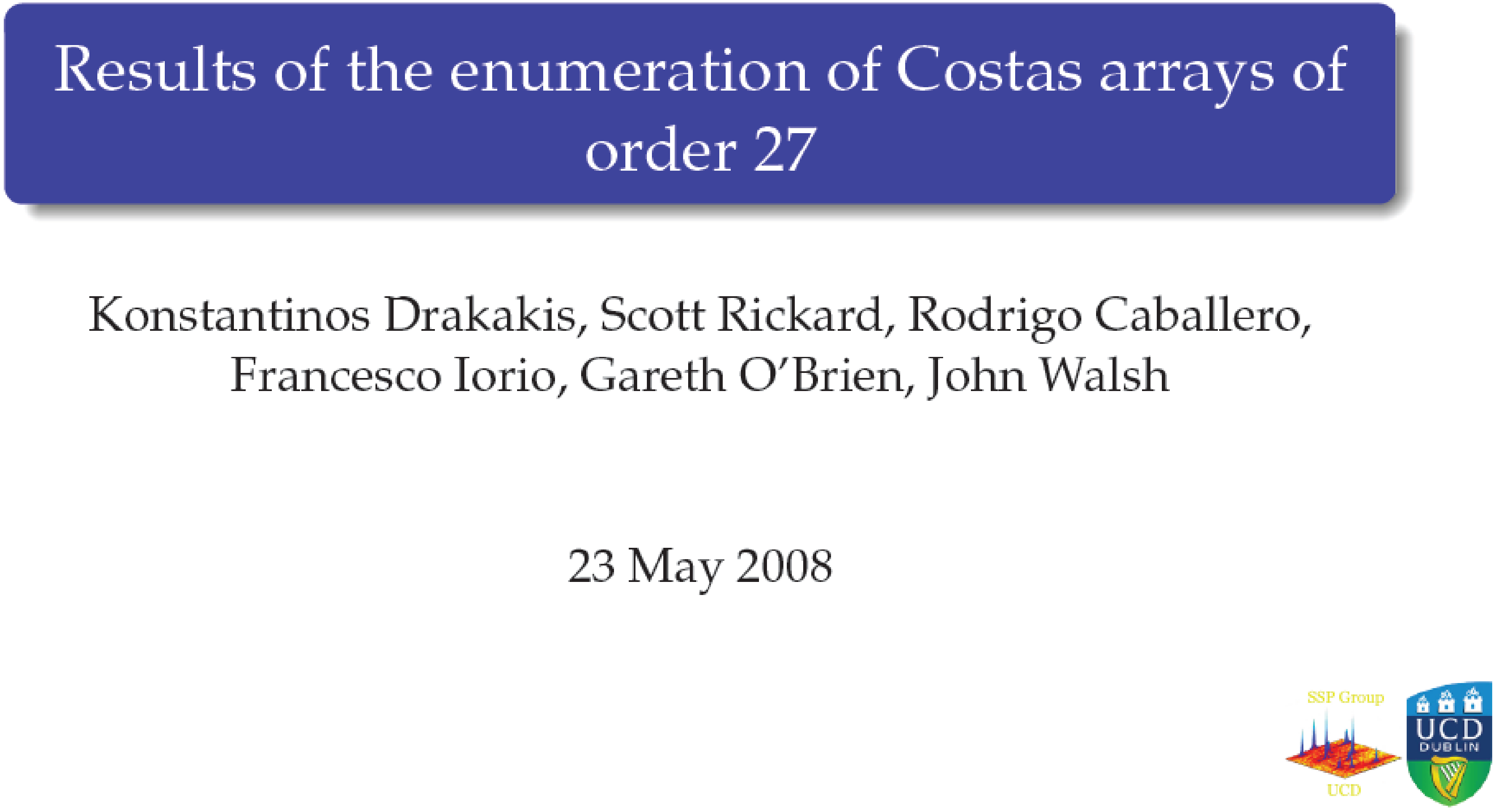

Results of the enumeration of Costas arrays of order 27

Konstantinos Drakakis, Scott Rickard, Rodrigo Caballero,
Francesco Iorio, Gareth O'Brien, John Walsh

23 May 2008

29 ECs of Costas arrays were found; 7 are symmetric:
$22 \cdot 8 + 7 \cdot 4 = 204$ Costas arrays of order 27 in total.

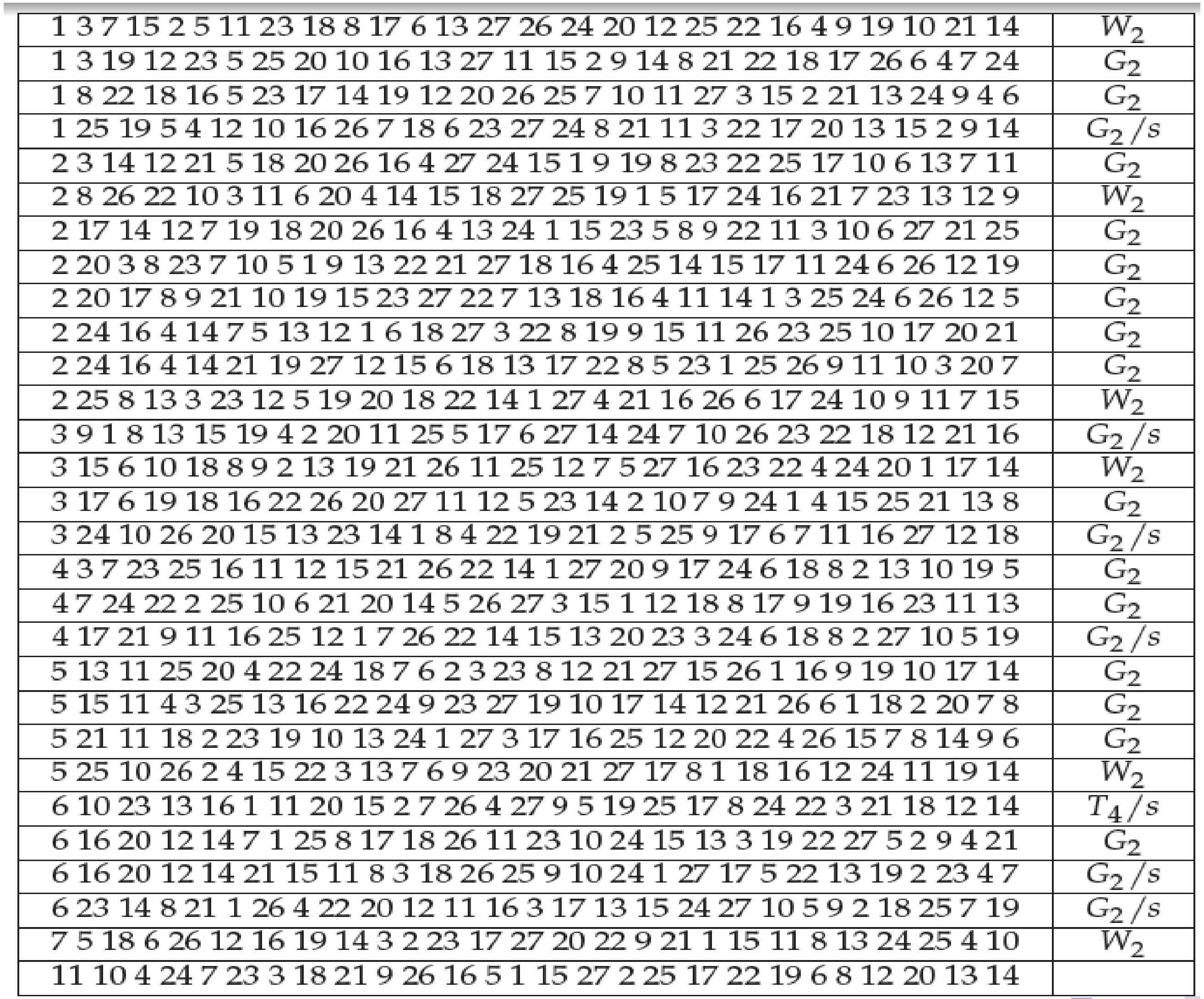

1 3 7 15 2 5 11 23 18 8 17 6 13 27 26 24 20 12 25 22 16 4 9 19 10 21 14	W_2
1 3 19 12 23 5 25 20 10 16 13 27 11 15 2 9 14 8 21 22 18 17 26 6 4 7 24	G_2
1 8 22 18 16 5 23 17 14 19 12 20 26 25 7 10 11 27 3 15 2 21 13 24 9 4 6	G_2
1 25 19 5 4 12 10 16 26 7 18 6 23 27 24 8 21 11 3 22 17 20 13 15 2 9 14	G_2/s
2 3 14 12 21 5 18 20 26 16 4 27 24 15 1 9 19 8 23 22 25 17 10 6 13 7 11	G_2
2 8 26 22 10 3 11 6 20 4 14 15 18 27 25 19 1 5 17 24 16 21 7 23 13 12 9	W_2
2 17 14 12 7 19 18 20 26 16 4 13 24 1 15 23 5 8 9 22 11 3 10 6 27 21 25	G_2
2 20 3 8 23 7 10 5 1 9 13 22 21 27 18 16 4 25 14 15 17 11 24 6 26 12 19	G_2
2 20 17 8 9 21 10 19 15 23 27 22 7 13 18 16 4 11 14 1 3 25 24 6 26 12 5	G_2
2 24 16 4 14 7 5 13 12 1 6 18 27 3 22 8 19 9 15 11 26 23 25 10 17 20 21	G_2
2 24 16 4 14 21 19 27 12 15 6 18 13 17 22 8 5 23 1 25 26 9 11 10 3 20 7	G_2
2 25 8 13 3 23 12 5 19 20 18 22 14 1 27 4 21 16 26 6 17 24 10 9 11 7 15	W_2
3 9 1 8 13 15 19 4 2 20 11 25 5 17 6 27 14 24 7 10 26 23 22 18 12 21 16	G_2/s
3 15 6 10 18 8 9 2 13 19 21 26 11 25 12 7 5 27 16 23 22 4 24 20 1 17 14	W_2
3 17 6 19 18 16 22 26 20 27 11 12 5 23 14 2 10 7 9 24 1 4 15 25 21 13 8	G_2
3 24 10 26 20 15 13 23 14 1 8 4 22 19 21 2 5 25 9 17 6 7 11 16 27 12 18	G_2/s
4 3 7 23 25 16 11 12 15 21 26 22 14 1 27 20 9 17 24 6 18 8 2 13 10 19 5	G_2
4 7 24 22 2 25 10 6 21 20 14 5 26 27 3 15 1 12 18 8 17 9 19 16 23 11 13	G_2
4 17 21 9 11 16 25 12 1 7 26 22 14 15 13 20 23 3 24 6 18 8 2 27 10 5 19	G_2/s
5 13 11 25 20 4 22 24 18 7 6 2 3 23 8 12 21 27 15 26 1 16 9 19 10 17 14	G_2
5 15 11 4 3 25 13 16 22 24 9 23 27 19 10 17 14 12 21 26 6 1 18 2 20 7 8	G_2
5 21 11 18 2 23 19 10 13 24 1 27 3 17 16 25 12 20 22 4 26 15 7 8 14 9 6	G_2
5 25 10 26 2 4 15 22 3 13 7 6 9 23 20 21 27 17 8 1 18 16 12 24 11 19 14	W_2
6 10 23 13 16 1 11 20 15 2 7 26 4 27 9 5 19 25 17 8 24 22 3 21 18 12 14	T_4/s
6 16 20 12 14 7 1 25 8 17 18 26 11 23 10 24 15 13 3 19 22 27 5 2 9 4 21	G_2
6 16 20 12 14 21 15 11 8 3 18 26 25 9 10 24 1 27 17 5 22 13 19 2 23 4 7	G_2/s
6 23 14 8 21 1 26 4 22 20 12 11 16 3 17 13 15 24 27 10 5 9 2 18 25 7 19	G_2/s
7 5 18 6 26 12 16 19 14 3 2 23 17 27 20 22 9 21 1 15 11 8 13 24 25 4 10	W_2
11 10 4 24 7 23 3 18 21 9 26 16 5 1 15 27 2 25 17 22 19 6 8 12 20 13 14	

Horizontal/vertical flips and transpositions of a Costas array are also Costas arrays: 1 → 8 (or 1 → 4 if symmetric). These are equivalence classes (EC) of Costas arrays.

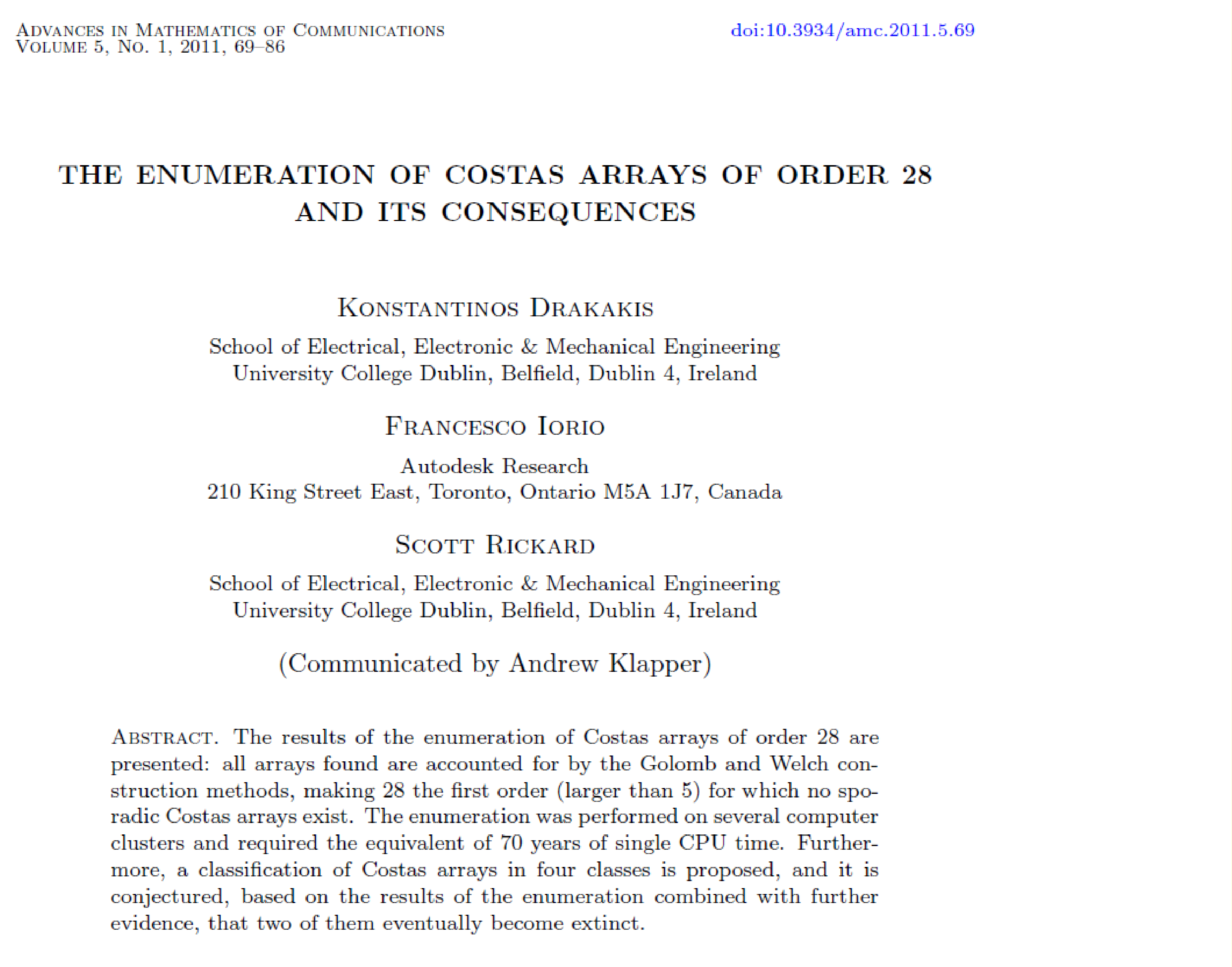

Advances in Mathematics of Communications
Volume 5, No. 1, 2011, 69–86

doi:10.3934/amc.2011.5.69

THE ENUMERATION OF COSTAS ARRAYS OF ORDER 28 AND ITS CONSEQUENCES

Konstantinos Drakakis

School of Electrical, Electronic & Mechanical Engineering
University College Dublin, Belfield, Dublin 4, Ireland

Francesco Iorio

Autodesk Research
210 King Street East, Toronto, Ontario M5A 1J7, Canada

Scott Rickard

School of Electrical, Electronic & Mechanical Engineering
University College Dublin, Belfield, Dublin 4, Ireland

(Communicated by Andrew Klapper)

Abstract. The results of the enumeration of Costas arrays of order 28 are presented: all arrays found are accounted for by the Golomb and Welch construction methods, making 28 the first order (larger than 5) for which no sporadic Costas arrays exist. The enumeration was performed on several computer clusters and required the equivalent of 70 years of single CPU time. Furthermore, a classification of Costas arrays in four classes is proposed, and it is conjectured, based on the results of the enumeration combined with further evidence, that two of them eventually become extinct.

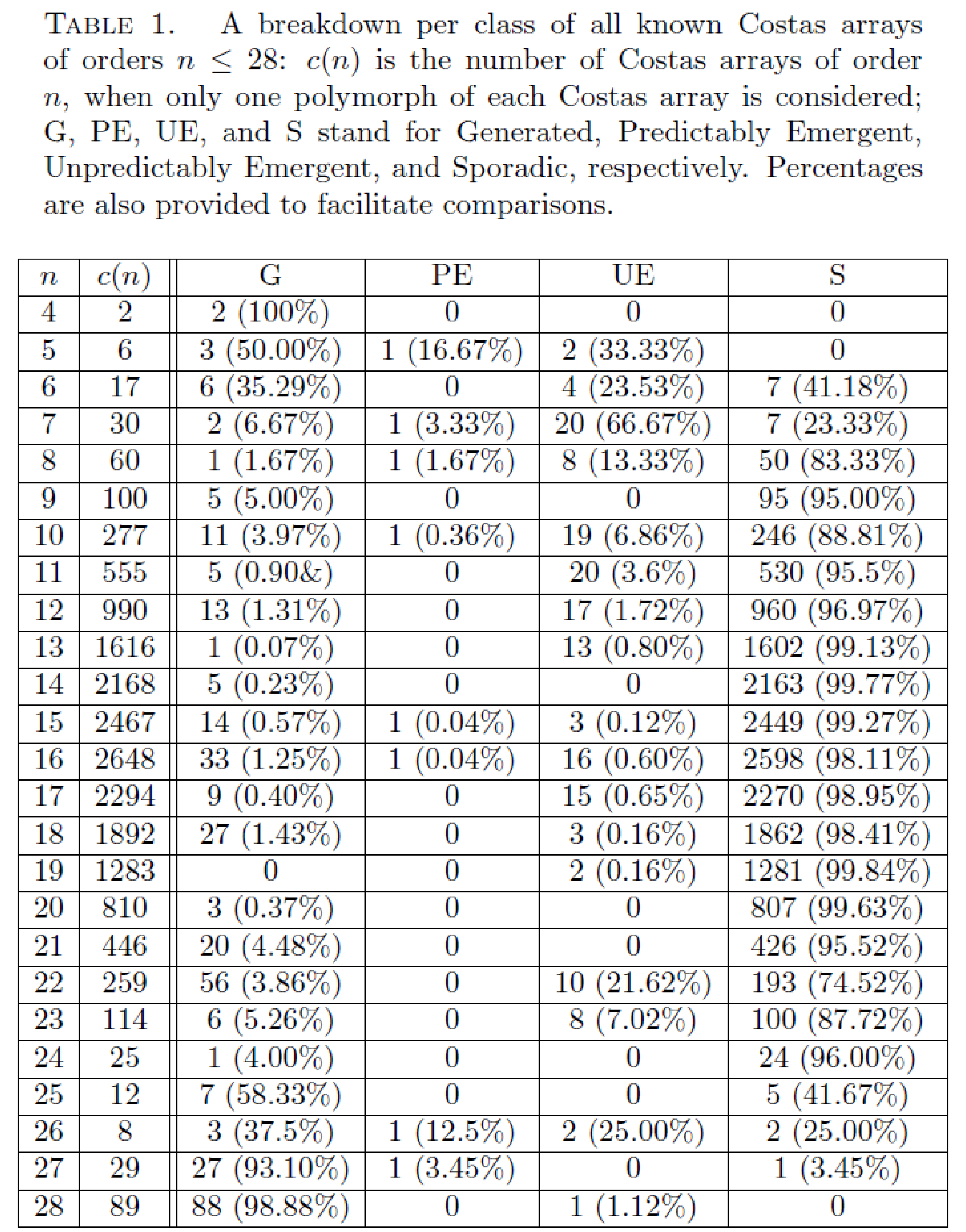

TABLE 1. A breakdown per class of all known Costas arrays of orders $n \leq 28$: $c(n)$ is the number of Costas arrays of order n, when only one polymorph of each Costas array is considered; G, PE, UE, and S stand for Generated, Predictably Emergent, Unpredictably Emergent, and Sporadic, respectively. Percentages are also provided to facilitate comparisons.

n	$c(n)$	G	PE	UE	S
4	2	2 (100%)	0	0	0
5	6	3 (50.00%)	1 (16.67%)	2 (33.33%)	0
6	17	6 (35.29%)	0	4 (23.53%)	7 (41.18%)
7	30	2 (6.67%)	1 (3.33%)	20 (66.67%)	7 (23.33%)
8	60	1 (1.67%)	1 (1.67%)	8 (13.33%)	50 (83.33%)
9	100	5 (5.00%)	0	0	95 (95.00%)
10	277	11 (3.97%)	1 (0.36%)	19 (6.86%)	246 (88.81%)
11	555	5 (0.90&)	0	20 (3.6%)	530 (95.5%)
12	990	13 (1.31%)	0	17 (1.72%)	960 (96.97%)
13	1616	1 (0.07%)	0	13 (0.80%)	1602 (99.13%)
14	2168	5 (0.23%)	0	0	2163 (99.77%)
15	2467	14 (0.57%)	1 (0.04%)	3 (0.12%)	2449 (99.27%)
16	2648	33 (1.25%)	1 (0.04%)	16 (0.60%)	2598 (98.11%)
17	2294	9 (0.40%)	0	15 (0.65%)	2270 (98.95%)
18	1892	27 (1.43%)	0	3 (0.16%)	1862 (98.41%)
19	1283	0	0	2 (0.16%)	1281 (99.84%)
20	810	3 (0.37%)	0	0	807 (99.63%)
21	446	20 (4.48%)	0	0	426 (95.52%)
22	259	56 (3.86%)	0	10 (21.62%)	193 (74.52%)
23	114	6 (5.26%)	0	8 (7.02%)	100 (87.72%)
24	25	1 (4.00%)	0	0	24 (96.00%)
25	12	7 (58.33%)	0	0	5 (41.67%)
26	8	3 (37.5%)	1 (12.5%)	2 (25.00%)	2 (25.00%)
27	29	27 (93.10%)	1 (3.45%)	0	1 (3.45%)
28	89	88 (98.88%)	0	1 (1.12%)	0

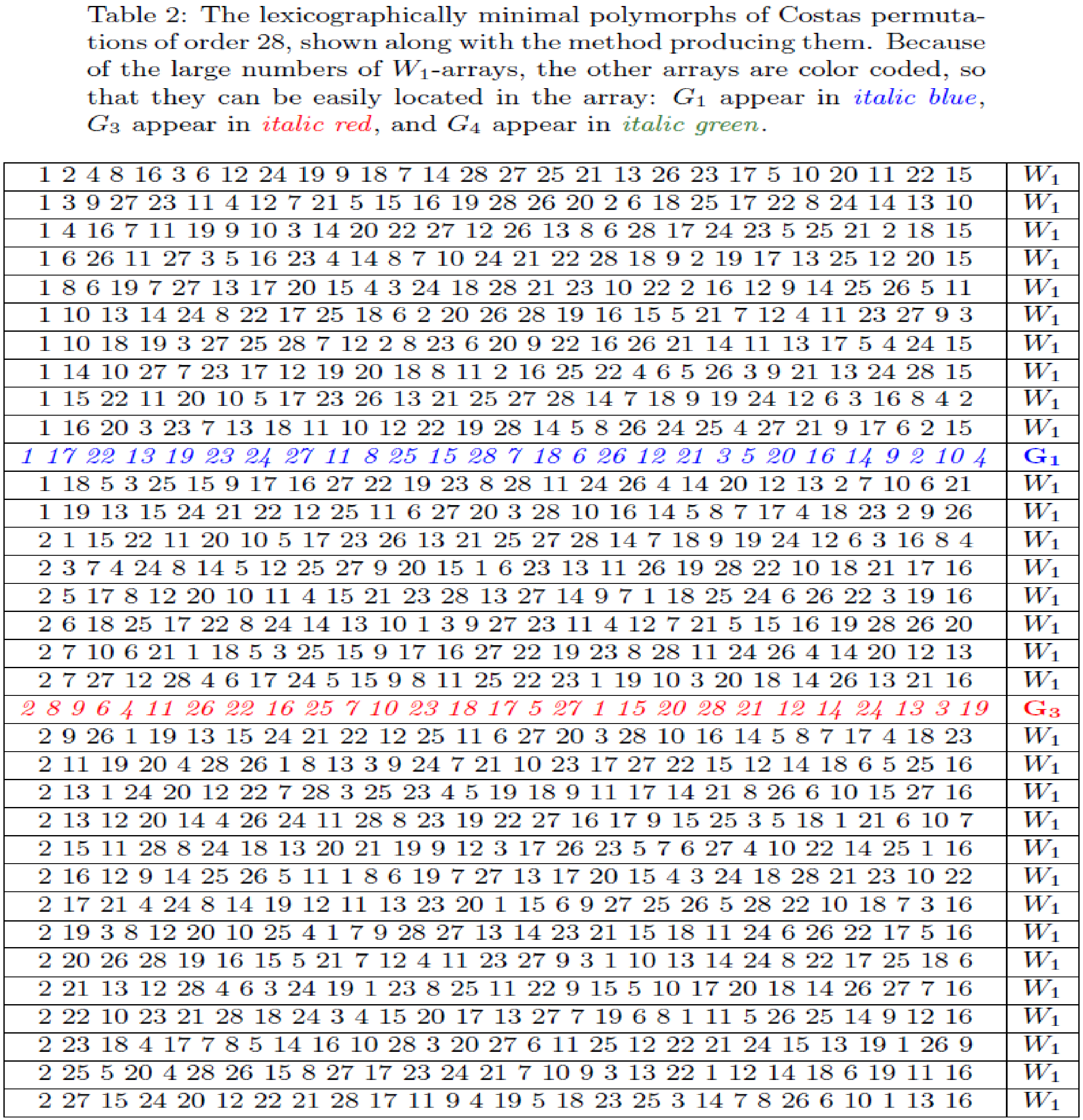

Table 2: The lexicographically minimal polymorphs of Costas permutations of order 28, shown along with the method producing them. Because of the large numbers of W_1-arrays, the other arrays are color coded, so that they can be easily located in the array: G_1 appear in *italic blue*, G_3 appear in *italic red*, and G_4 appear in *italic green*.

1 2 4 8 16 3 6 12 24 19 9 18 7 14 28 27 25 21 13 26 23 17 5 10 20 11 22 15	W_1
1 3 9 27 23 11 4 12 7 21 5 15 16 19 28 26 20 2 6 18 25 17 22 8 24 14 13 10	W_1
1 4 16 7 11 19 9 10 3 14 20 22 27 12 26 13 8 6 28 17 24 23 5 25 21 2 18 15	W_1
1 6 26 11 27 3 5 16 23 4 14 8 7 10 24 21 22 28 18 9 2 19 17 13 25 12 20 15	W_1
1 8 6 19 7 27 13 17 20 15 4 3 24 18 28 21 23 10 22 2 16 12 9 14 25 26 5 11	W_1
1 10 13 14 24 8 22 17 25 18 6 2 20 26 28 19 16 15 5 21 7 12 4 11 23 27 9 3	W_1
1 10 18 19 3 27 25 28 7 12 2 8 23 6 20 9 22 16 26 21 14 11 13 17 5 4 24 15	W_1
1 14 10 27 7 23 17 12 19 20 18 8 11 2 16 25 22 4 6 5 26 3 9 21 13 24 28 15	W_1
1 15 22 11 20 10 5 17 23 26 13 21 25 27 28 14 7 18 9 19 24 12 6 3 16 8 4 2	W_1
1 16 20 3 23 7 13 18 11 10 12 22 19 28 14 5 8 26 24 25 4 27 21 9 17 6 2 15	W_1
1 17 22 13 19 23 24 27 11 8 25 15 28 7 18 6 26 12 21 3 5 20 16 14 9 2 10 4	$\mathbf{G_1}$
1 18 5 3 25 15 9 17 16 27 22 19 23 8 28 11 24 26 4 14 20 12 13 2 7 10 6 21	W_1
1 19 13 15 24 21 22 12 25 11 6 27 20 3 28 10 16 14 5 8 7 17 4 18 23 2 9 26	W_1
2 1 15 22 11 20 10 5 17 23 26 13 21 25 27 28 14 7 18 9 19 24 12 6 3 16 8 4	W_1
2 3 7 4 24 8 14 5 12 25 27 9 20 15 1 6 23 13 11 26 19 28 22 10 18 21 17 16	W_1
2 5 17 8 12 20 10 11 4 15 21 23 28 13 27 14 9 7 1 18 25 24 6 26 22 3 19 16	W_1
2 6 18 25 17 22 8 24 14 13 10 1 3 9 27 23 11 4 12 7 21 5 15 16 19 28 26 20	W_1
2 7 10 6 21 1 18 5 3 25 15 9 17 16 27 22 19 23 8 28 11 24 26 4 14 20 12 13	W_1
2 7 27 12 28 4 6 17 24 5 15 9 8 11 25 22 23 1 19 10 3 20 18 14 26 13 21 16	W_1
2 8 9 6 4 11 26 22 16 25 7 10 23 18 17 5 27 1 15 20 28 21 12 14 24 13 3 19	$\mathbf{G_3}$
2 9 26 1 19 13 15 24 21 22 12 25 11 6 27 20 3 28 10 16 14 5 8 7 17 4 18 23	W_1
2 11 19 20 4 28 26 1 8 13 3 9 24 7 21 10 23 17 27 22 15 12 14 18 6 5 25 16	W_1
2 13 1 24 20 12 22 7 28 3 25 23 4 5 19 18 9 11 17 14 21 8 26 6 10 15 27 16	W_1
2 13 12 20 14 4 26 24 11 28 8 23 19 22 27 16 17 9 15 25 3 5 18 1 21 6 10 7	W_1
2 15 11 28 8 24 18 13 20 21 19 9 12 3 17 26 23 5 7 6 27 4 10 22 14 25 1 16	W_1
2 16 12 9 14 25 26 5 11 1 8 6 19 7 27 13 17 20 15 4 3 24 18 28 21 23 10 22	W_1
2 17 21 4 24 8 14 19 12 11 13 23 20 1 15 6 9 27 25 26 5 28 22 10 18 7 3 16	W_1
2 19 3 8 12 20 10 25 4 1 7 9 28 27 13 14 23 21 15 18 11 24 6 26 22 17 5 16	W_1
2 20 26 28 19 16 15 5 21 7 12 4 11 23 27 9 3 1 10 13 14 24 8 22 17 25 18 6	W_1
2 21 13 12 28 4 6 3 24 19 1 23 8 25 11 22 9 15 5 10 17 20 18 14 26 27 7 16	W_1
2 22 10 23 21 28 18 24 3 4 15 20 17 13 27 7 19 6 8 1 11 5 26 25 14 9 12 16	W_1
2 23 18 4 17 7 8 5 14 16 10 28 3 20 27 6 11 25 12 22 21 24 15 13 19 1 26 9	W_1
2 25 5 20 4 28 26 15 8 27 17 23 24 21 7 10 9 3 13 22 1 12 14 18 6 19 11 16	W_1
2 27 15 24 20 12 22 21 28 17 11 9 4 19 5 18 23 25 3 14 7 8 26 6 10 1 13 16	W_1

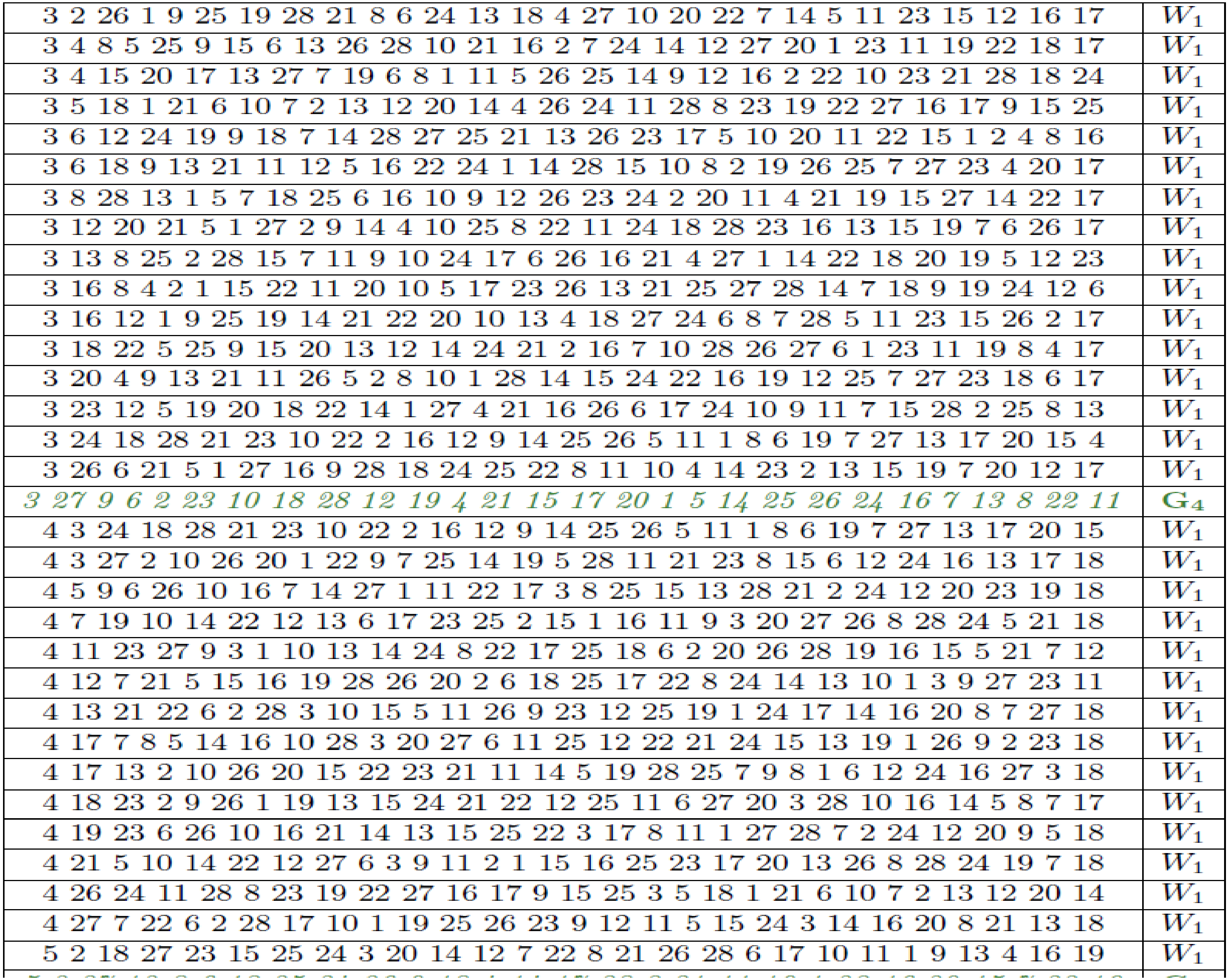

3 2 26 1 9 25 19 28 21 8 6 24 13 18 4 27 10 20 22 7 14 5 11 23 15 12 16 17	W_1
3 4 8 5 25 9 15 6 13 26 28 10 21 16 2 7 24 14 12 27 20 1 23 11 19 22 18 17	W_1
3 4 15 20 17 13 27 7 19 6 8 1 11 5 26 25 14 9 12 16 2 22 10 23 21 28 18 24	W_1
3 5 18 1 21 6 10 7 2 13 12 20 14 4 26 24 11 28 8 23 19 22 27 16 17 9 15 25	W_1
3 6 12 24 19 9 18 7 14 28 27 25 21 13 26 23 17 5 10 20 11 22 15 1 2 4 8 16	W_1
3 6 18 9 13 21 11 12 5 16 22 24 1 14 28 15 10 8 2 19 26 25 7 27 23 4 20 17	W_1
3 8 28 13 1 5 7 18 25 6 16 10 9 12 26 23 24 2 20 11 4 21 19 15 27 14 22 17	W_1
3 12 20 21 5 1 27 2 9 14 4 10 25 8 22 11 24 18 28 23 16 13 15 19 7 6 26 17	W_1
3 13 8 25 2 28 15 7 11 9 10 24 17 6 26 16 21 4 27 1 14 22 18 20 19 5 12 23	W_1
3 16 8 4 2 1 15 22 11 20 10 5 17 23 26 13 21 25 27 28 14 7 18 9 19 24 12 6	W_1
3 16 12 1 9 25 19 14 21 22 20 10 13 4 18 27 24 6 8 7 28 5 11 23 15 26 2 17	W_1
3 18 22 5 25 9 15 20 13 12 14 24 21 2 16 7 10 28 26 27 6 1 23 11 19 8 4 17	W_1
3 20 4 9 13 21 11 26 5 2 8 10 1 28 14 15 24 22 16 19 12 25 7 27 23 18 6 17	W_1
3 23 12 5 19 20 18 22 14 1 27 4 21 16 26 6 17 24 10 9 11 7 15 28 2 25 8 13	W_1
3 24 18 28 21 23 10 22 2 16 12 9 14 25 26 5 11 1 8 6 19 7 27 13 17 20 15 4	W_1
3 26 6 21 5 1 27 16 9 28 18 24 25 22 8 11 10 4 14 23 2 13 15 19 7 20 12 17	W_1
3 27 9 6 2 23 10 18 28 12 19 4 21 15 17 20 1 5 14 25 26 24 16 7 13 8 22 11	G_4
4 3 24 18 28 21 23 10 22 2 16 12 9 14 25 26 5 11 1 8 6 19 7 27 13 17 20 15	W_1
4 3 27 2 10 26 20 1 22 9 7 25 14 19 5 28 11 21 23 8 15 6 12 24 16 13 17 18	W_1
4 5 9 6 26 10 16 7 14 27 1 11 22 17 3 8 25 15 13 28 21 2 24 12 20 23 19 18	W_1
4 7 19 10 14 22 12 13 6 17 23 25 2 15 1 16 11 9 3 20 27 26 8 28 24 5 21 18	W_1
4 11 23 27 9 3 1 10 13 14 24 8 22 17 25 18 6 2 20 26 28 19 16 15 5 21 7 12	W_1
4 12 7 21 5 15 16 19 28 26 20 2 6 18 25 17 22 8 24 14 13 10 1 3 9 27 23 11	W_1
4 13 21 22 6 2 28 3 10 15 5 11 26 9 23 12 25 19 1 24 17 14 16 20 8 7 27 18	W_1
4 17 7 8 5 14 16 10 28 3 20 27 6 11 25 12 22 21 24 15 13 19 1 26 9 2 23 18	W_1
4 17 13 2 10 26 20 15 22 23 21 11 14 5 19 28 25 7 9 8 1 6 12 24 16 27 3 18	W_1
4 18 23 2 9 26 1 19 13 15 24 21 22 12 25 11 6 27 20 3 28 10 16 14 5 8 7 17	W_1
4 19 23 6 26 10 16 21 14 13 15 25 22 3 17 8 11 1 27 28 7 2 24 12 20 9 5 18	W_1
4 21 5 10 14 22 12 27 6 3 9 11 2 1 15 16 25 23 17 20 13 26 8 28 24 19 7 18	W_1
4 26 24 11 28 8 23 19 22 27 16 17 9 15 25 3 5 18 1 21 6 10 7 2 13 12 20 14	W_1
4 27 7 22 6 2 28 17 10 1 19 25 26 23 9 12 11 5 15 24 3 14 16 20 8 21 13 18	W_1
5 2 18 27 23 15 25 24 3 20 14 12 7 22 8 21 26 28 6 17 10 11 1 9 13 4 16 19	W_1

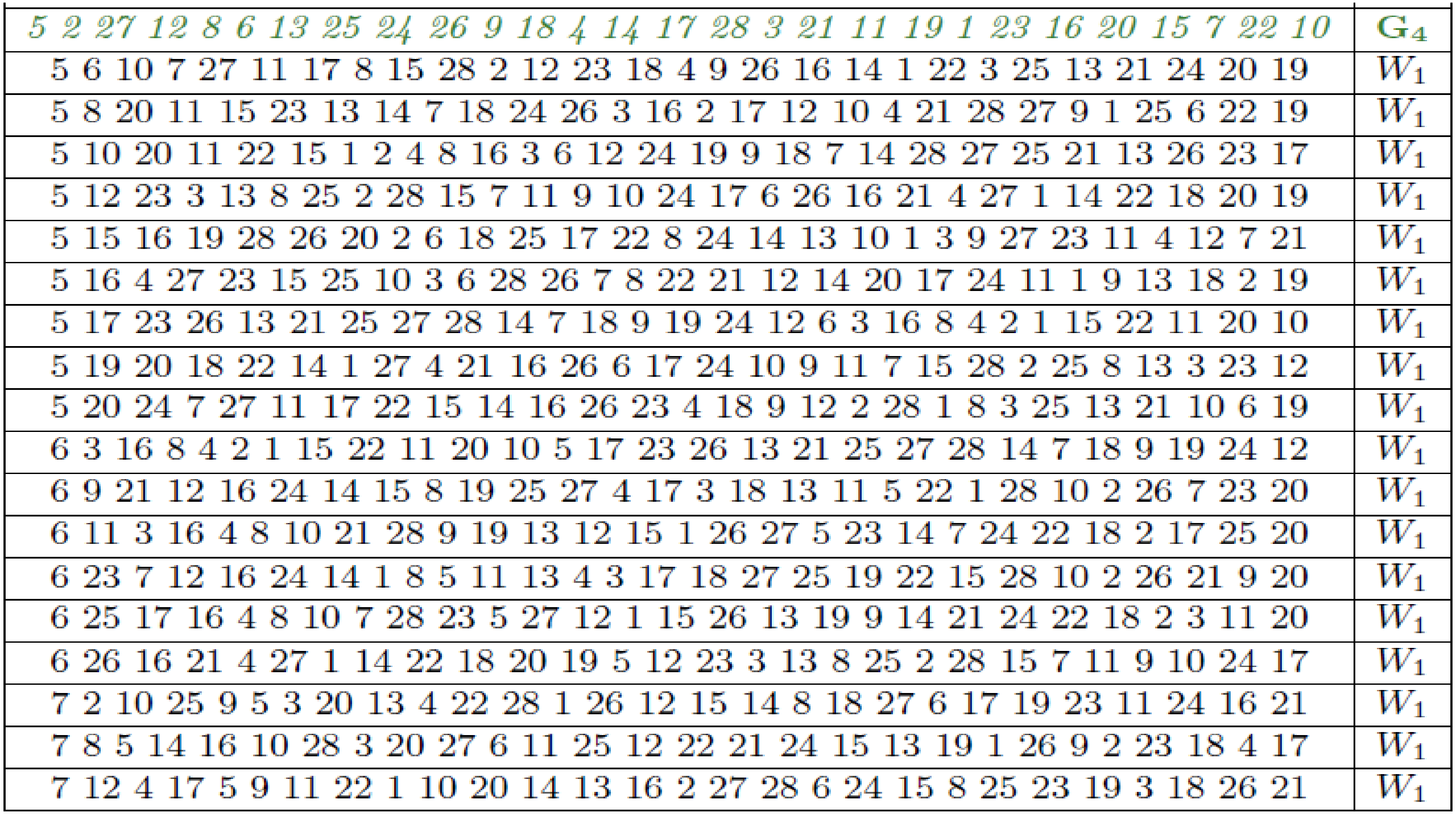

5 2 27 12 8 6 13 25 24 26 9 18 4 14 17 28 3 21 11 19 1 23 16 20 15 7 22 10	$\mathbf{G}_4$
5 6 10 7 27 11 17 8 15 28 2 12 23 18 4 9 26 16 14 1 22 3 25 13 21 24 20 19	W_1
5 8 20 11 15 23 13 14 7 18 24 26 3 16 2 17 12 10 4 21 28 27 9 1 25 6 22 19	W_1
5 10 20 11 22 15 1 2 4 8 16 3 6 12 24 19 9 18 7 14 28 27 25 21 13 26 23 17	W_1
5 12 23 3 13 8 25 2 28 15 7 11 9 10 24 17 6 26 16 21 4 27 1 14 22 18 20 19	W_1
5 15 16 19 28 26 20 2 6 18 25 17 22 8 24 14 13 10 1 3 9 27 23 11 4 12 7 21	W_1
5 16 4 27 23 15 25 10 3 6 28 26 7 8 22 21 12 14 20 17 24 11 1 9 13 18 2 19	W_1
5 17 23 26 13 21 25 27 28 14 7 18 9 19 24 12 6 3 16 8 4 2 1 15 22 11 20 10	W_1
5 19 20 18 22 14 1 27 4 21 16 26 6 17 24 10 9 11 7 15 28 2 25 8 13 3 23 12	W_1
5 20 24 7 27 11 17 22 15 14 16 26 23 4 18 9 12 2 28 1 8 3 25 13 21 10 6 19	W_1
6 3 16 8 4 2 1 15 22 11 20 10 5 17 23 26 13 21 25 27 28 14 7 18 9 19 24 12	W_1
6 9 21 12 16 24 14 15 8 19 25 27 4 17 3 18 13 11 5 22 1 28 10 2 26 7 23 20	W_1
6 11 3 16 4 8 10 21 28 9 19 13 12 15 1 26 27 5 23 14 7 24 22 18 2 17 25 20	W_1
6 23 7 12 16 24 14 1 8 5 11 13 4 3 17 18 27 25 19 22 15 28 10 2 26 21 9 20	W_1
6 25 17 16 4 8 10 7 28 23 5 27 12 1 15 26 13 19 9 14 21 24 22 18 2 3 11 20	W_1
6 26 16 21 4 27 1 14 22 18 20 19 5 12 23 3 13 8 25 2 28 15 7 11 9 10 24 17	W_1
7 2 10 25 9 5 3 20 13 4 22 28 1 26 12 15 14 8 18 27 6 17 19 23 11 24 16 21	W_1
7 8 5 14 16 10 28 3 20 27 6 11 25 12 22 21 24 15 13 19 1 26 9 2 23 18 4 17	W_1
7 12 4 17 5 9 11 22 1 10 20 14 13 16 2 27 28 6 24 15 8 25 23 19 3 18 26 21	W_1

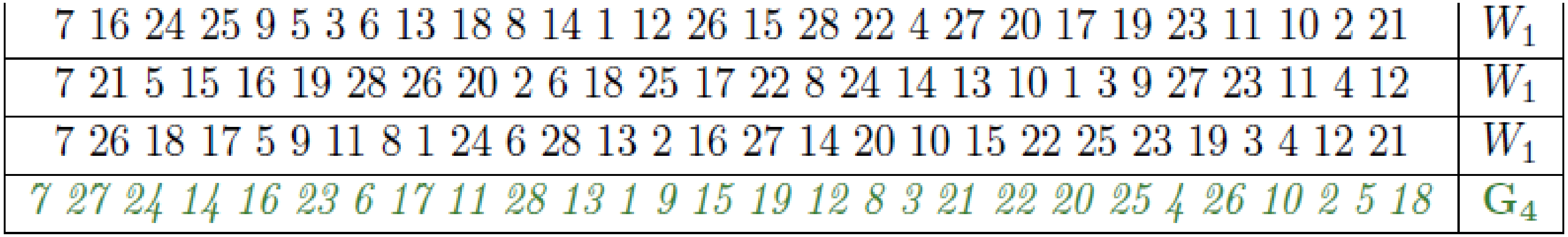

7 16 24 25 9 5 3 6 13 18 8 14 1 12 26 15 28 22 4 27 20 17 19 23 11 10 2 21	W_1
7 21 5 15 16 19 28 26 20 2 6 18 25 17 22 8 24 14 13 10 1 3 9 27 23 11 4 12	W_1
7 26 18 17 5 9 11 8 1 24 6 28 13 2 16 27 14 20 10 15 22 25 23 19 3 4 12 21	W_1
7 27 24 14 16 23 6 17 11 28 13 1 9 15 19 12 8 3 21 22 20 25 4 26 10 2 5 18	$\mathbf{G}_4$

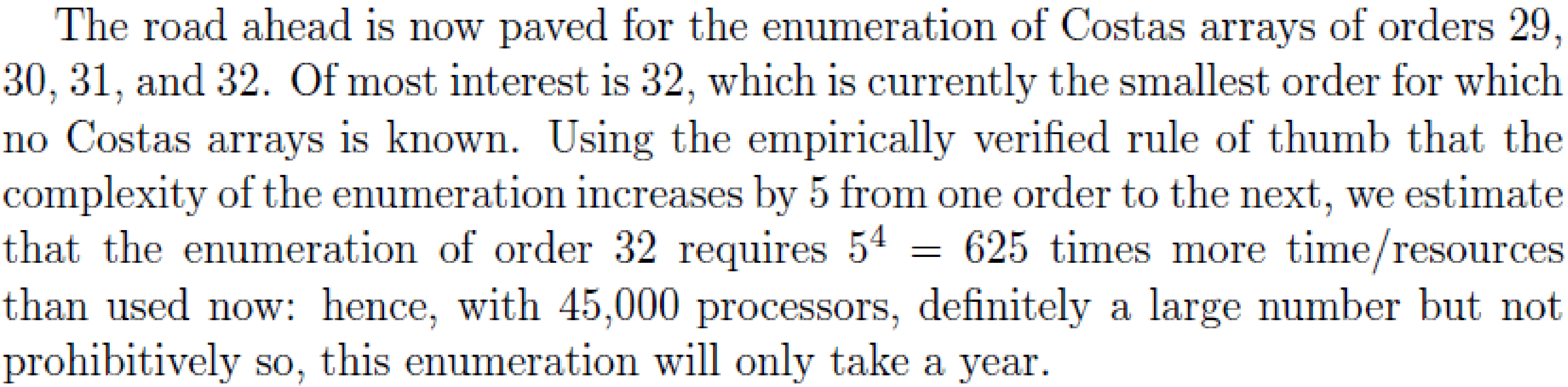

The road ahead is now paved for the enumeration of Costas arrays of orders 29, 30, 31, and 32. Of most interest is 32, which is currently the smallest order for which no Costas arrays is known. Using the empirically verified rule of thumb that the complexity of the enumeration increases by 5 from one order to the next, we estimate that the enumeration of order 32 requires $5^4 = 625$ times more time/resources than used now: hence, with 45,000 processors, definitely a large number but not prohibitively so, this enumeration will only take a year.

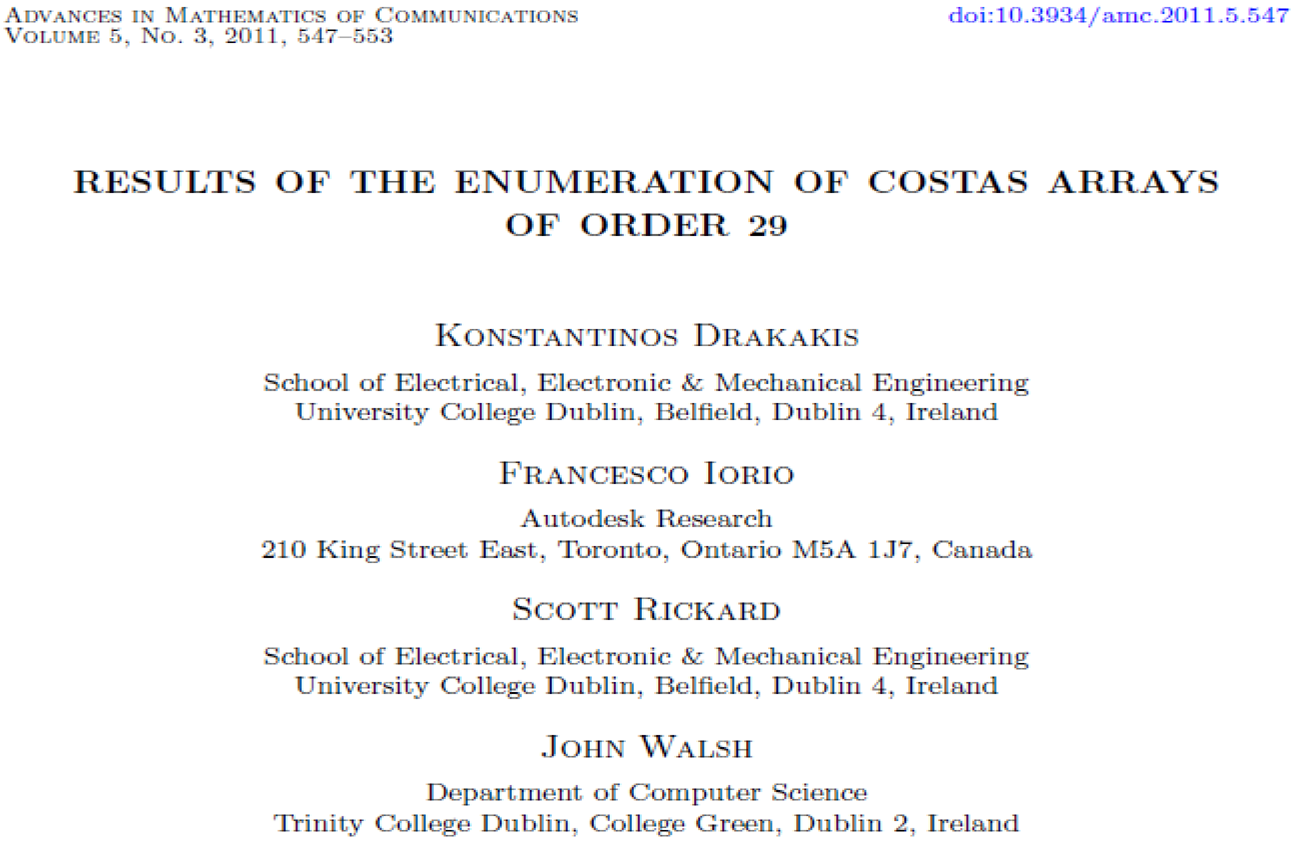

Advances in Mathematics of Communications
Volume 5, No. 3, 2011, 547–553
doi:10.3934/amc.2011.5.547

RESULTS OF THE ENUMERATION OF COSTAS ARRAYS OF ORDER 29

Konstantinos Drakakis

School of Electrical, Electronic & Mechanical Engineering
University College Dublin, Belfield, Dublin 4, Ireland

Francesco Iorio

Autodesk Research
210 King Street East, Toronto, Ontario M5A 1J7, Canada

Scott Rickard

School of Electrical, Electronic & Mechanical Engineering
University College Dublin, Belfield, Dublin 4, Ireland

John Walsh

Department of Computer Science
Trinity College Dublin, College Green, Dublin 2, Ireland

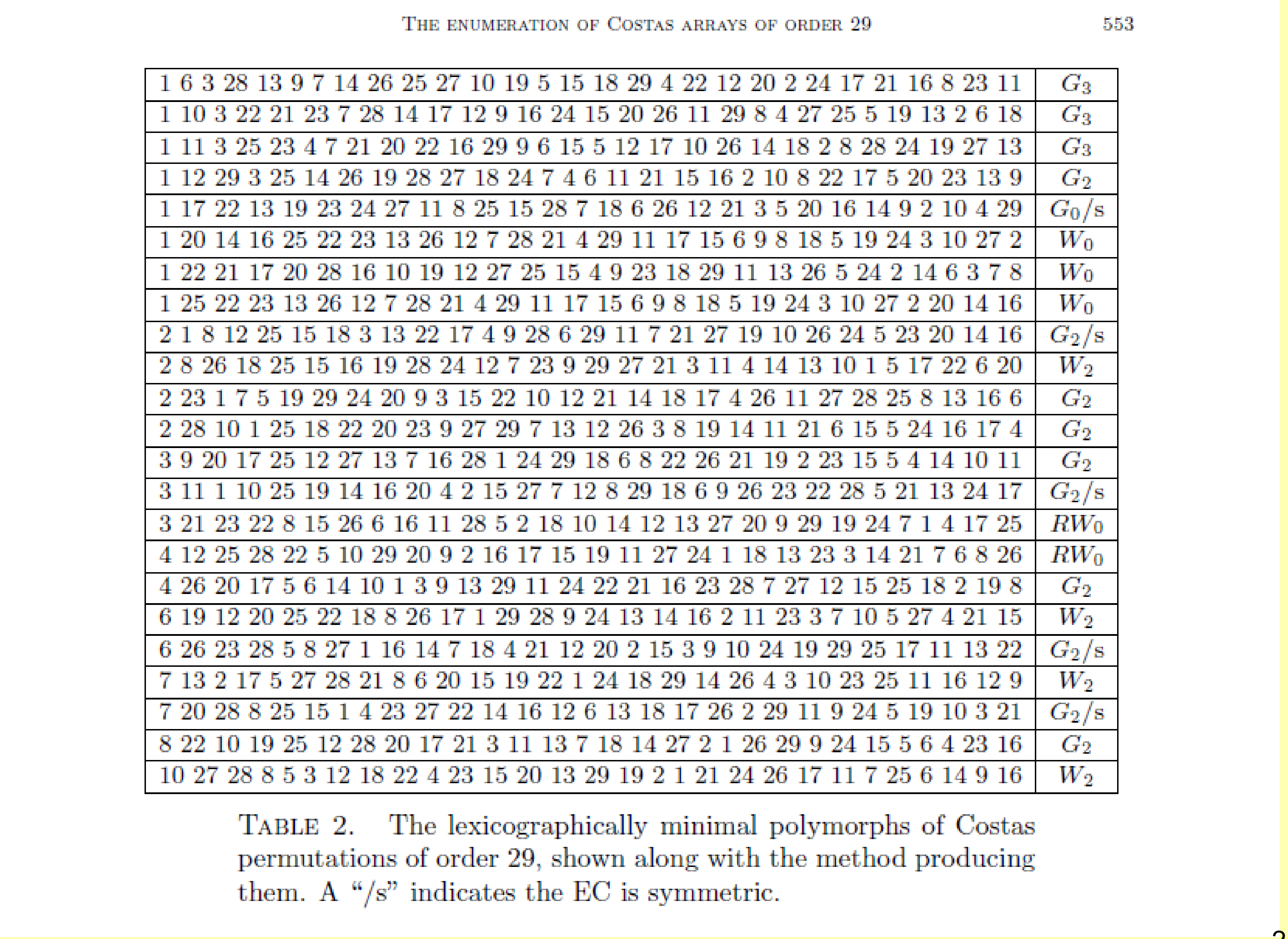

THE ENUMERATION OF COSTAS ARRAYS OF ORDER 29 553

1 6 3 28 13 9 7 14 26 25 27 10 19 5 15 18 29 4 22 12 20 2 24 17 21 16 8 23 11	G_3
1 10 3 22 21 23 7 28 14 17 12 9 16 24 15 20 26 11 29 8 4 27 25 5 19 13 2 6 18	G_3
1 11 3 25 23 4 7 21 20 22 16 29 9 6 15 5 12 17 10 26 14 18 2 8 28 24 19 27 13	G_3
1 12 29 3 25 14 26 19 28 27 18 24 7 4 6 11 21 15 16 2 10 8 22 17 5 20 23 13 9	G_2
1 17 22 13 19 23 24 27 11 8 25 15 28 7 18 6 26 12 21 3 5 20 16 14 9 2 10 4 29	G_0/s
1 20 14 16 25 22 23 13 26 12 7 28 21 4 29 11 17 15 6 9 8 18 5 19 24 3 10 27 2	W_0
1 22 21 17 20 28 16 10 19 12 27 25 15 4 9 23 18 29 11 13 26 5 24 2 14 6 3 7 8	W_0
1 25 22 23 13 26 12 7 28 21 4 29 11 17 15 6 9 8 18 5 19 24 3 10 27 2 20 14 16	W_0
2 1 8 12 25 15 18 3 13 22 17 4 9 28 6 29 11 7 21 27 19 10 26 24 5 23 20 14 16	G_2/s
2 8 26 18 25 15 16 19 28 24 12 7 23 9 29 27 21 3 11 4 14 13 10 1 5 17 22 6 20	W_2
2 23 1 7 5 19 29 24 20 9 3 15 22 10 12 21 14 18 17 4 26 11 27 28 25 8 13 16 6	G_2
2 28 10 1 25 18 22 20 23 9 27 29 7 13 12 26 3 8 19 14 11 21 6 15 5 24 16 17 4	G_2
3 9 20 17 25 12 27 13 7 16 28 1 24 29 18 6 8 22 26 21 19 2 23 15 5 4 14 10 11	G_2
3 11 1 10 25 19 14 16 20 4 2 15 27 7 12 8 29 18 6 9 26 23 22 28 5 21 13 24 17	G_2/s
3 21 23 22 8 15 26 6 16 11 28 5 2 18 10 14 12 13 27 20 9 29 19 24 7 1 4 17 25	RW_0
4 12 25 28 22 5 10 29 20 9 2 16 17 15 19 11 27 24 1 18 13 23 3 14 21 7 6 8 26	RW_0
4 26 20 17 5 6 14 10 1 3 9 13 29 11 24 22 21 16 23 28 7 27 12 15 25 18 2 19 8	G_2
6 19 12 20 25 22 18 8 26 17 1 29 28 9 24 13 14 16 2 11 23 3 7 10 5 27 4 21 15	W_2
6 26 23 28 5 8 27 1 16 14 7 18 4 21 12 20 2 15 3 9 10 24 19 29 25 17 11 13 22	G_2/s
7 13 2 17 5 27 28 21 8 6 20 15 19 22 1 24 18 29 14 26 4 3 10 23 25 11 16 12 9	W_2
7 20 28 8 25 15 1 4 23 27 22 14 16 12 6 13 18 17 26 2 29 11 9 24 5 19 10 3 21	G_2/s
8 22 10 19 25 12 28 20 17 21 3 11 13 7 18 14 27 2 1 26 29 9 24 15 5 6 4 23 16	G_2
10 27 28 8 5 3 12 18 22 4 23 15 20 13 29 19 2 1 21 24 26 17 11 7 25 6 14 9 16	W_2

TABLE 2. The lexicographically minimal polymorphs of Costas permutations of order 29, shown along with the method producing them. A "/s" indicates the EC is symmetric.

What happens when $f_n - f_{n-1} \neq \dfrac{1}{t_b}$?

{4 7 1 6 5 2 3}

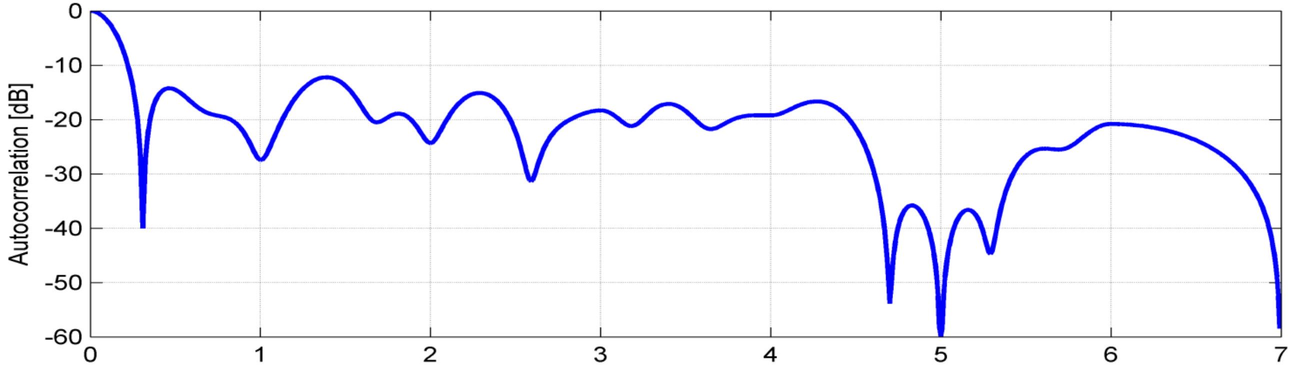

$$f_n - f_{n-1} = \frac{1}{2t_b}$$

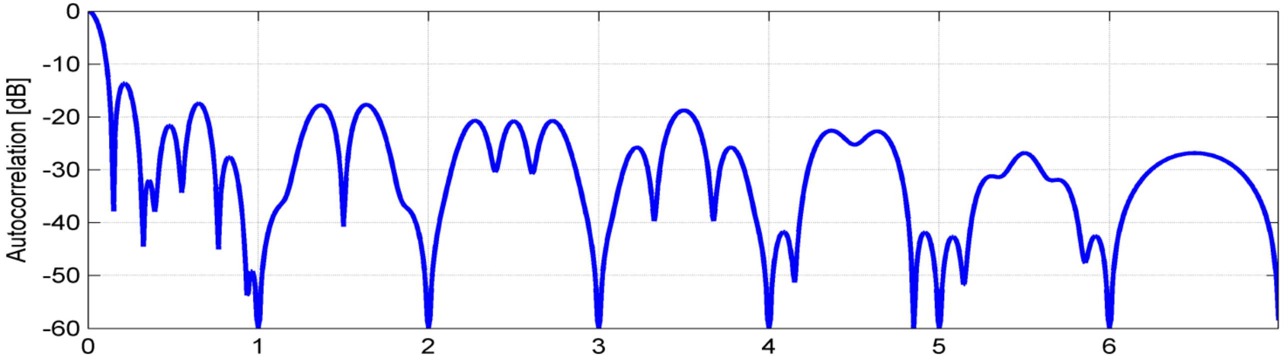

$$f_n - f_{n-1} = \frac{1}{t_b}$$

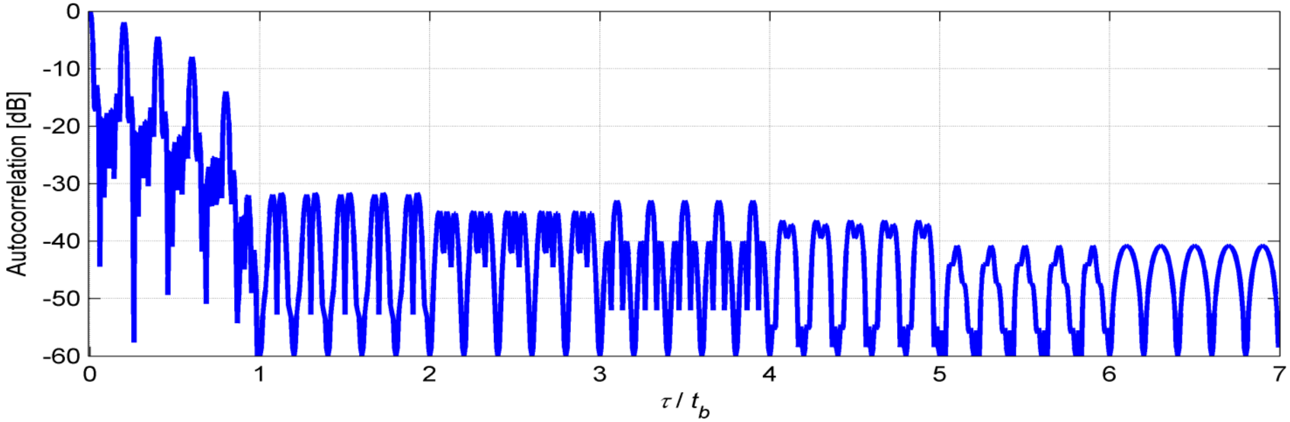

$$f_n - f_{n-1} = \frac{5}{t_b}$$

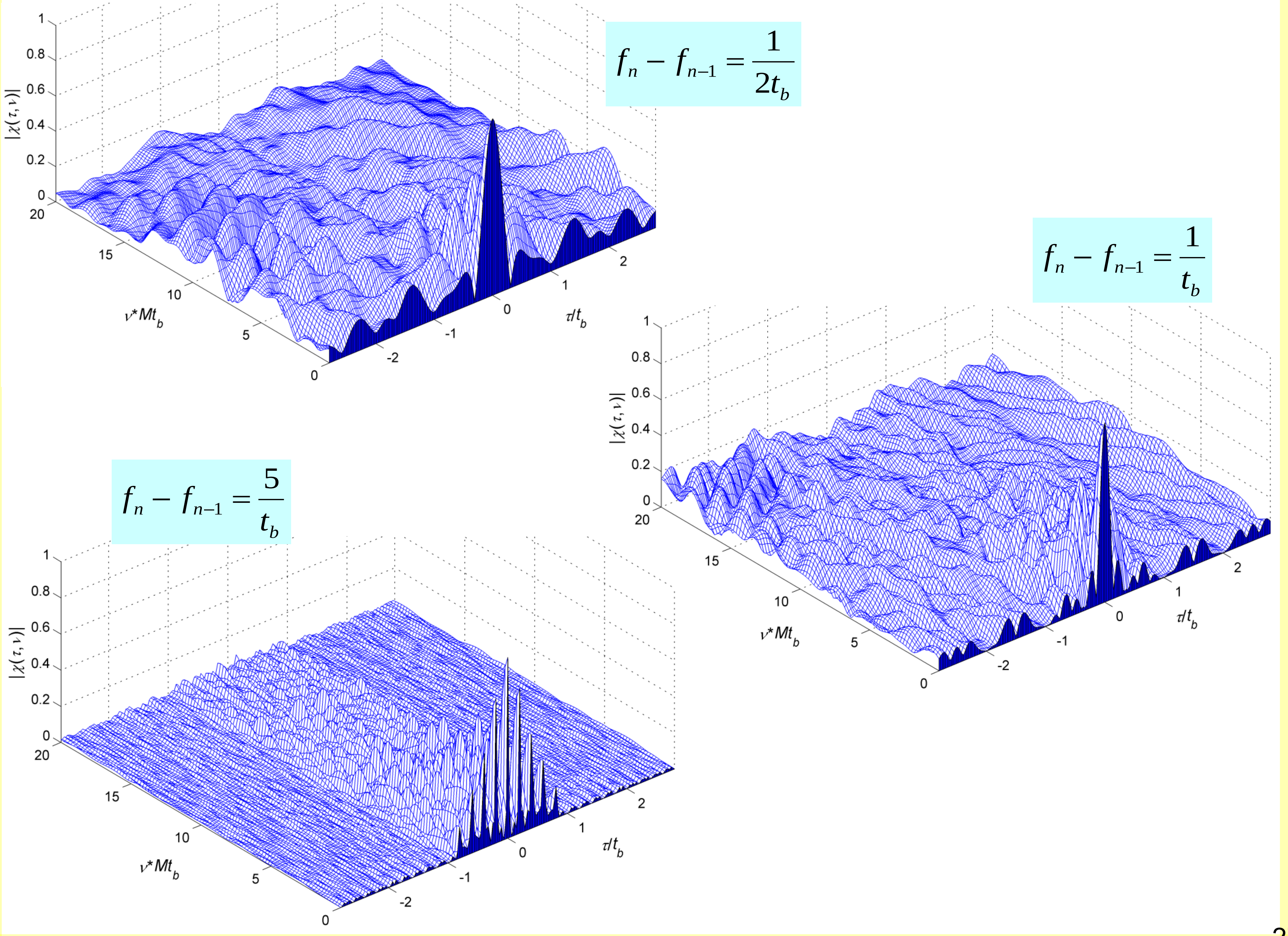

$$f_n - f_{n-1} = \frac{1}{2t_b}$$

$$f_n - f_{n-1} = \frac{1}{t_b}$$

$$f_n - f_{n-1} = \frac{5}{t_b}$$

Tentative use of modified Costas waveforms in GESTRA radar

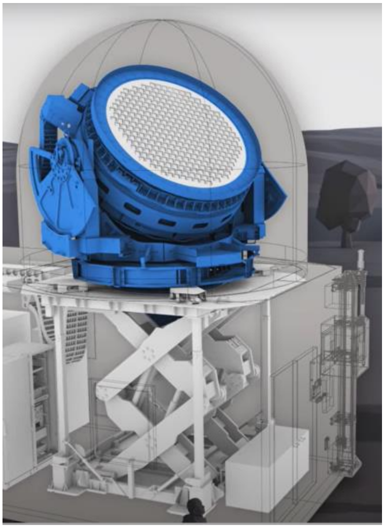

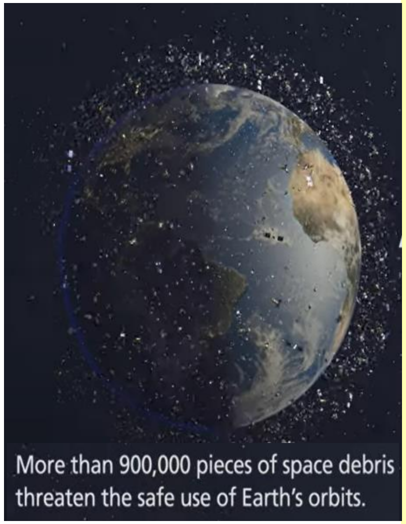

More than 900,000 pieces of space debris threaten the safe use of Earth's orbits.

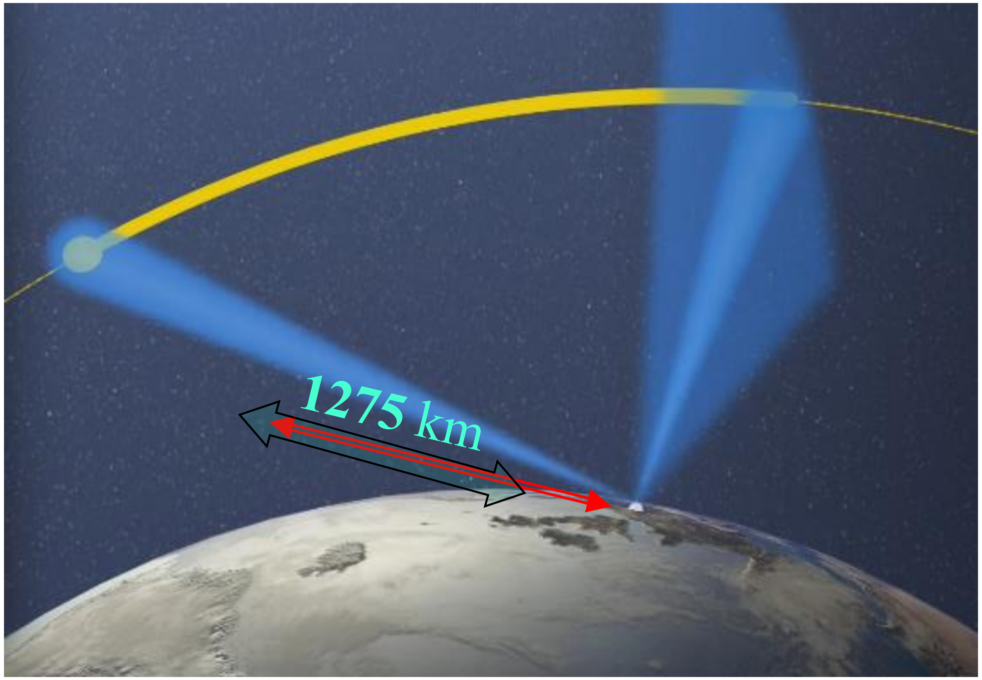

Maximum target range = 3000 km
maximum range-rate = 7 km/s
$\boldsymbol{t_p}$ = Pulse width = 0.0085 s (8.5 msec)

$$\therefore\ ct_p/2 = 1275\,\text{km}$$

$$f_c = 1.33\,\text{GHz}\ ,\ BW = 2\,\text{MHz}$$

$$t_p = 8.5\,\text{msec}$$

$$M \approx 130 \Rightarrow \text{pulse compression} = M^2 = 16900$$

$$\text{Delay resolution} = \Delta R = ct_p/\left(2M^2\right) = 75\text{m}$$

$$\text{Range-rate resolution} = \Delta\dot{R} = c/\left(2\,f_c\,t_p\right) = 13\,\text{m/s}$$

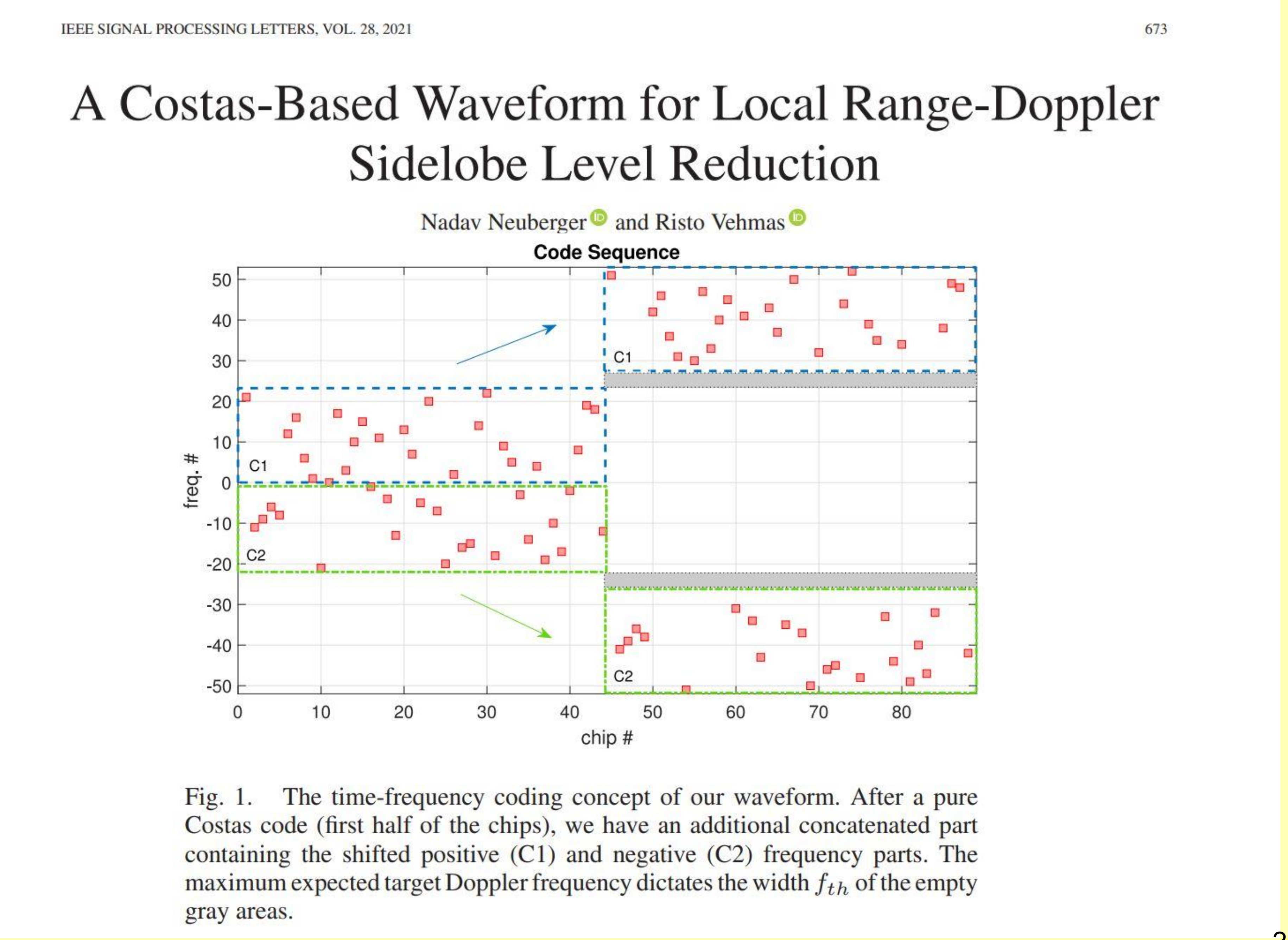

IEEE SIGNAL PROCESSING LETTERS, VOL. 28, 2021 673

A Costas-Based Waveform for Local Range-Doppler Sidelobe Level Reduction

Nadav Neuberger and Risto Vehmas

Fig. 1. The time-frequency coding concept of our waveform. After a pure Costas code (first half of the chips), we have an additional concatenated part containing the shifted positive (C1) and negative (C2) frequency parts. The maximum expected target Doppler frequency dictates the width f_{th} of the empty gray areas.

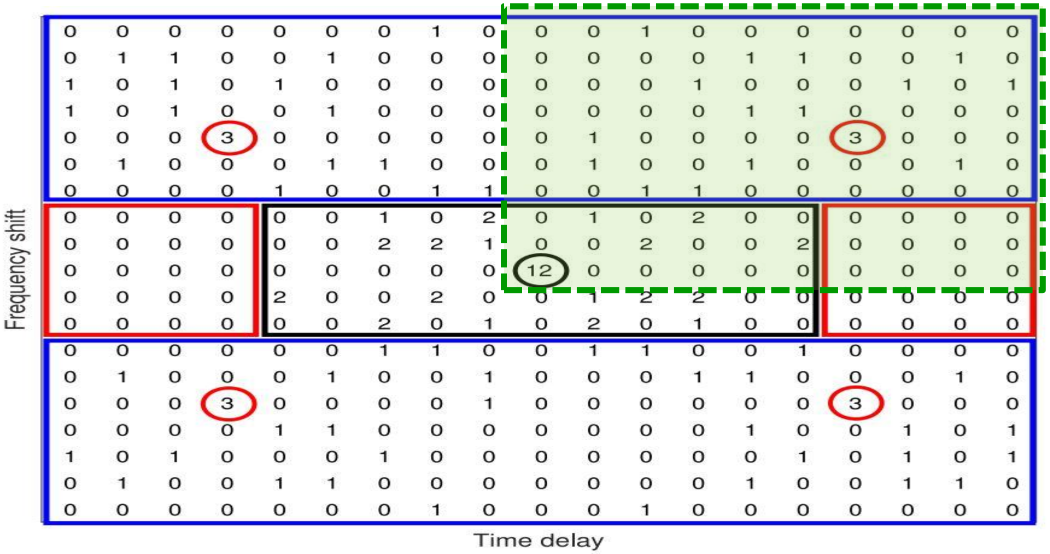

0	0	0	0	0	0	0	1	0	0	0	1	0	0	0	0	0	0	0
0	1	1	0	0	1	0	0	0	0	0	0	0	1	1	0	0	1	0
1	0	1	0	1	0	0	0	0	0	0	0	1	0	0	0	1	0	1
1	0	1	0	0	1	0	0	0	0	0	0	0	1	1	0	0	0	0
0	0	0	3	0	0	0	0	0	0	1	0	0	0	0	3	0	0	0
0	1	0	0	0	1	1	0	0	0	1	0	0	1	0	0	0	1	0
0	0	0	0	1	0	0	1	1	0	0	1	1	0	0	0	0	0	0
0	0	0	0	0	0	1	0	2	0	1	0	2	0	0	0	0	0	0
0	0	0	0	0	0	2	2	1	0	0	2	0	0	2	0	0	0	0
0	0	0	0	0	0	0	0	0	12	0	0	0	0	0	0	0	0	0
0	0	0	0	2	0	0	2	0	0	1	2	2	0	0	0	0	0	0
0	0	0	0	0	0	2	0	1	0	2	0	1	0	0	0	0	0	0
0	0	0	0	0	0	1	1	0	0	1	1	0	0	1	0	0	0	0
0	1	0	0	0	1	0	0	1	0	0	0	1	1	0	0	0	1	0
0	0	0	3	0	0	0	0	1	0	0	0	0	0	0	3	0	0	0
0	0	0	0	1	1	0	0	0	0	0	0	0	1	0	0	1	0	1
1	0	1	0	0	0	1	0	0	0	0	0	0	0	1	0	1	0	1
0	1	0	0	1	1	0	0	0	0	0	0	0	1	0	0	1	1	0
0	0	0	0	0	0	0	1	0	0	0	1	0	0	0	0	0	0	0

Fig. 2. The DAF of our waveform for code length $M = 12$. The area A^c is

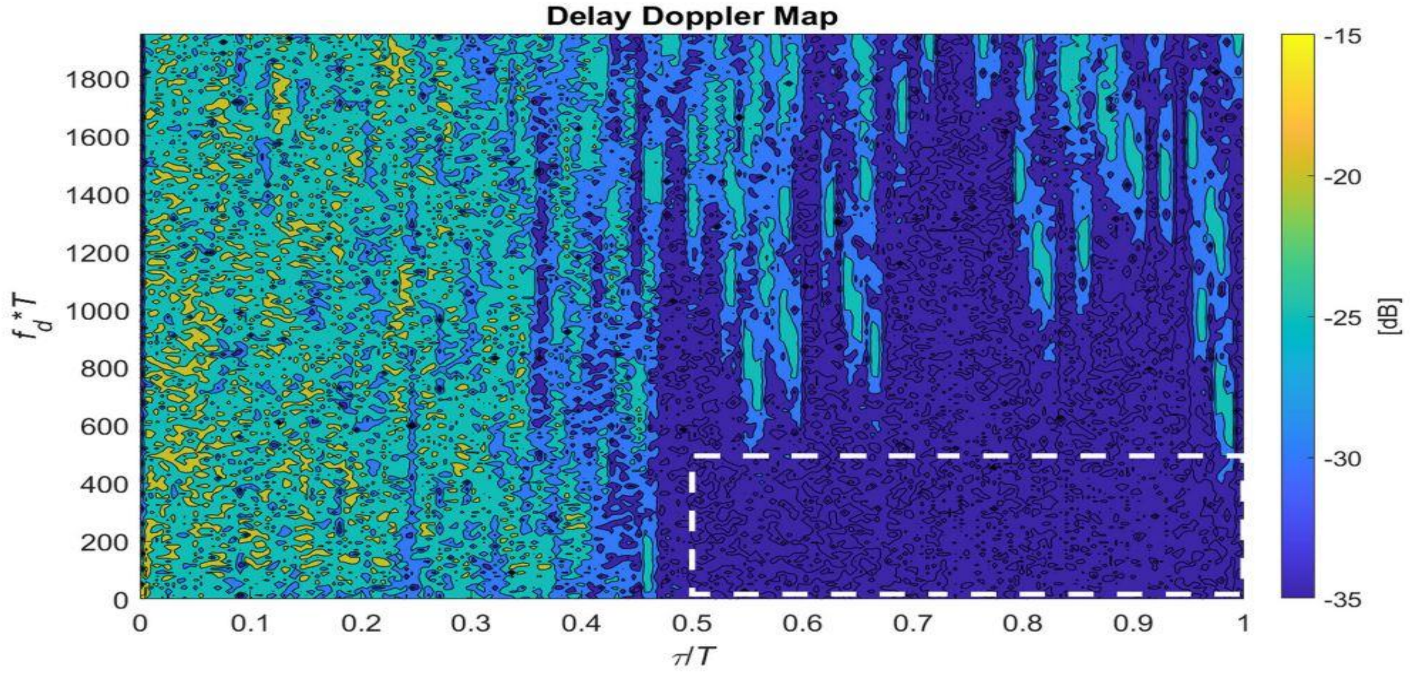

AF of a modified Costas pulse, $M = 100$

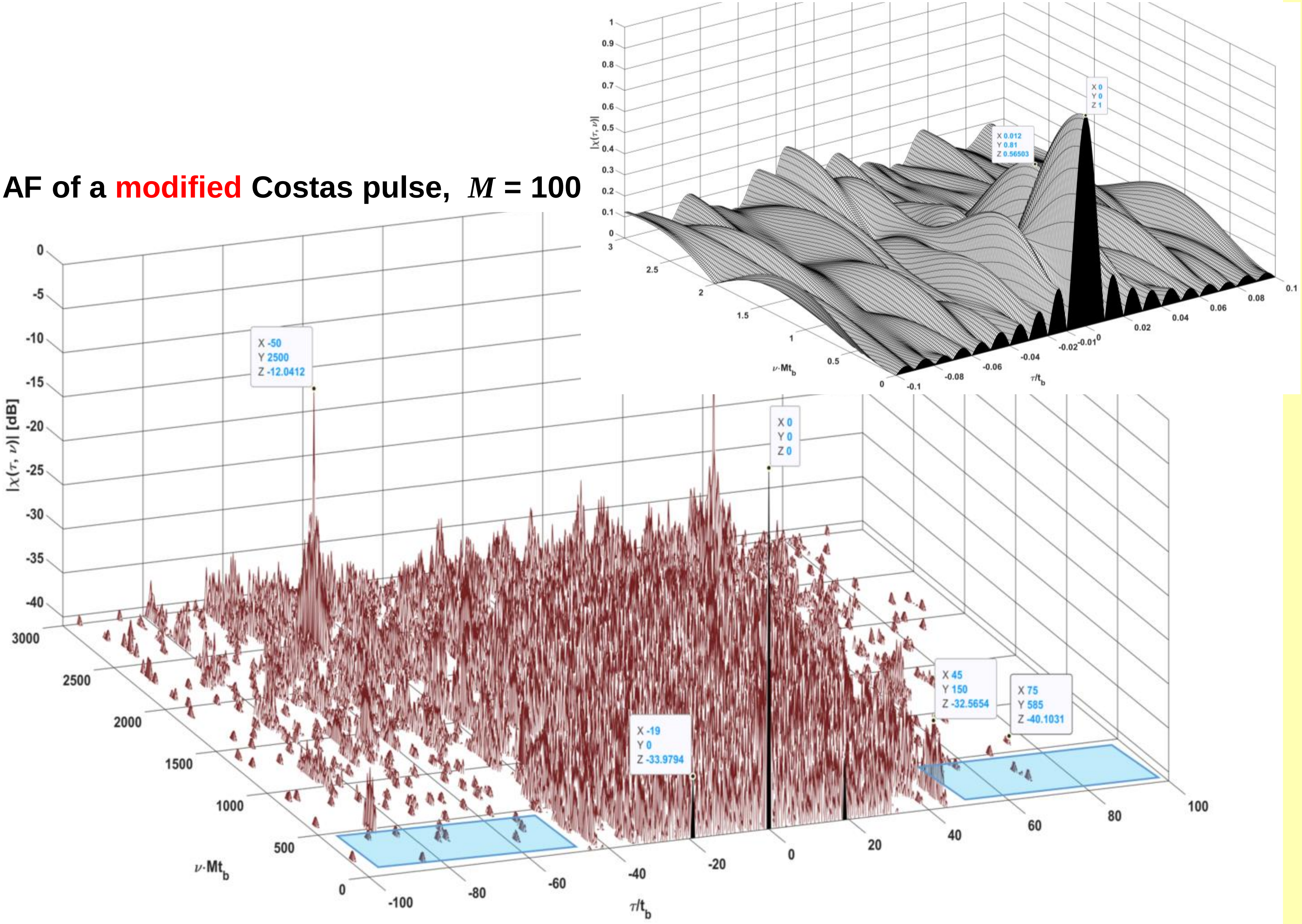

PHASE CODING, Code Comparison

- Bi-phase codes (bi-polar, binary)
  - easy to implement
  - can achieve significant range sidelobe reduction
  - thumbtack AF (Doppler intolerant)

- Poly-phase codes
  - typically higher range sidelobes than bi-phase
  - ridge-type AF (Doppler tolerant)

Bi-phase:

- Barker
- MPSL

Poly-phase:

- Frank
- P3 and P4
- P(n,k)

$$u(t) = \frac{1}{\sqrt{Nt_b}} \sum_{n=0}^{N-1} u_n\left(t - nt_b\right)$$

$$u_n(t) = \begin{cases} \exp\left(j\phi_n\right); & 0 \le t \le t_b \\ 0 \ ; & \text{elsewhere} \end{cases}$$

Binary code

The phase of the RF carrier switches between two values 180^0 degrees apart. Can be describe by a sequence of ±1's

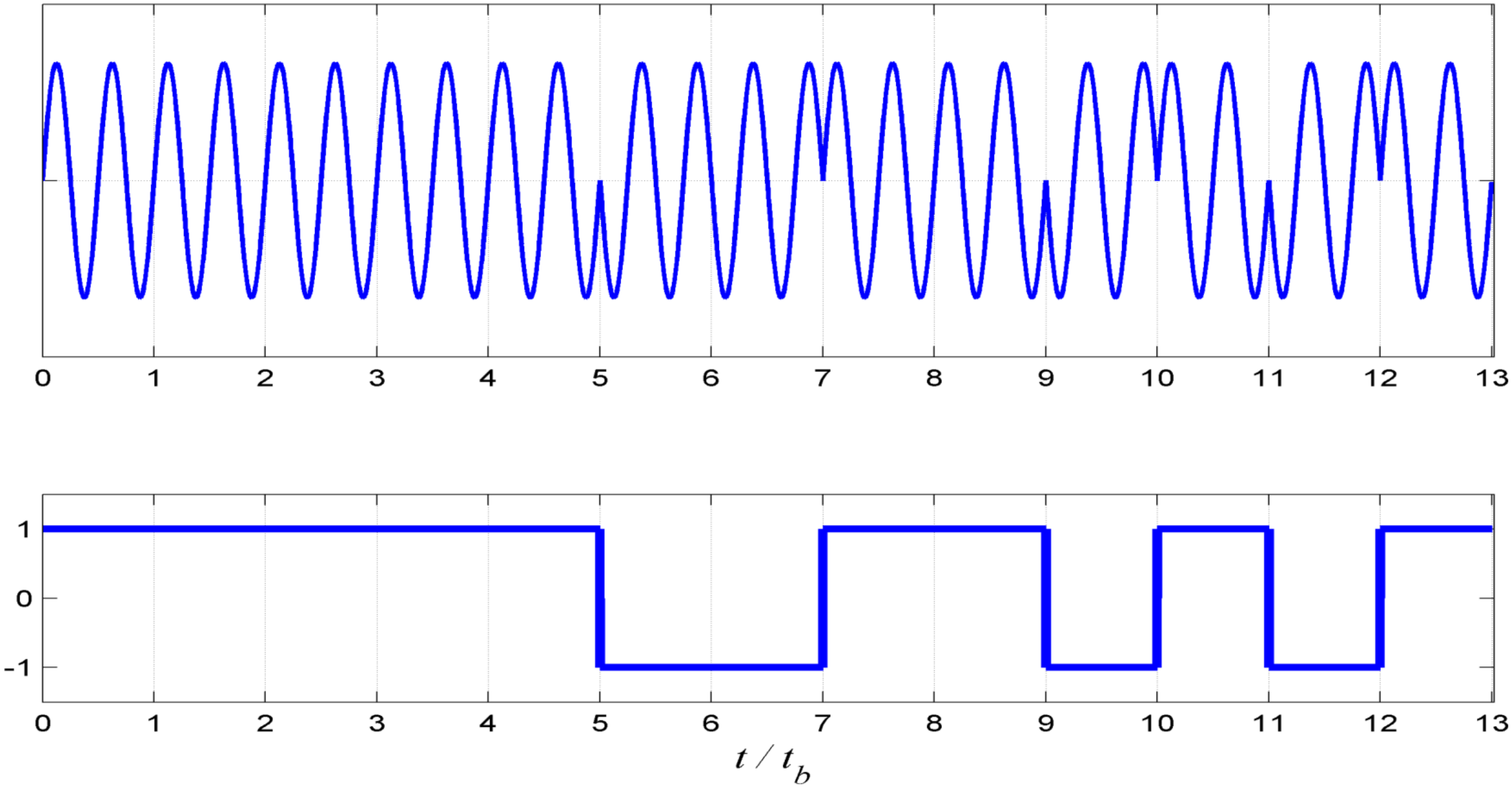

Barker codes: Magnitude of ACF sidelobes ≤ 1/N

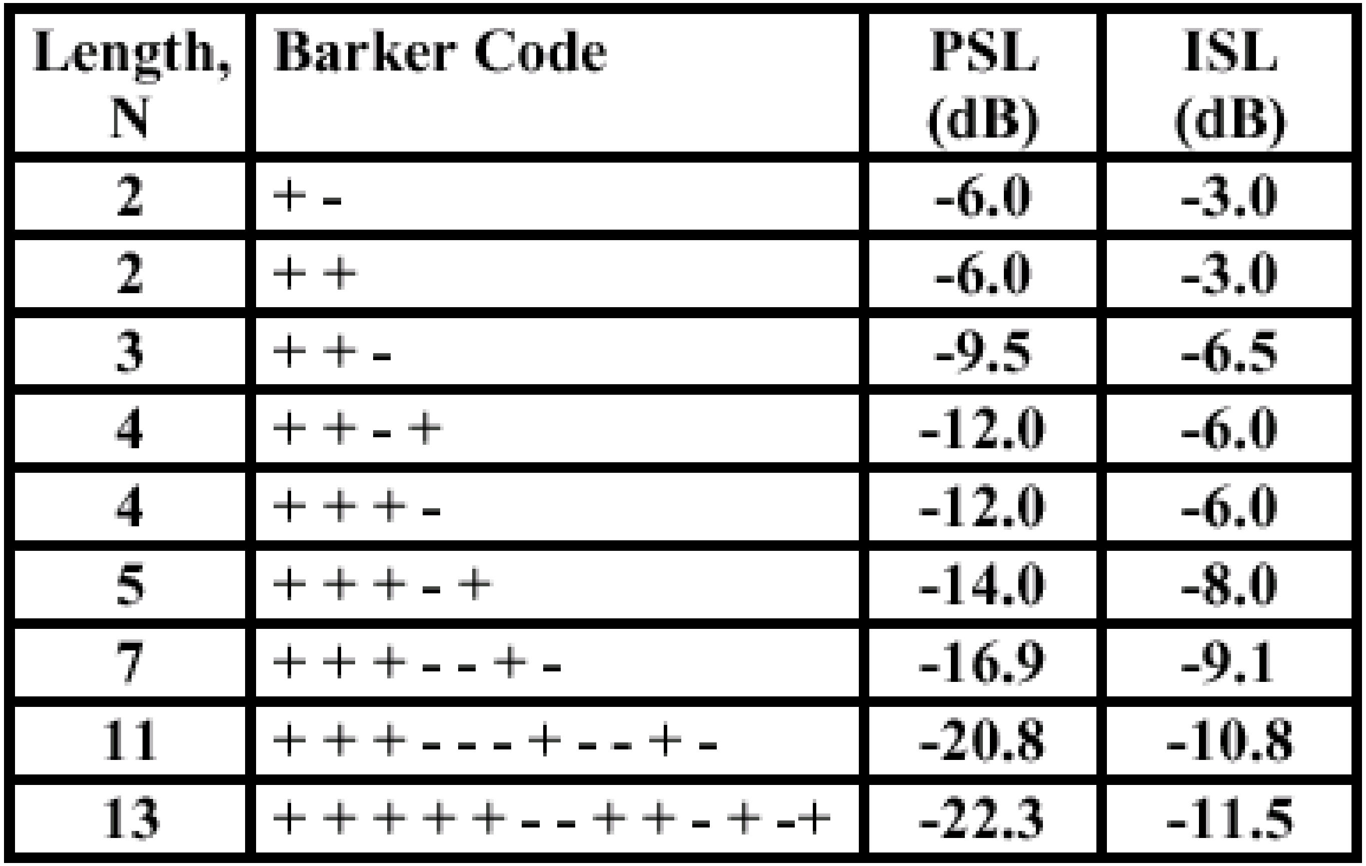

Length, N	Barker Code	PSL (dB)	ISL (dB)
2	+ -	-6.0	-3.0
2	+ +	-6.0	-3.0
3	+ + -	-9.5	-6.5
4	+ + - +	-12.0	-6.0
4	+ + + -	-12.0	-6.0
5	+ + + - +	-14.0	-8.0
7	+ + + - - + -	-16.9	-9.1
11	+ + + - - - + - - + -	-20.8	-10.8
13	+ + + + + - - + + - + -+	-22.3	-11.5

Barker 13

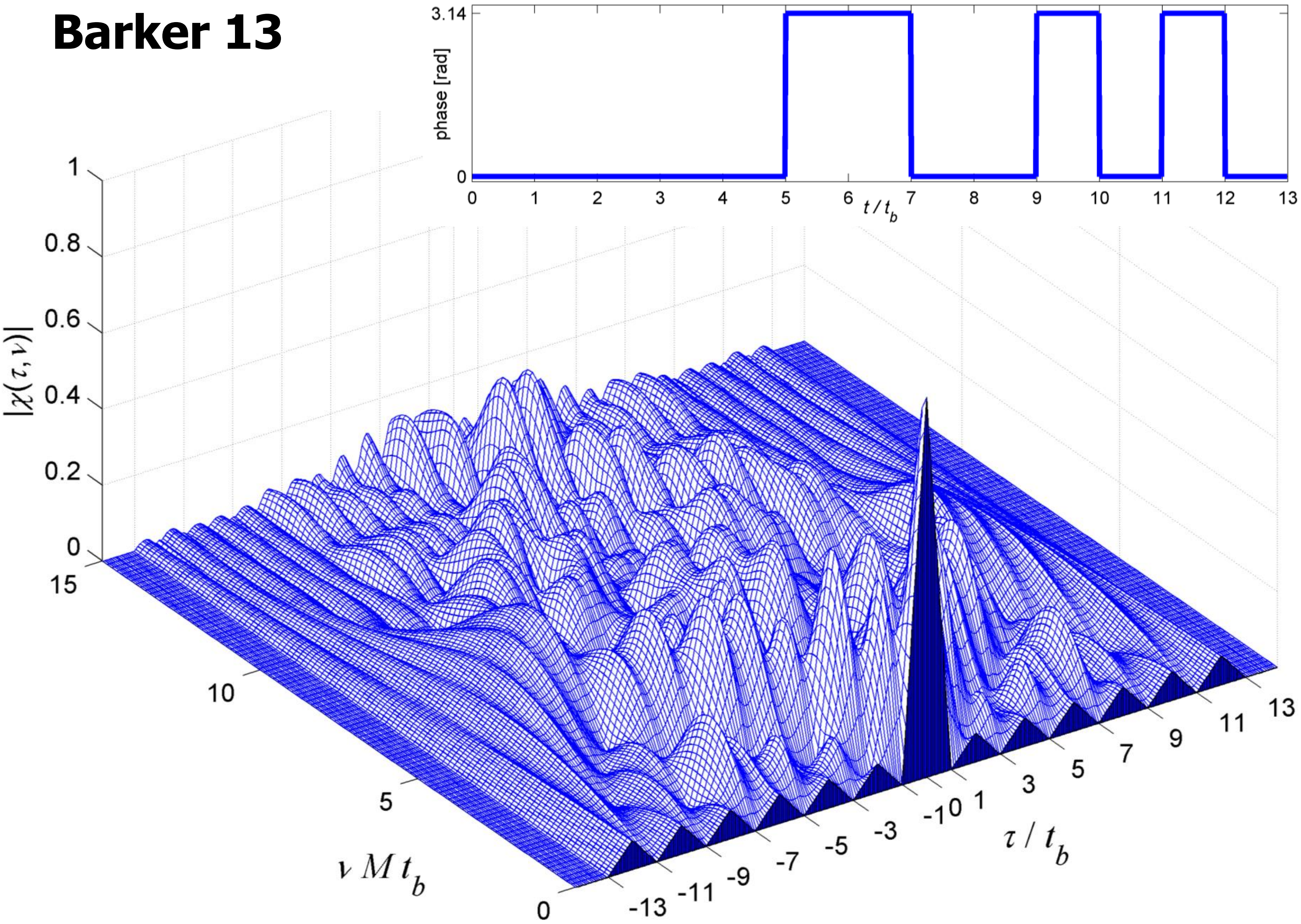
3.14
phase [rad]
0
0 1 2 3 4 5 6 7 8 9 10 11 12 13
t / t_b
1
0.8
0.6
0.4
0.2
0
$|\chi(\tau,\nu)|$
15
10
5
0
$\nu M t_b$
-13 -11 -9 -7 -5 -3 -1 0 1 3 5 7 9 11 13
τ / t_b

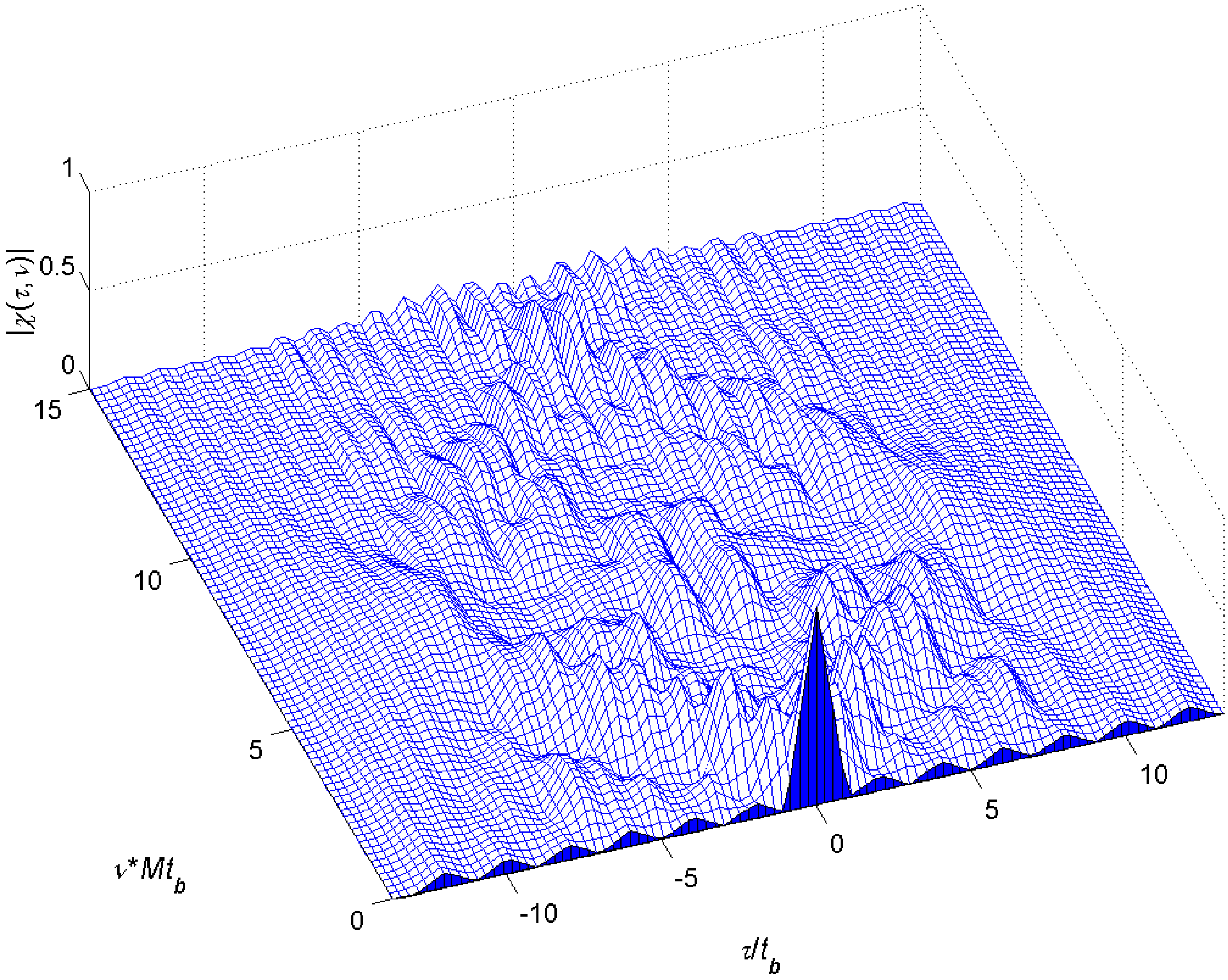
1
0.5
0
$|\chi(\tau,\nu)|$
15
10
5
0
ν*Mt_b
-10
-5
0
5
10
τ/t_b

Ambiguity function of the 13-element Barker code showing some of the area where the range-Doppler sidelobes exceed 1/13

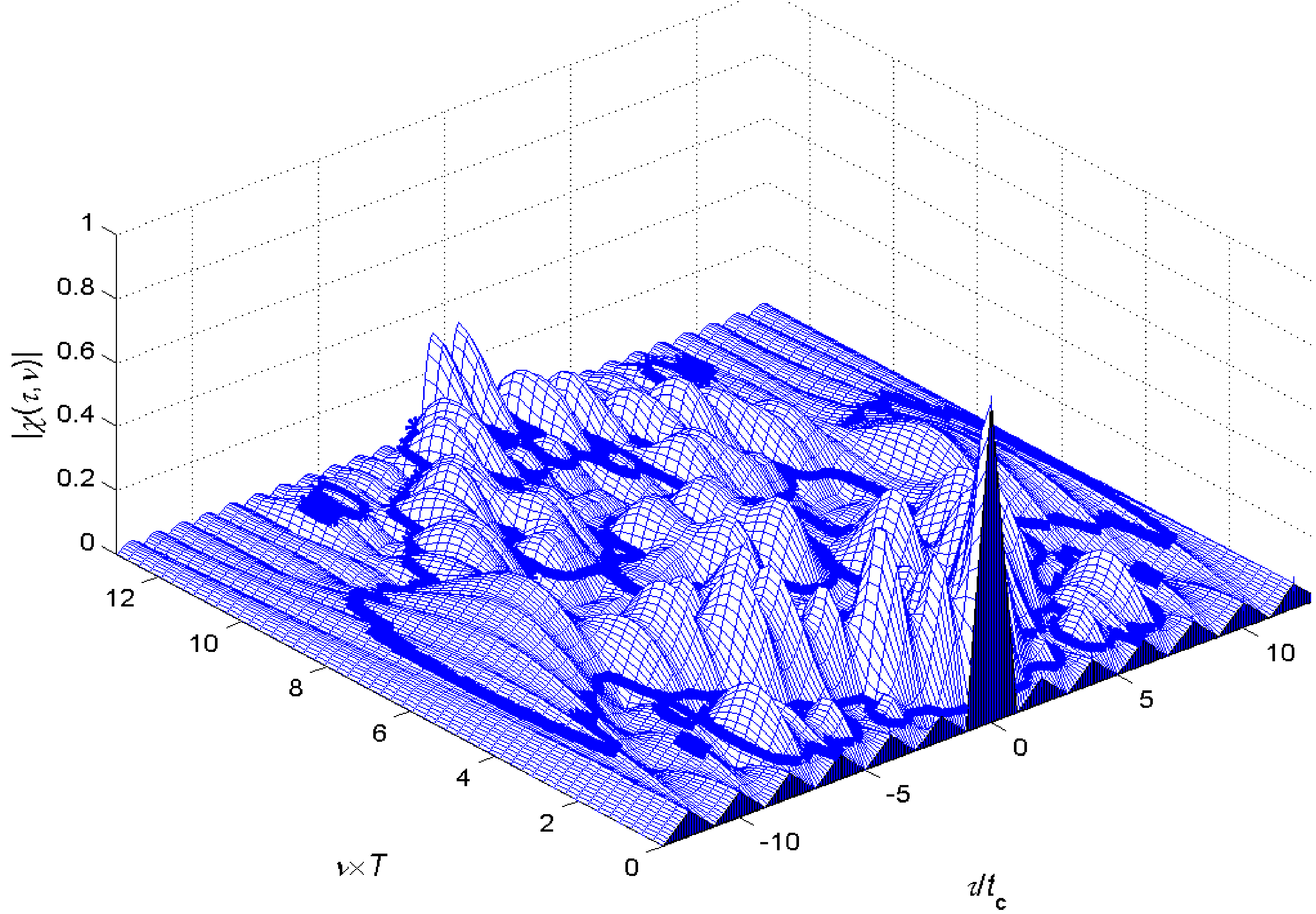

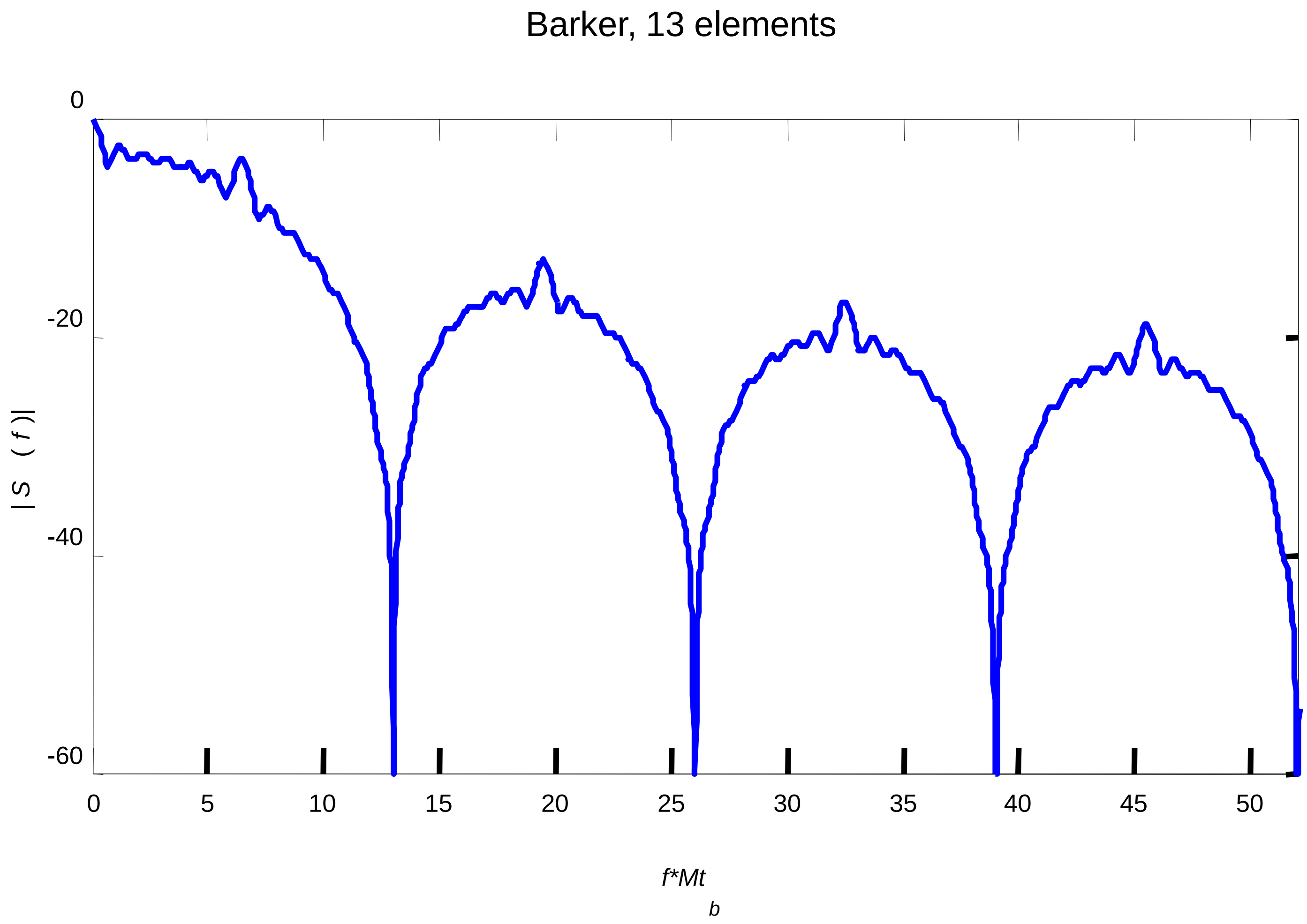
Barker, 13 elements
0
-20
-40
-60
|S (f)|
0
5
10
15
20
25
30
35
40
45
50
f*Mt
b

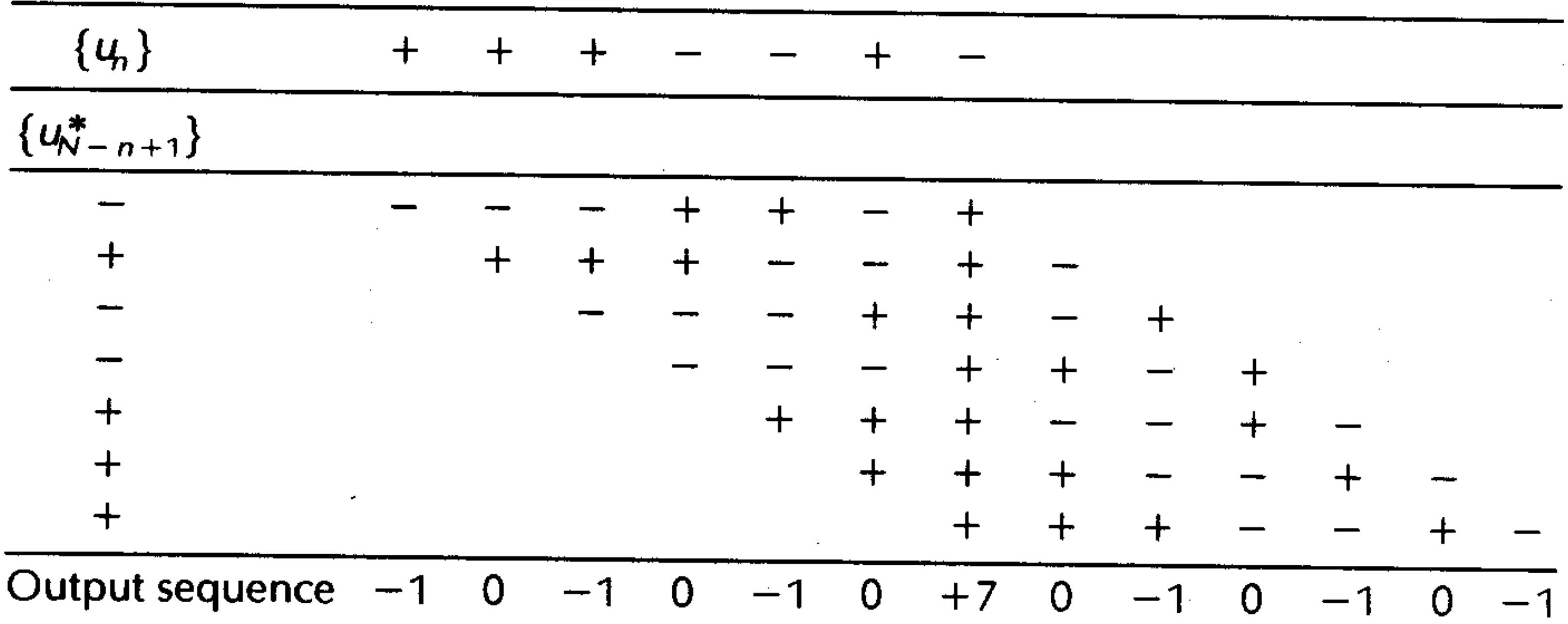

Table 8.3 The Autocorrelation Sequence of a Barker Code of Length 7

$\{u_n\}$	+	+	+	−	−	+	−						
$\{u^*_{N-n+1}\}$													
−	−	−	−	+	+	−	+						
+		+	+	+	−	−	+	−					
−			−	−	−	+	+	−	+				
−				−	−	−	+	+	−	+			
+					+	+	+	−	−	+	−		
+						+	+	+	−	−	+	−	
+							+	+	+	−	−	+	−
Output sequence	−1	0	−1	0	−1	0	+7	0	−1	0	−1	0	−1

The Search For Longer Codes

- The limited number of chips associated with Barker phase codes has led to the search for longer codes in order to increase the pulse compression gain.
- Combining Barker codes is one example of extending the code length. For example,

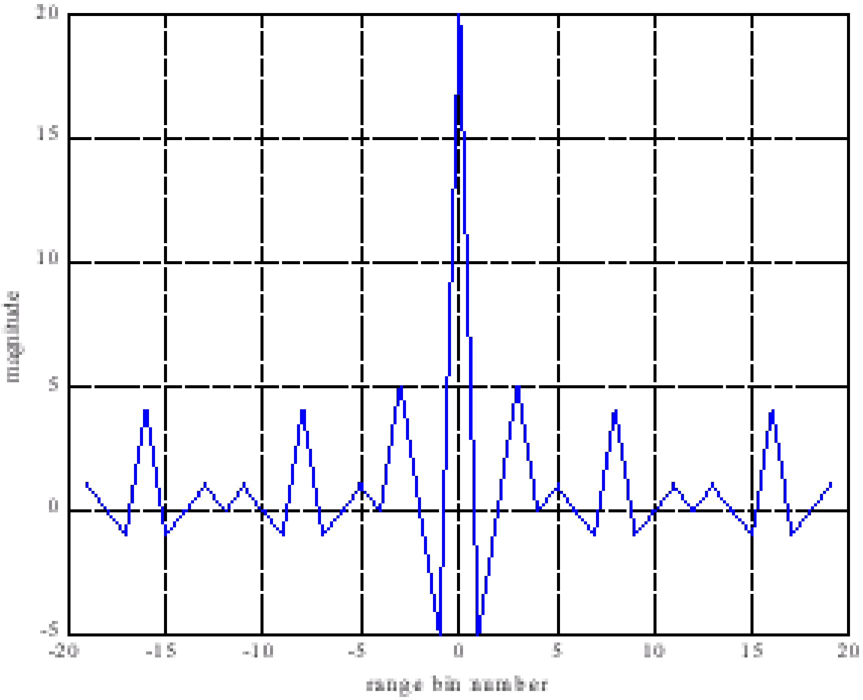

5 Bit Barker : + + + - +

4 Bit Barker: + + - +

Combined Code: + + - + + + - + + + - + - - + - + + - +

1 1 1 1 1 -1 -1 1 1 -1 1 -1 1 1 1 1 1 1 -1 -1 1 1 -1 1 -1 1 -1 -1 -1 -1 -1 1 1 -1 -1 1 -1 1 -1

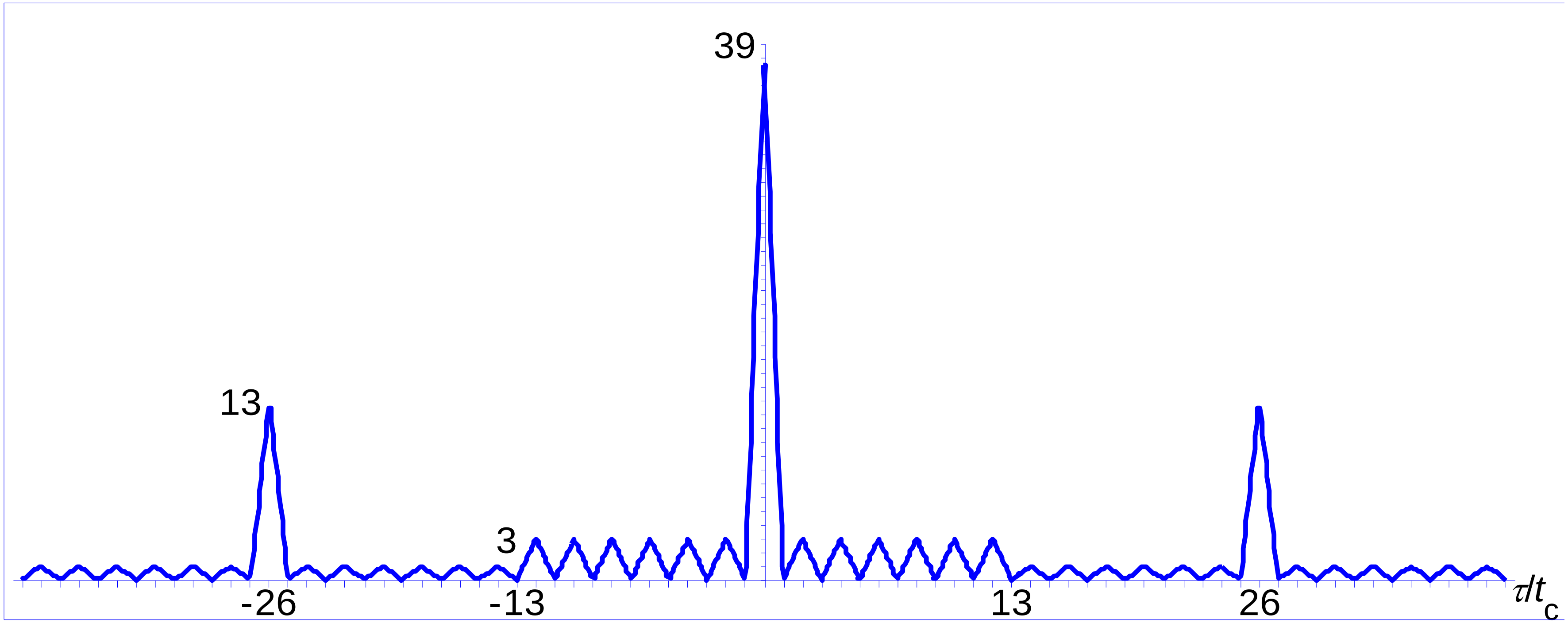

Autocorrelation function of the nested Barker 13 and Barker 3 code

Barker 13 nested in Barker 13

```
   1     1     1     1     1    -1    -1     1     1    -1     1    -1     1
   1     1     1     1     1    -1    -1     1     1    -1     1    -1     1
   1     1     1     1     1    -1    -1     1     1    -1     1    -1     1
   1     1     1     1     1    -1    -1     1     1    -1     1    -1     1
   1     1     1     1     1    -1    -1     1     1    -1     1    -1     1
  -1    -1    -1    -1    -1     1     1    -1    -1     1    -1     1    -1
  -1    -1    -1    -1    -1     1     1    -1    -1     1    -1     1    -1
   1     1     1     1     1    -1    -1     1     1    -1     1    -1     1
   1     1     1     1     1    -1    -1     1     1    -1     1    -1     1
  -1    -1    -1    -1    -1     1     1    -1    -1     1    -1     1    -1
   1     1     1     1     1    -1    -1     1     1    -1     1    -1     1
  -1    -1    -1    -1    -1     1     1    -1    -1     1    -1     1    -1
   1     1     1     1     1    -1    -1     1     1    -1     1    -1     1
```

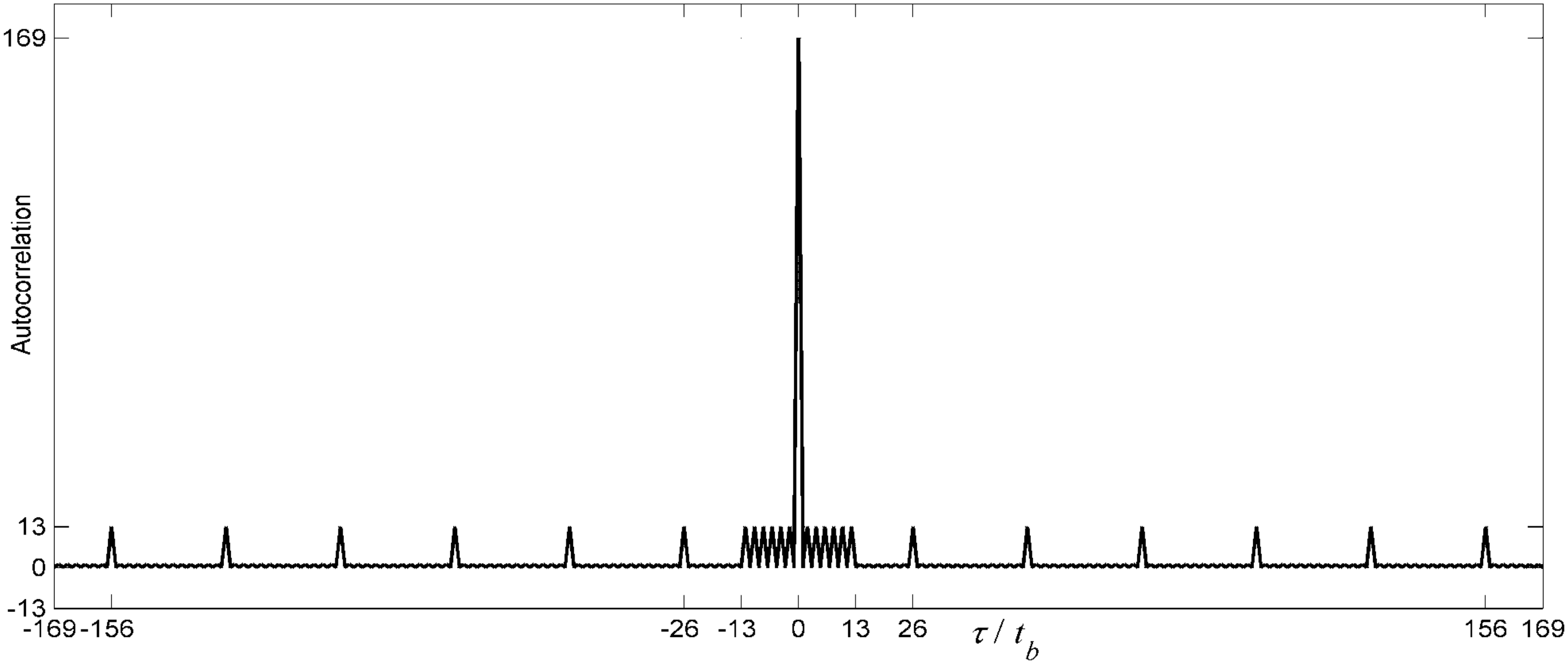

Good ISL, N = 169

```
  -1    -1    -1     1     1     1     1     1    -1    -1    -1     1     1
   1    -1    -1    -1    -1    -1     1     1     1    -1    -1     1     1
   1    -1     1     1     1    -1    -1    -1     1    -1    -1    -1     1
   1     1    -1    -1    -1     1    -1     1    -1    -1     1     1     1
  -1    -1    -1    -1    -1    -1    -1     1    -1     1     1     1     1
   1    -1     1    -1    -1    -1     1    -1    -1     1    -1     1    -1
  -1    -1    -1    -1    -1     1    -1    -1    -1     1    -1     1    -1
   1     1     1     1     1    -1    -1    -1     1    -1    -1    -1    -1
   1    -1     1    -1    -1    -1    -1     1    -1     1    -1     1    -1
  -1     1    -1    -1     1     1     1     1     1    -1     1     1    -1
   1     1    -1     1     1     1    -1     1     1    -1     1     1     1
  -1     1     1    -1    -1     1    -1    -1     1    -1     1    -1    -1
   1    -1    -1     1    -1    -1     1    -1     1    -1    -1     1    -1
```

Jedwab, Ferguson & Knauer,
Simon Fraser Univ., 2004

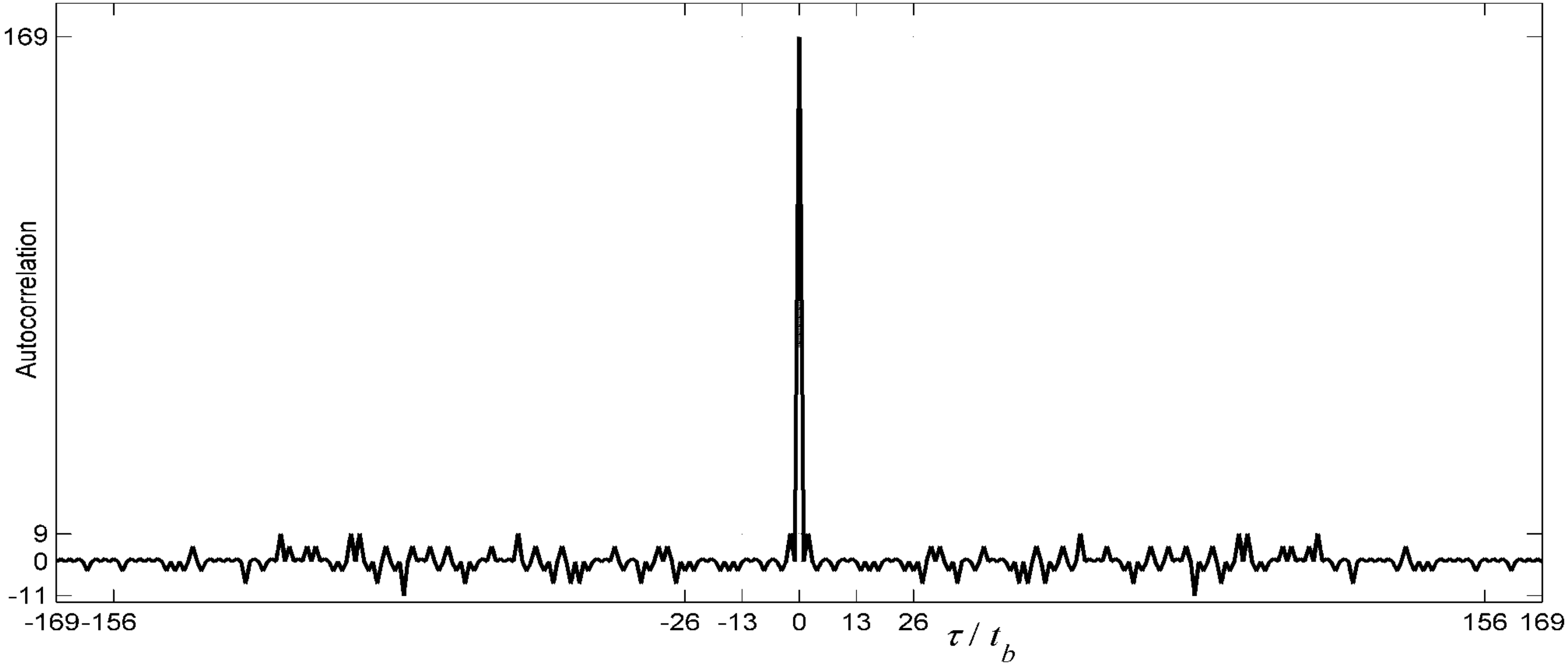

SKEW-SYMMETRY

Skew symmetric means one of the interleaved halves of a code is symmetric, the other anti-symmetric. For example with the 13 bit Barker:

1111100110101 = 1110111 interleaved with 110100.

One of Golay's papers pointed out how for most lengths, at least up to perhaps length 70, the maximum merit factor is achieved with skew symmetric sequences.

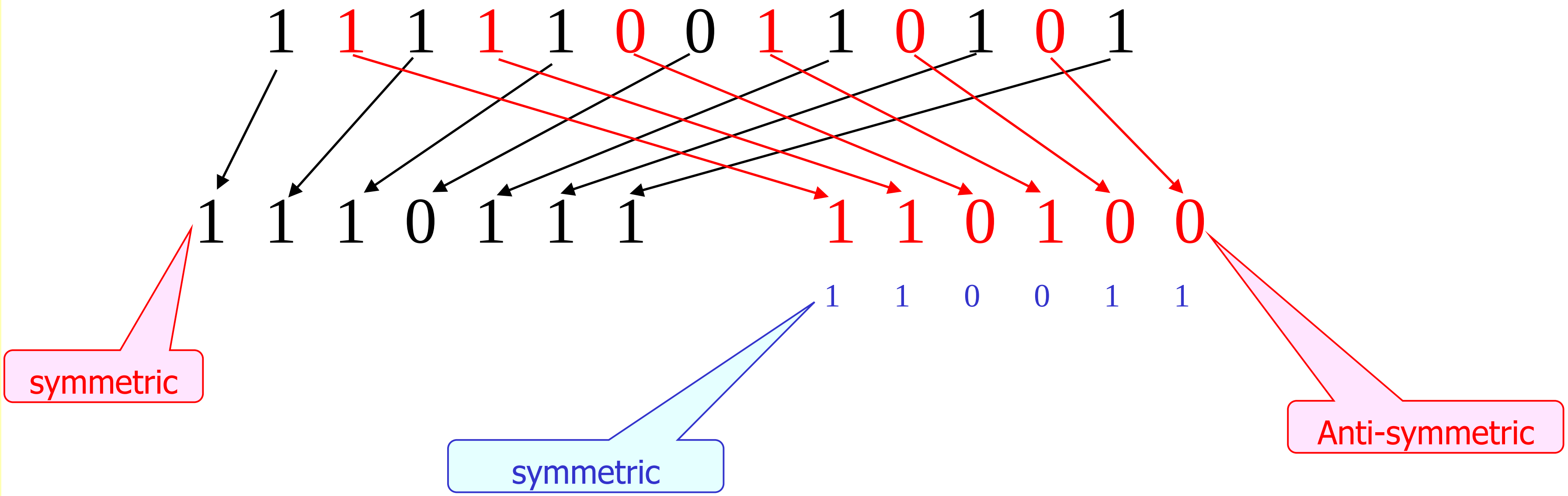

SKEW-SYMMETRY – another view

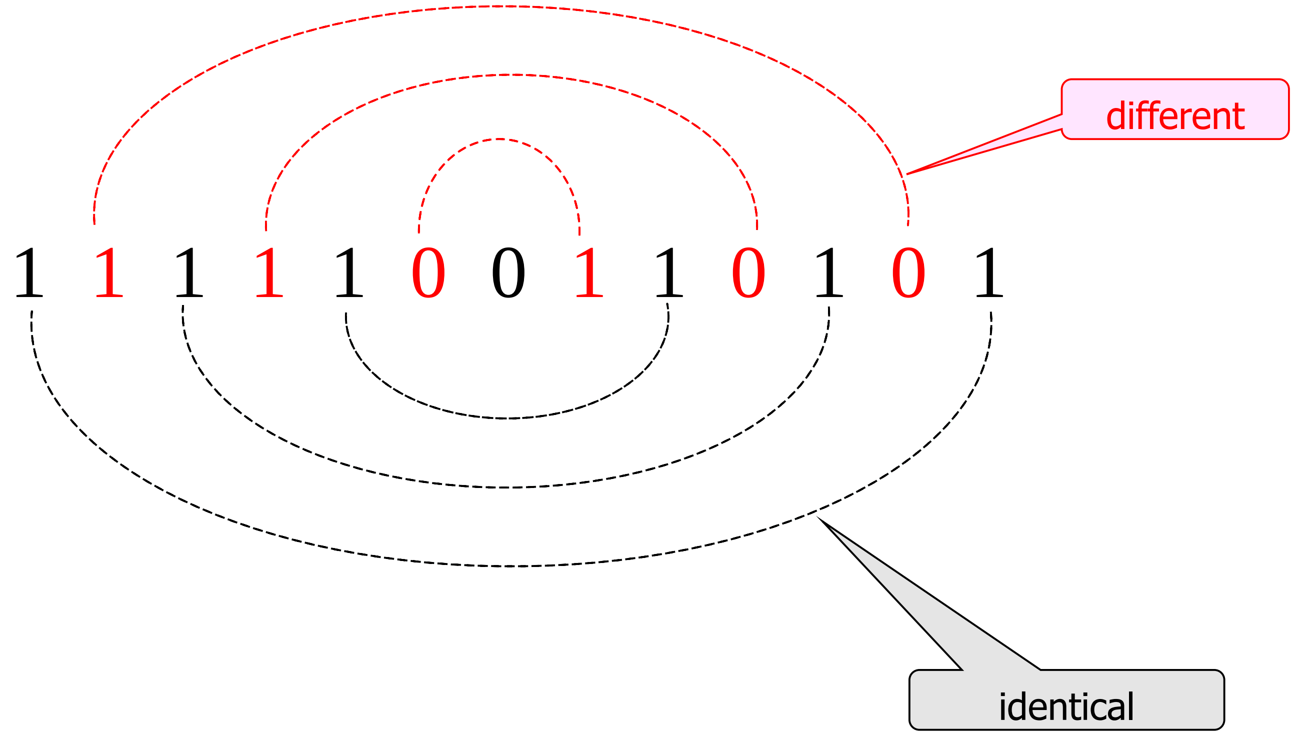

1 1 1 1 1 0 0 1 1 0 1 0 1

different

identical

Frank polyphase code

$$N = M^2$$

Constructed from the rows of an MxM array:

$$\phi_{p,q} = \frac{2\pi}{M}(p-1)(q-1) \quad , \quad p = 1,2,\ldots,M \ , \ q = 1,2,\ldots,M$$

$$N = 16$$

$$\begin{matrix} 0 & 0 & 0 & 0 \\ 0 & \frac{\pi}{2} & \pi & \frac{3\pi}{2} \\ 0 & \pi & 2\pi & 3\pi \\ 0 & \frac{3\pi}{2} & 3\pi & \frac{9\pi}{2} \end{matrix} \qquad \begin{matrix} 1 & 1 & 1 & 1 \\ 1 & \mathrm{j} & -1 & -\mathrm{j} \\ 1 & -1 & 1 & -1 \\ 1 & -\mathrm{j} & -1 & \mathrm{j} \end{matrix}$$

$$\phi_{p,q} \qquad\qquad u_{p,q} = \exp\left(j\phi_{p,q}\right)$$

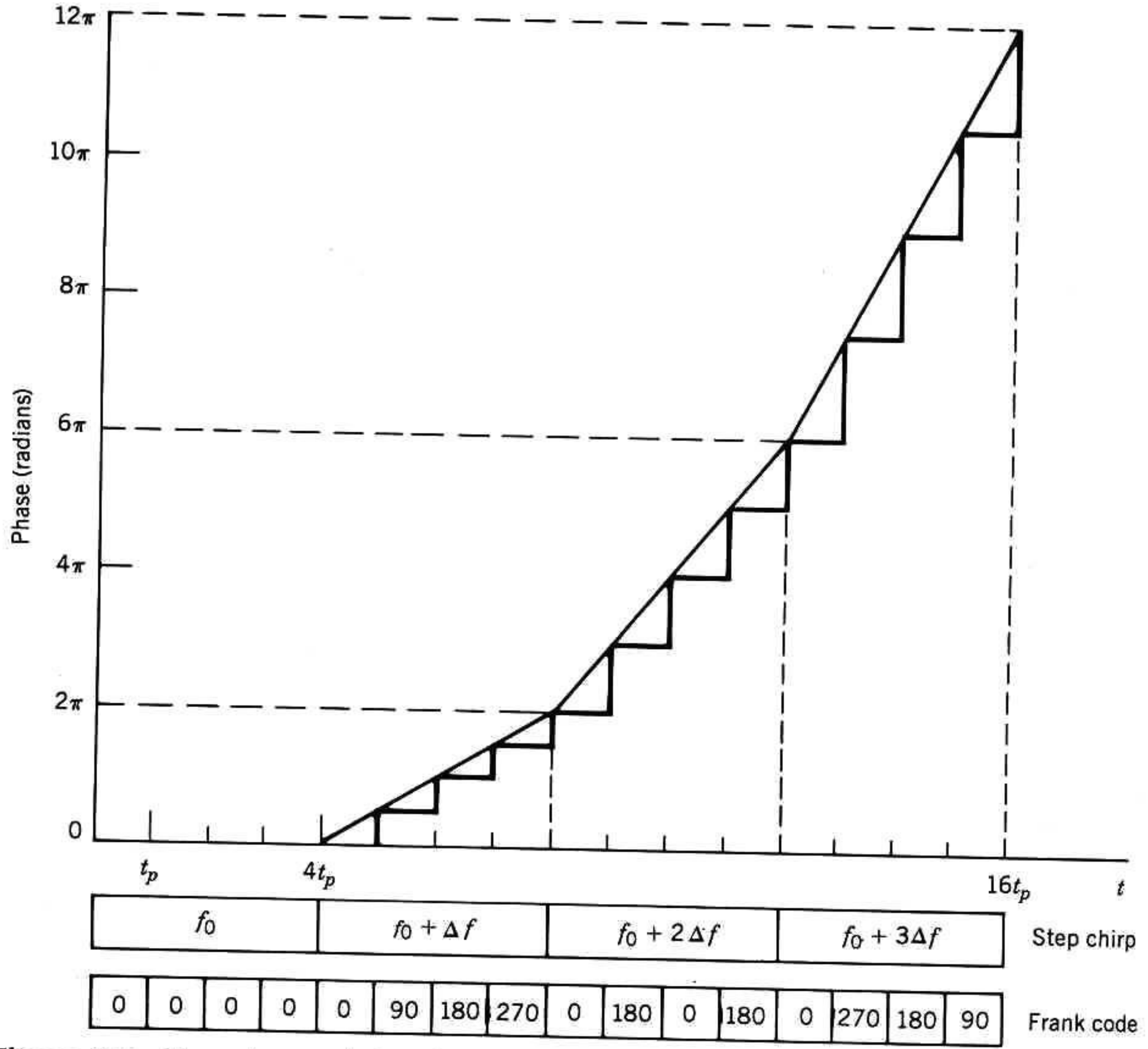

Figure 8.7 The phase relationship between quantized linear FM and Frank coded signals. (Source: F. F. Kretschmer, Jr. and B. L. Lewis, "Polyphase Pulse Compression Waveforms," Naval Research Laboratory Report 8540, 1982.)

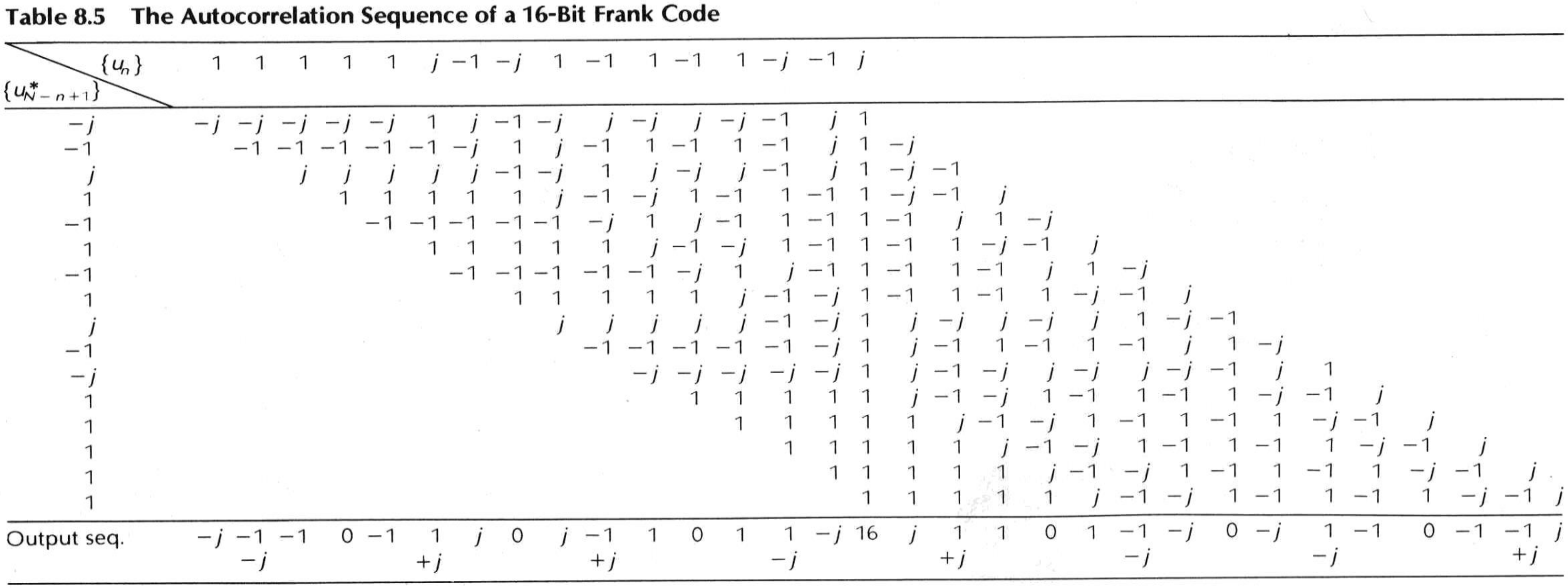

Table 8.5 The Autocorrelation Sequence of a 16-Bit Frank Code

$\{u_n\}$ $\{u^*_{N-n+1}\}$	1	1	1	1	1	j	-1	-j	1	-1	1	-1	1	-j	-1	j															
-j	-j	-j	-j	-j	-j	1	j	-1	-j	j	-j	j	-j	-1	j	1															
-1		-1	-1	-1	-1	-1	-j	1	j	-1	1	-1	1	-1	j	1	-j														
j			j	j	j	j	j	-1	-j	1	j	-j	j	-j	j	1	-j	-1													
1				1	1	1	1	1	j	-1	-j	1	-1	1	-1	1	-j	-1	j												
-1					-1	-1	-1	-1	-1	-j	1	j	-1	1	-1	1	-1	j	1	-j											
1						1	1	1	1	1	j	-1	-j	1	-1	1	-1	1	-j	-1	j										
-1							-1	-1	-1	-1	-1	-j	1	j	-1	1	-1	1	-1	j	1	-j									
1								1	1	1	1	1	j	-1	-j	1	-1	1	-1	1	-j	-1	j								
j									j	j	j	j	j	-1	-j	1	j	-j	j	-j	j	1	-j	-1							
-1										-1	-1	-1	-1	-1	-j	1	j	-1	1	-1	1	-1	j	1	-j						
-j											-j	-j	-j	-j	-j	1	j	-1	-j	j	-j	j	-j	-1	j	1					
1												1	1	1	1	1	j	-1	-j	1	-1	1	-1	1	-j	-1	j				
1													1	1	1	1	1	j	-1	-j	1	-1	1	-1	1	-j	-1	j			
1														1	1	1	1	1	j	-1	-j	1	-1	1	-1	1	-j	-1	j		
1															1	1	1	1	1	j	-1	-j	1	-1	1	-1	1	-j	-1	j	
1																1	1	1	1	1	j	-1	-j	1	-1	1	-1	1	-j	-1	j
Output seq.	-j	-1 -j	-1	0	-1	1 +j	j	0	j	-1 +j	1	0	1	1 -j	-j	16	j	1 +j	1	0	1	-1 -j	-j	0	-j	1 -j	-1	0	-1	-1 +j	j

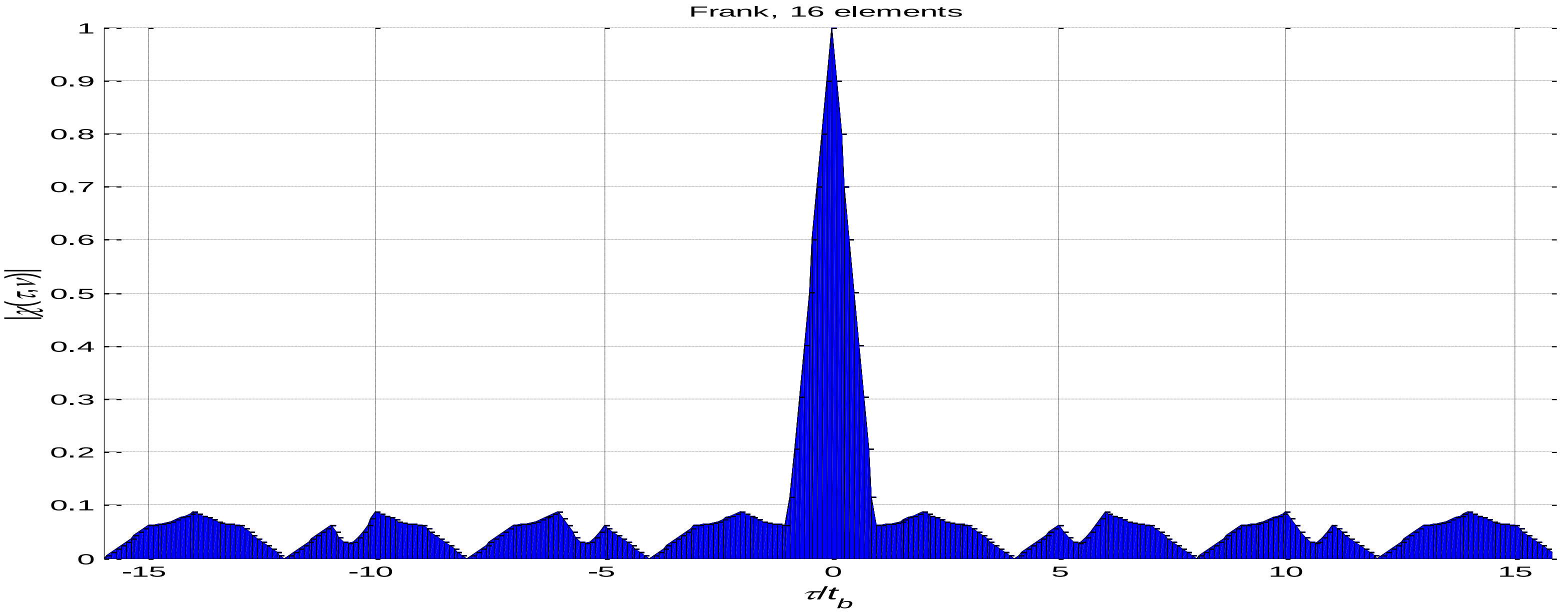

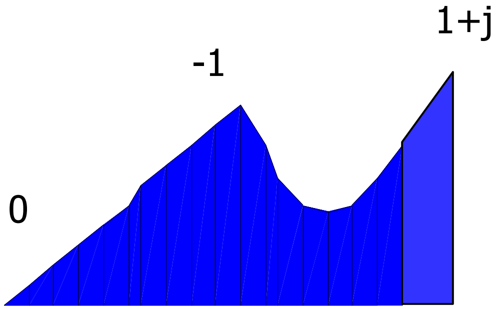

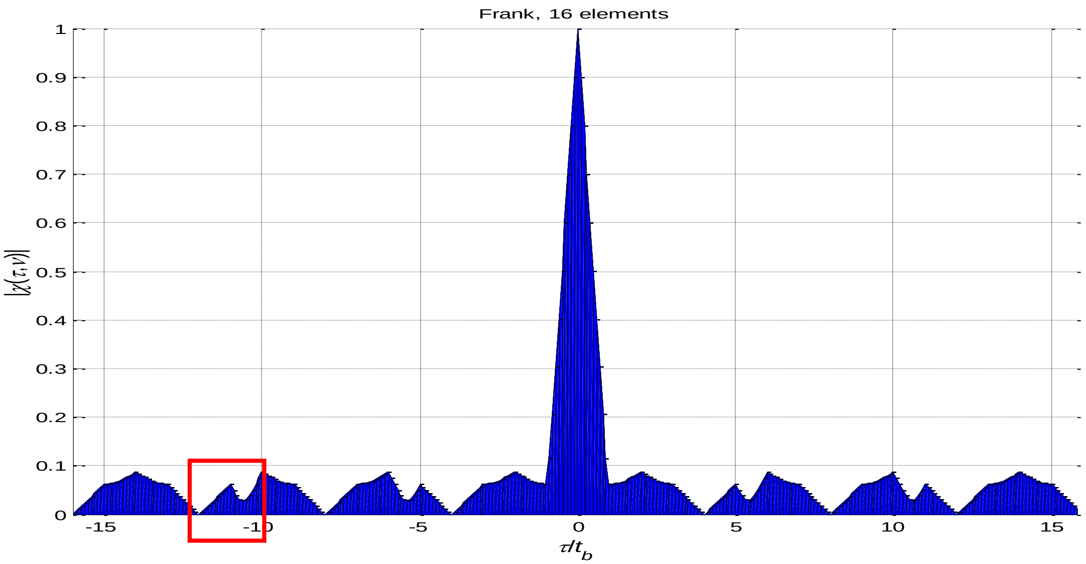

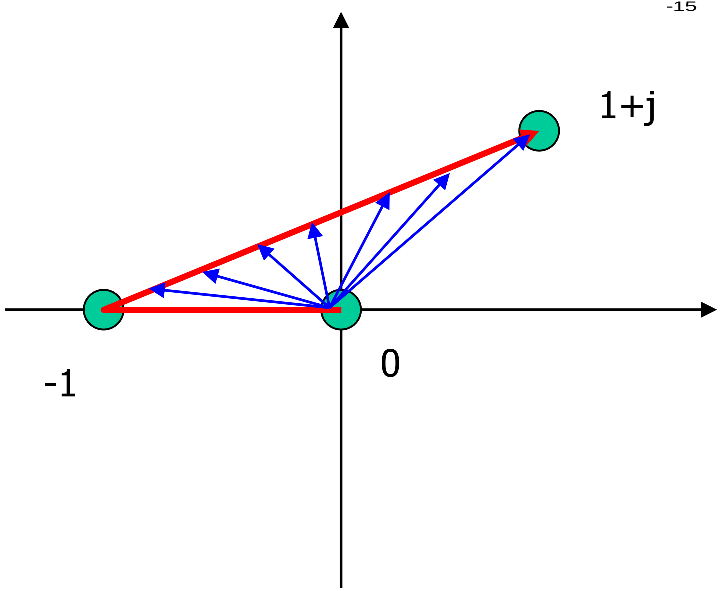

The ACF is constructed from straight lines between nt_b and $(n+1)t_b$, on the complex plain. The magnitude of the ACF can have curved lines.

Frank 16

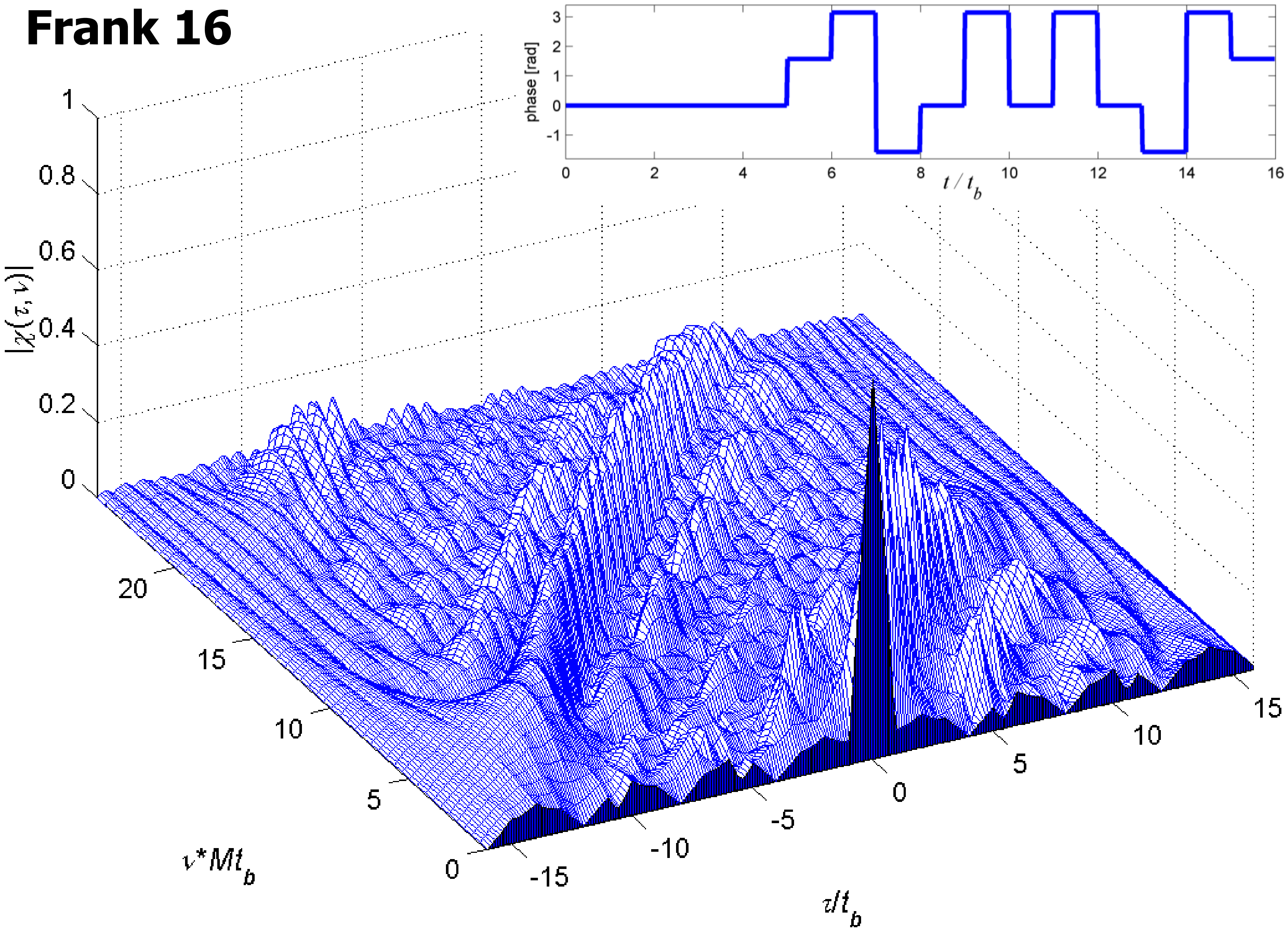
phase [rad]
3
2
1
0
-1
0
2
4
6
8
10
12
14
16
t / t_b
|χ(τ,ν)|
1
0.8
0.6
0.4
0.2
0
ν*Mt_b
0
5
10
15
20
τ/t_b
-15
-10
-5
0
5
10
15

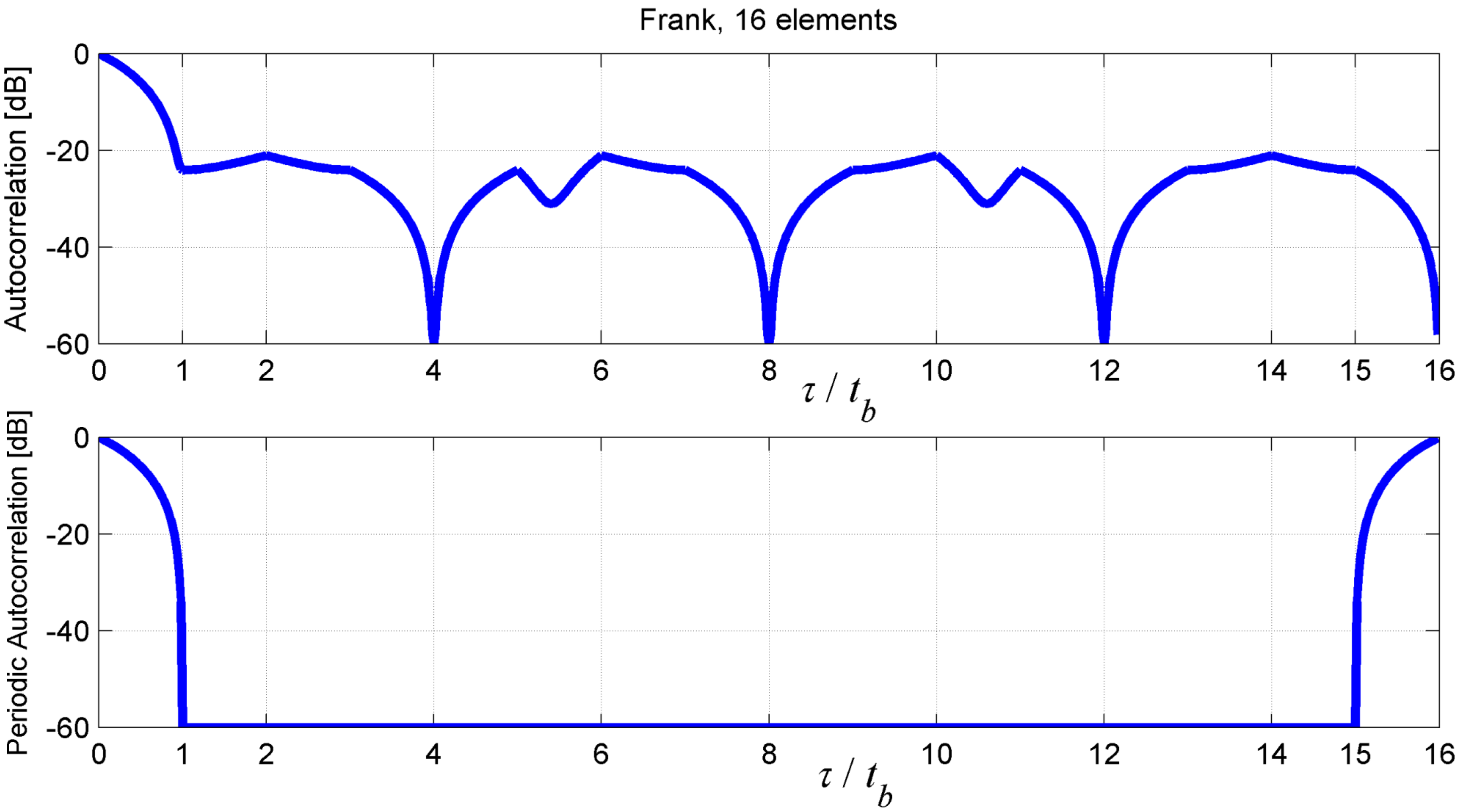

Frank codes exhibit perfect periodic autocorrelation

P3 and P4 polyphase coding

P3

$$\phi_m = \begin{cases} \dfrac{\pi}{M}(m-1)^2 \;\; ; \quad m=1,2,\ldots,M \;\; ; \quad M \text{ even} \\ \\ \dfrac{\pi}{M}(m-1)m \;\; ; \quad m=1,2,\ldots,M \;\; ; \quad M \text{ odd} \end{cases}$$

P4

$$\phi_m = \frac{\pi}{M}(m-1)^2 - \pi(m-1) \;\; ; \quad m=1,2,\ldots,M$$

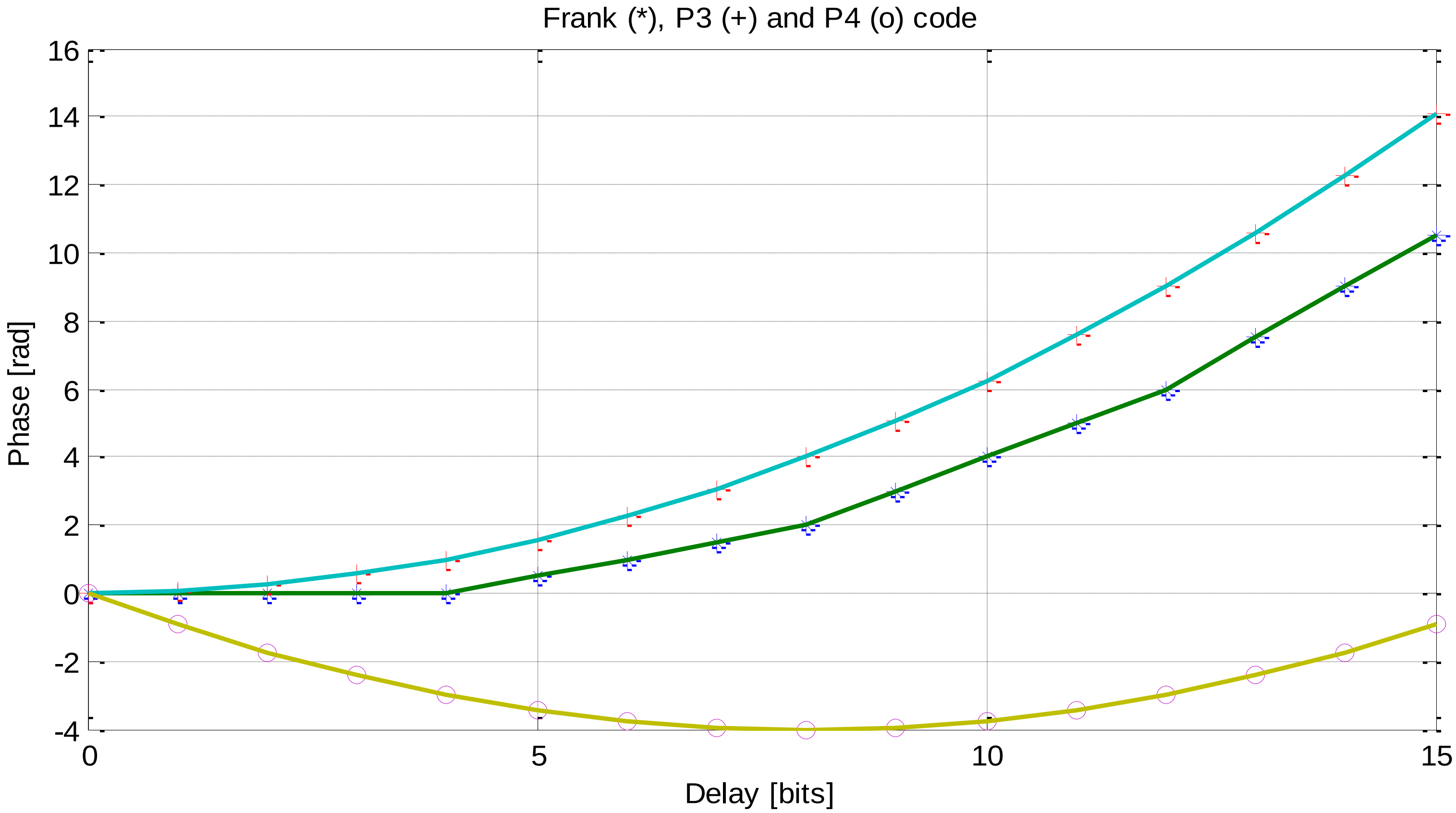

P4 25 elements

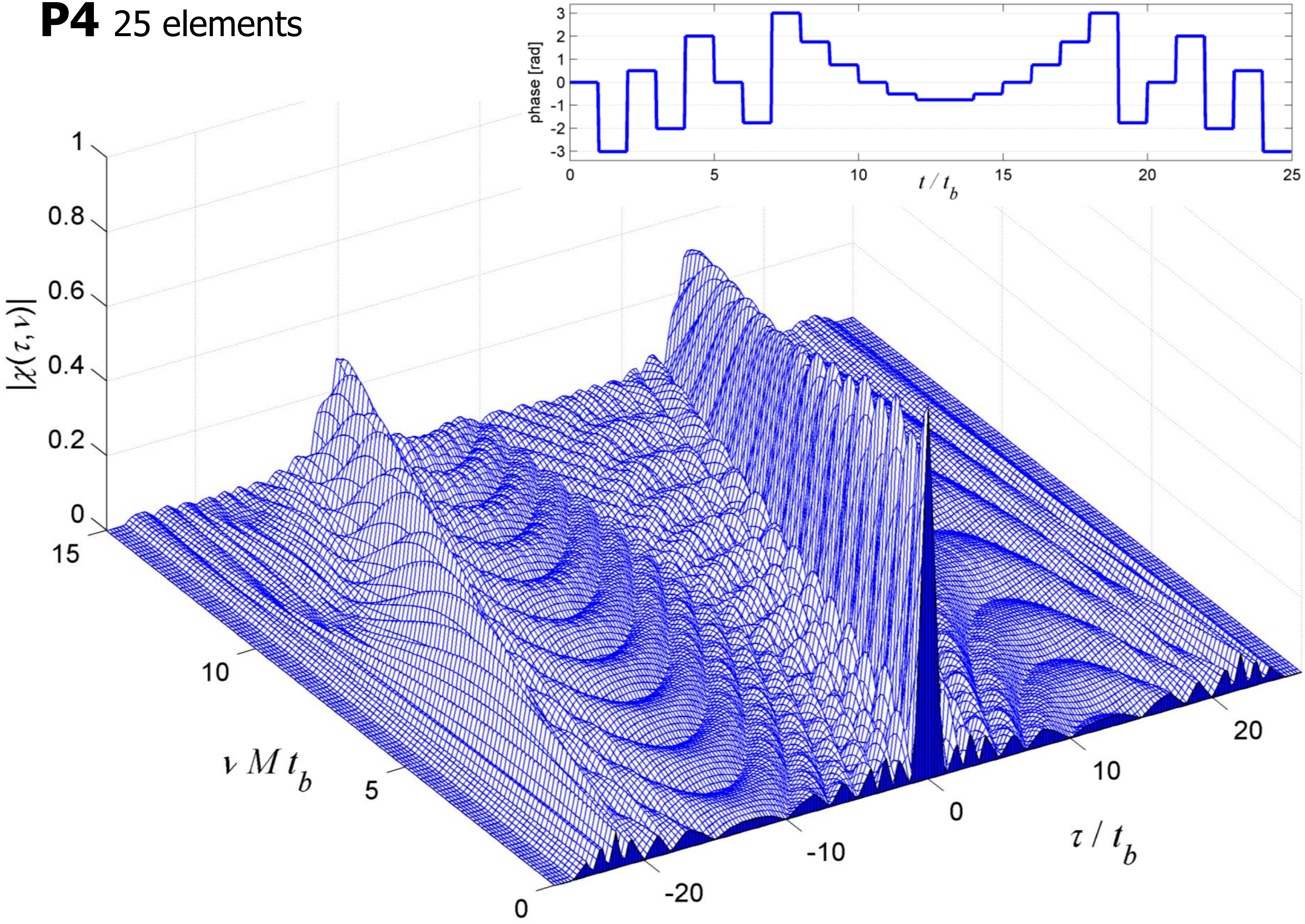

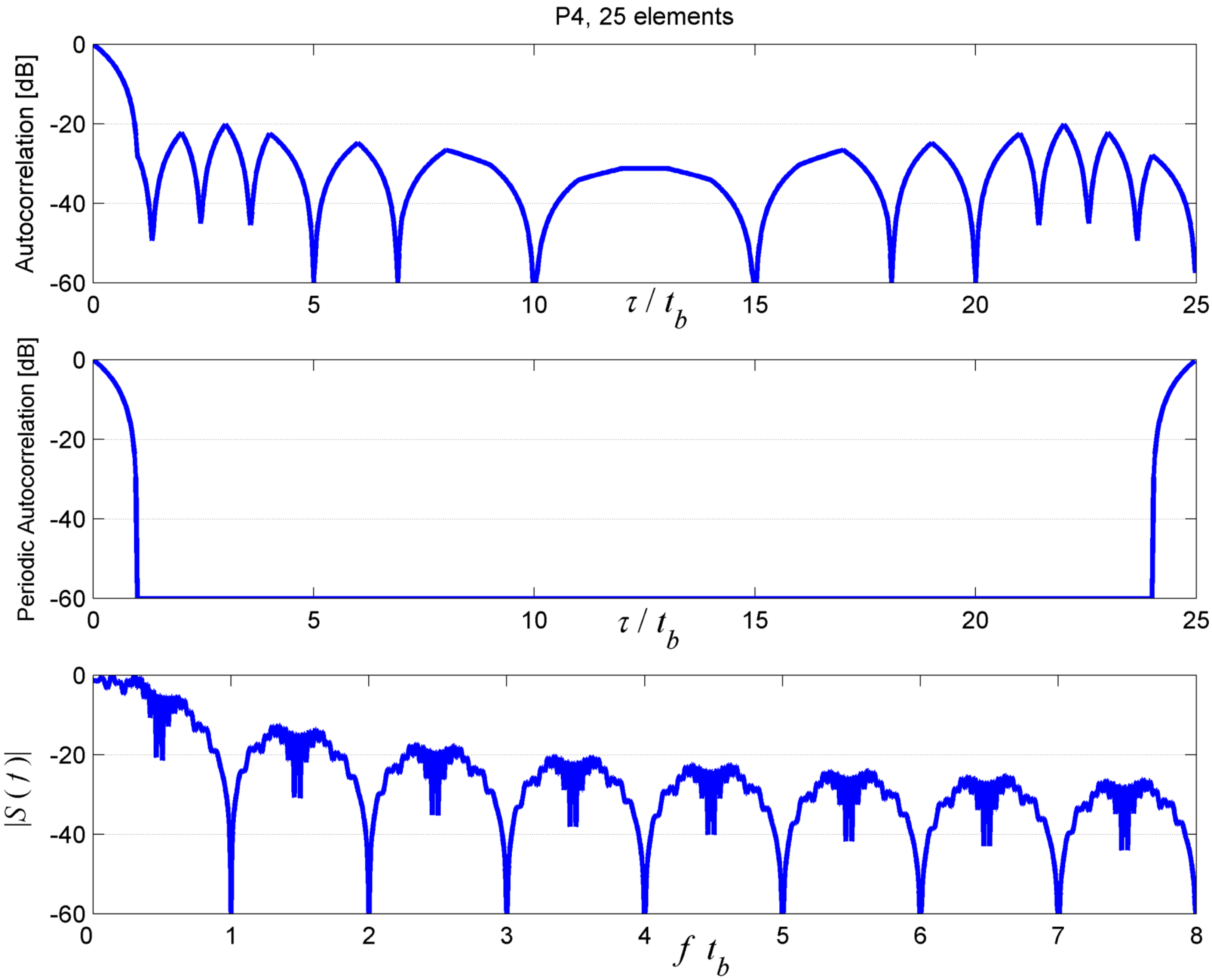
P4, 25 elements
Autocorrelation [dB]
0
-20
-40
-60
0
5
10
15
20
25
τ / t_b
Periodic Autocorrelation [dB]
0
-20
-40
-60
0
5
10
15
20
25
τ / t_b
|S (f)|
0
-20
-40
-60
0
1
2
3
4
5
6
7
8
f t_b

Px poly-phase code of length M=16 (See “Radar Signals”, p. 118)

$$\phi_k = \pi/8*[9\ 3\ 13\ 7\ 3\ 1\ 15\ 13\ 13\ 15\ 1\ 3\ 7\ 13\ 3\ 9\ ]$$

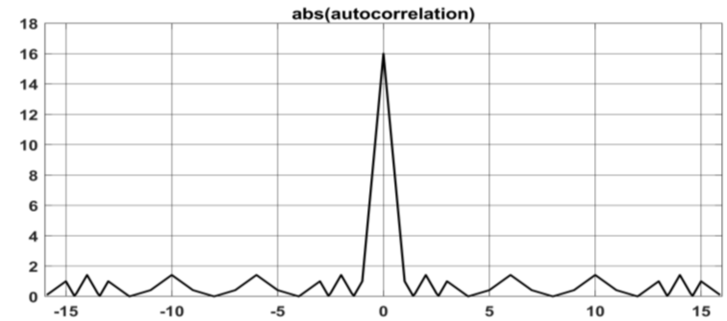

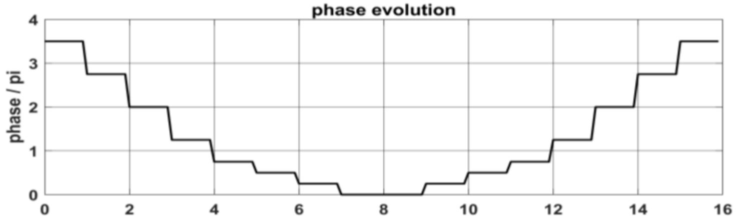

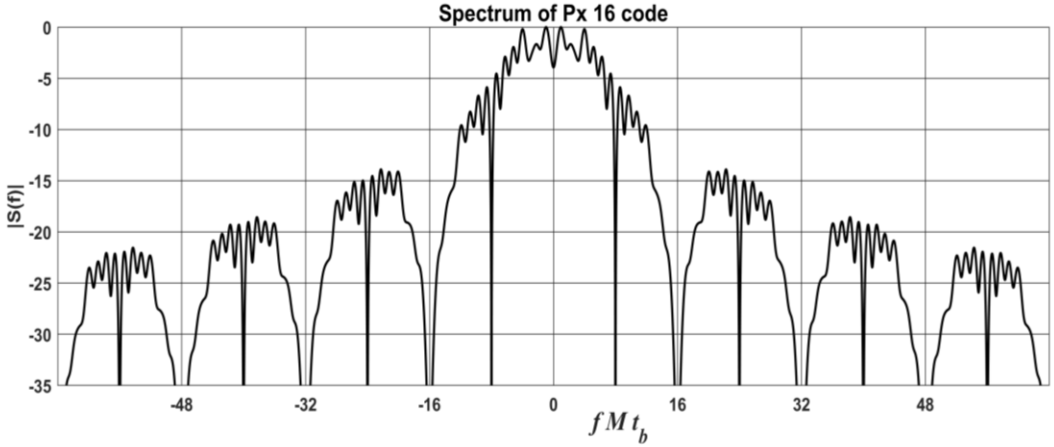

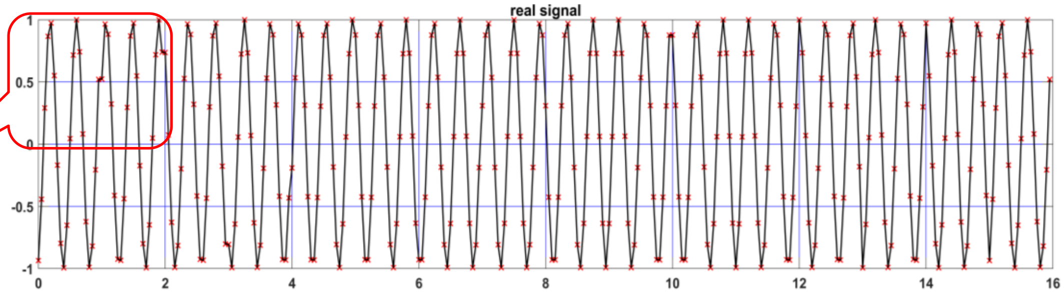

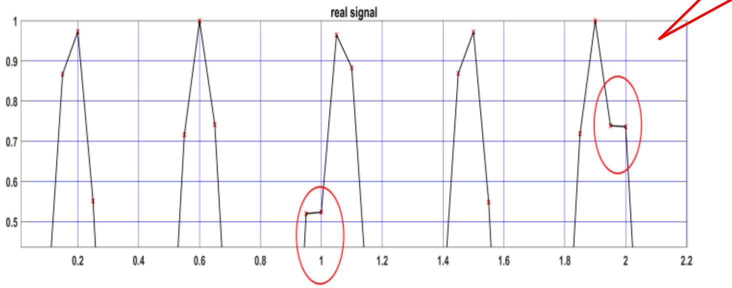

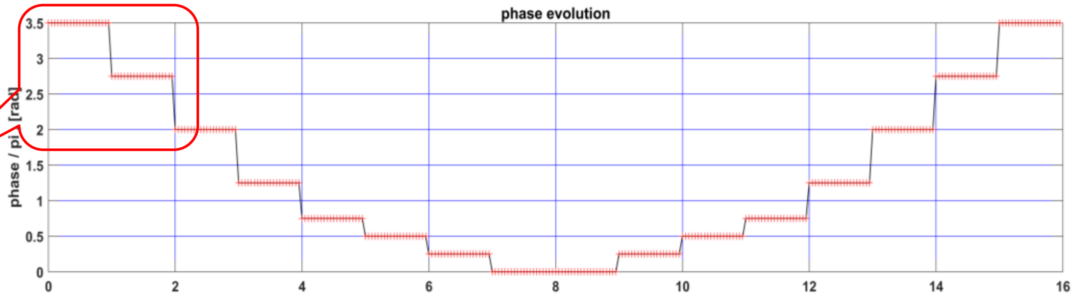

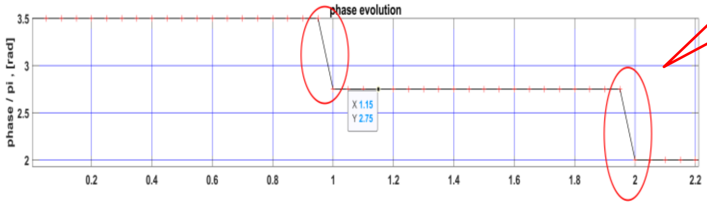

NON-LINEAR FM

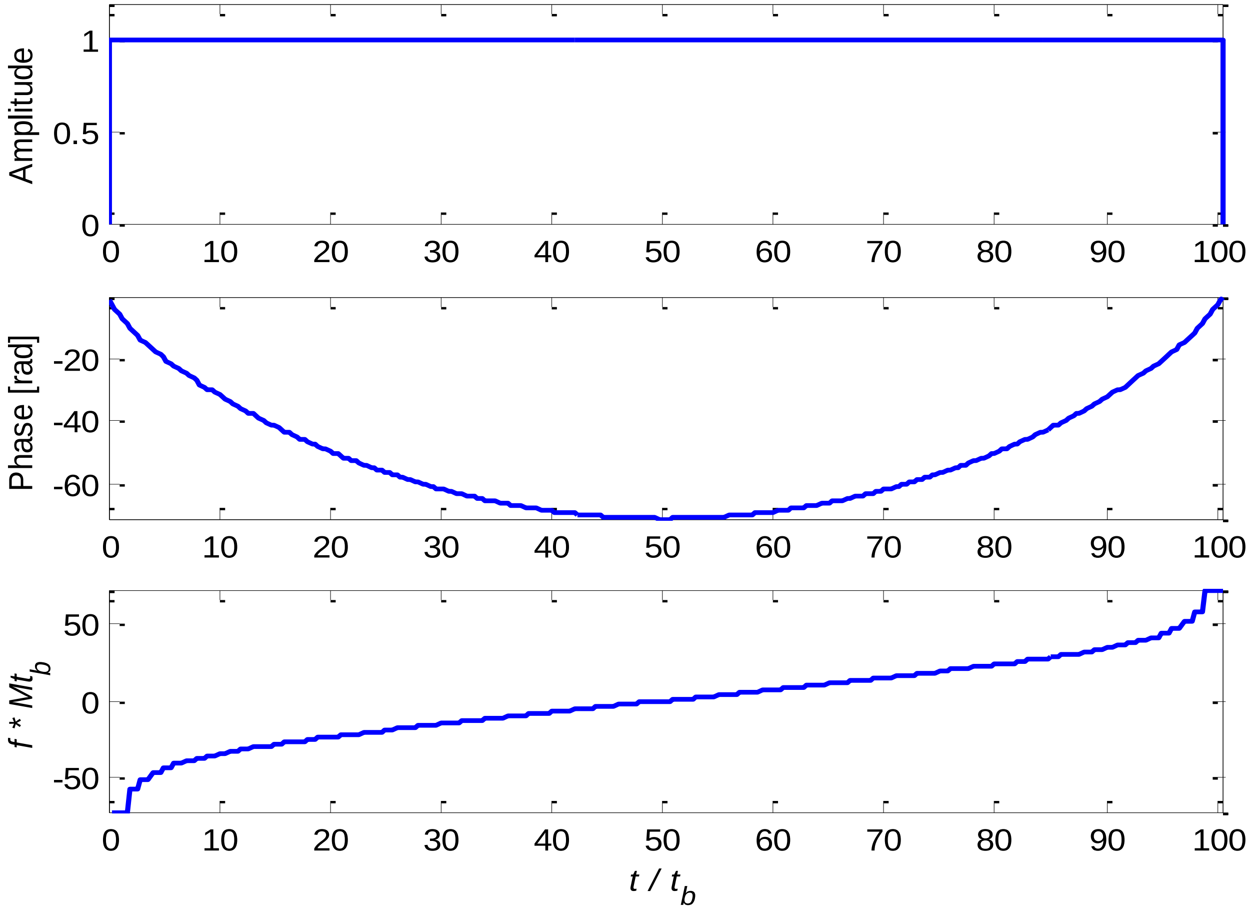

$$f(k)=\frac{k}{2M}\left[B_L+B_C\frac{1}{\sqrt{1-\frac{k^2}{M^2}}}\right]\quad ;\quad k=-(M-1),.....,-1,0,1,2,...,(M-1)$$

B_L=0.55

B_C=0.18

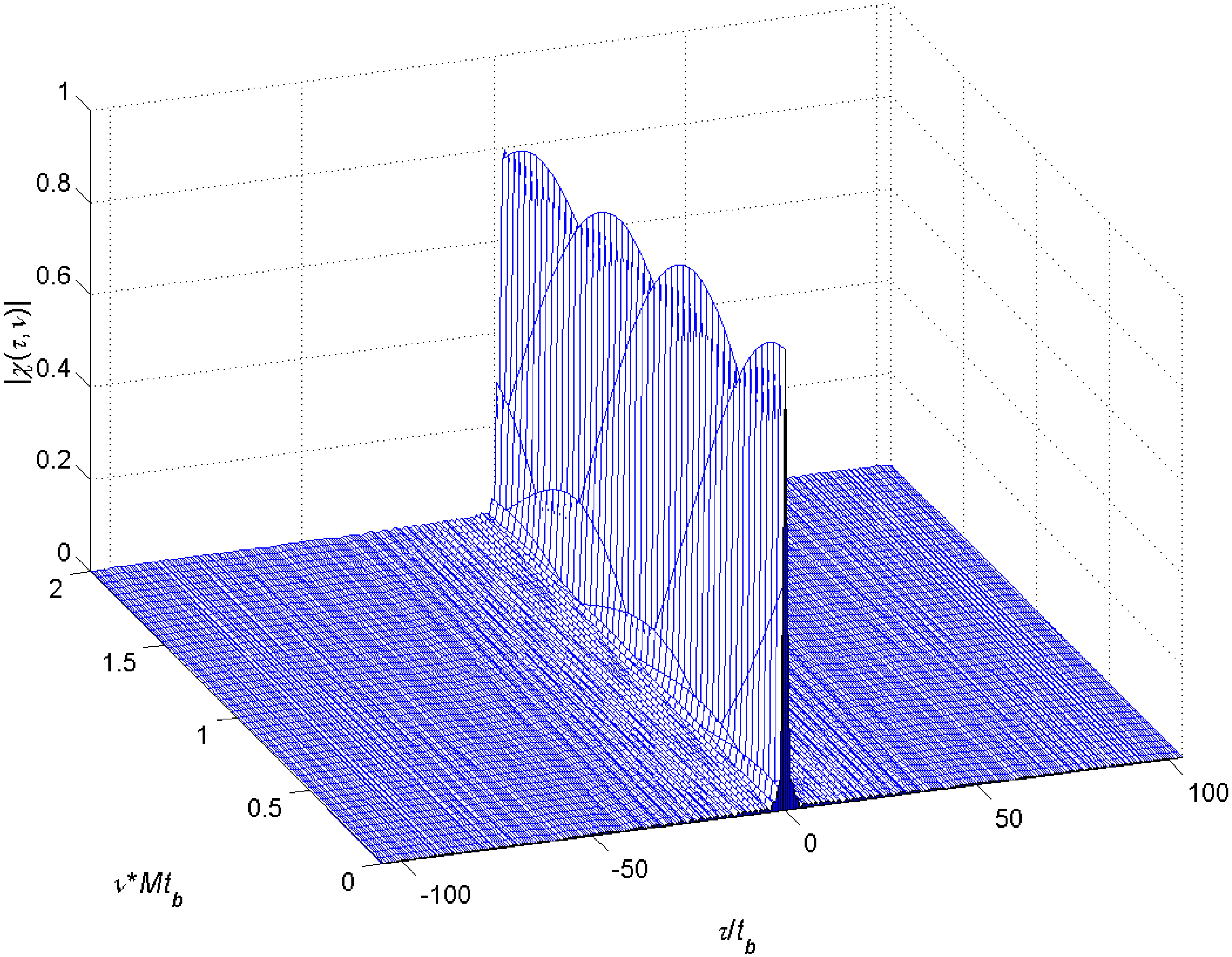
1
0.8
0.6
0.4
0.2
0
$|\chi(\tau,\nu)|$
2
1.5
1
0.5
0
$\nu * M t_b$
-100
-50
0
50
100
τ / t_b

P(n,k) code

- P4 is a phase-coded signal with discrete phases that are samples from the continuous phase of LFM.
- P(n,k) is a phase-coded signal with discrete phase that are samples from the continuous phase of NLFM.

$$W\left(f\right)=k+(1+k)\cos^{n}\left(\pi\ f/B\right),\quad \left|f\right|\le B/2$$

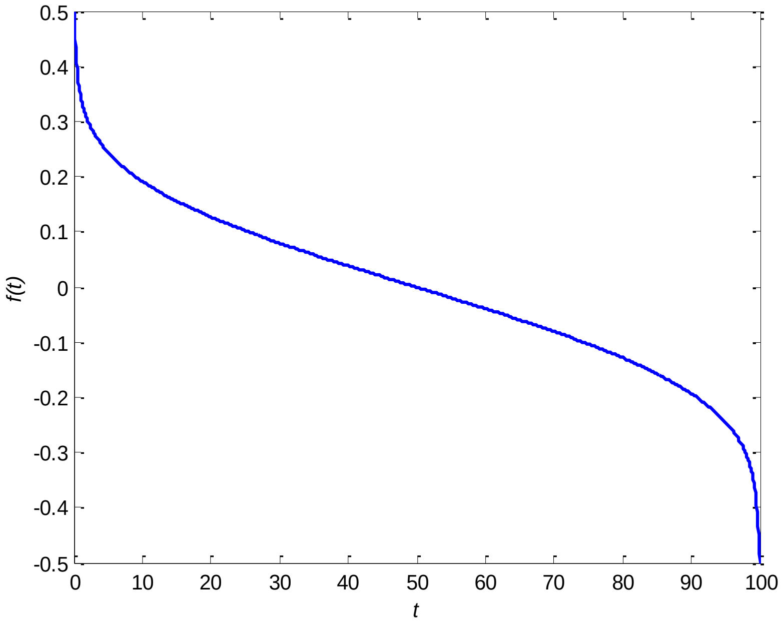

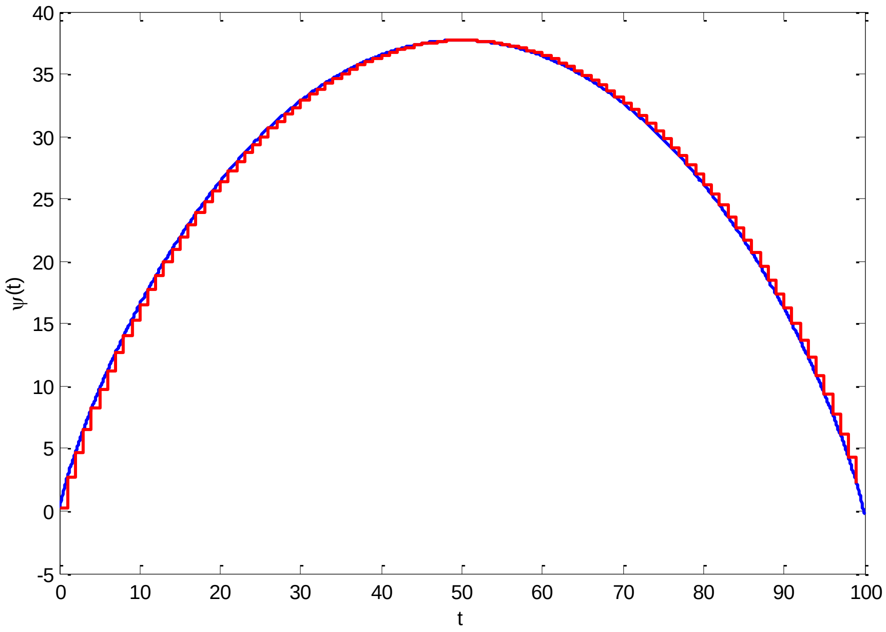

Felhauer T.:"Design and analysis of new P(n,k) polyphase pulse compression codes", *IEEE Trans. Aerospace and Electronic Systems*, Vol.30 (3), July 1994, pp. 865-874.

Any frequency-modulated signal can be converted to a phase-coded waveform.
Use: `u_phase = 2*cumsum(f_basic);`

(P(n,k) code)

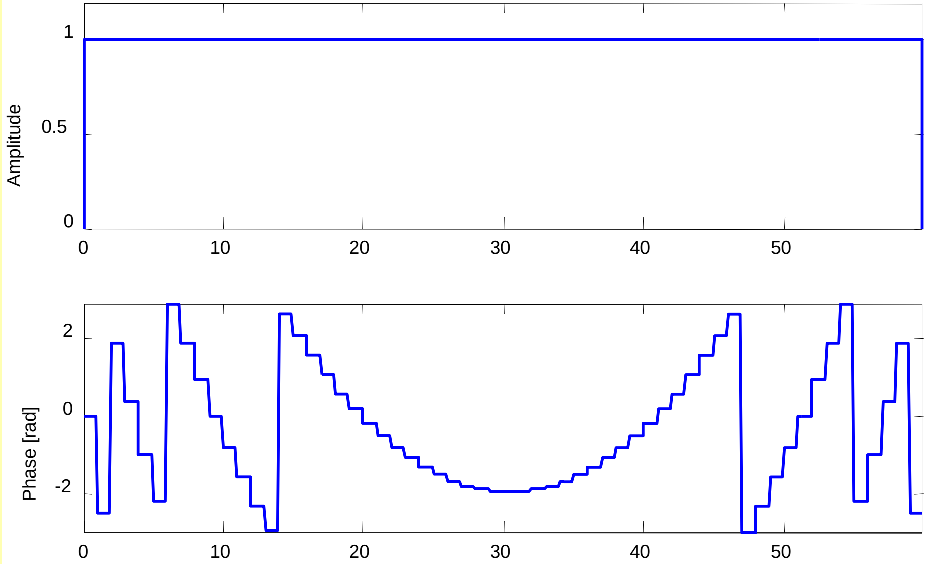
Amplitude
1
0.5
0
0
10
20
30
40
50
Phase [rad]
2
0
-2
0
10
20
30
40
50

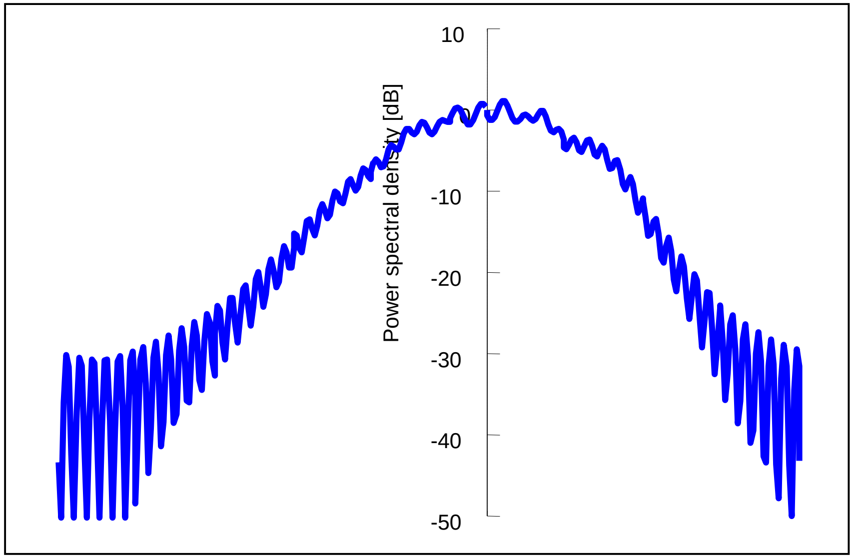
Power spectral density [dB]
10
0
-10
-20
-30
-40
-50

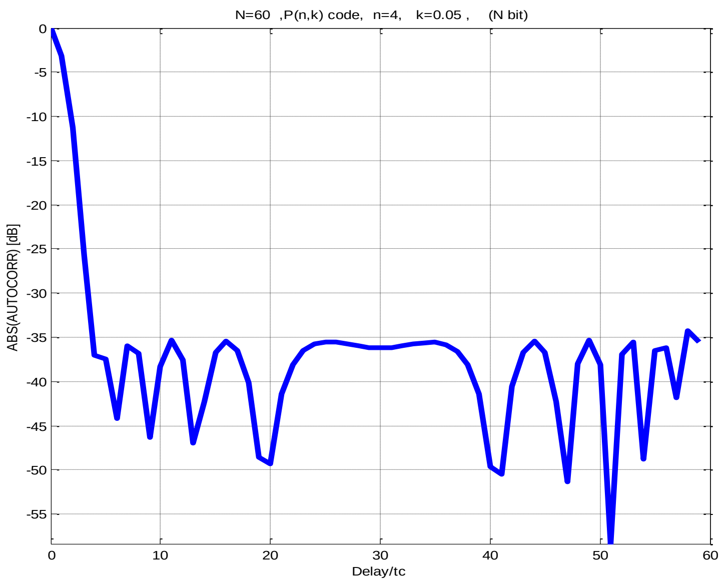
N=60 ,P(n,k) code, n=4, k=0.05 , (N bit)
ABS(AUTOCORR) [dB]
0
-5
-10
-15
-20
-25
-30
-35
-40
-45
-50
-55
0
10
20
30
40
50
60
Delay/tc

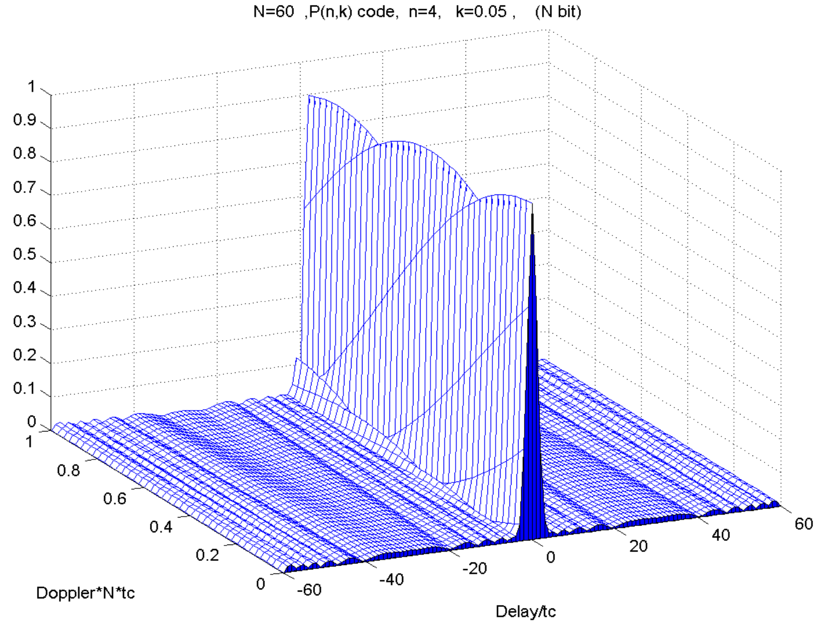
N=60 ,P(n,k) code, n=4, k=0.05 , (N bit)
1
0.9
0.8
0.7
0.6
0.5
0.4
0.3
0.2
0.1
0
1
0.8
0.6
0.4
0.2
0
Doppler*N*tc
-60
-40
-20
0
20
40
60
Delay/tc

Polyphase Barker codes

Allowing any phase values (non-binary) can lead to lower sidelobes. However, the outer most sidelobe is always 1 (for any polyphase or binary code).

The *Polyphase* sequence with minimal peak-to-peak sidelobe ratio excluding the outer most sidelobe are called *generalized Barker sequence* or *Polyphase Barker*.

Case 1: Phases are restricted to values that are the k'th roots of unity (e.g. k=2 gives the original Barker codes or k=6 for sextic Barker codes).

Case 2: No restriction on the values to the k'th roots of unity. Examples of such sequences are now known for all M≤36

Golomb, S. W. and Scholtz, R. A. “Generalized Barker sequences”, IEEE Trans. on Information Theory, **IT-11**, (4), Apr. 1965, pp. 533-537.

Bomer L. and Antweiler M. “Polyphase Barker sequences”, Electronic Letters, **25**, (3), Nov. 1989, pp. 1577-1579.

Normalized form* of known polyphase Barker codes

M	**Peak sidelobe**	**Phase values [º]**
4	0.5	104 313
5	0.77	73 225.3 90.6
6	1	58.2 175.9 354.1 234.2
7	0.522	106.4 93 316.7 60.5 270.7
8	0.662	72.1 28.6 294.3 151.7 251.2 63.3
9	0.430	38.7 41.5 270.2 215.1 40.5 160.7 334.3[e1]
10	0.832	60.2 132.1 142.8 18.3 10.7 230.8 22.9 242.9
11	0.892	34.1 259 266.5 327.9 158.4 13.7 22.7 221.5 94.5
12	0.908	104.8 163 170.9 344.3 241 185.5 282.2 147.6 209 78.7
13	0.721	115.8 114.8 248.4 213.4 123.1 154.9 140.2 12.7 149.6 303.5 121.6
14	0.968	66.8 133.5 202.2 100.4 37.5 235.8 167.2 86 168.7 33.5 143.1 13.3
15	0.805	17.8 5.5 5.4 142.4 212 298.1 123.9 91.6 1.3 206 314.2 156.5 23.9
16	0.933	26.5 38.5 97.3 49.4 305.8 286.5 197 65.7 241.3 137.5 319.1 47.9 178.5 303
17	0.733	5.3 18.5 278.4 307.6 67.3 149 207.5 70.6 301.2 282.8 137.3 6.5 120.5 327.9 186
18		**(?)**
19	0.980	53.3 24.7 90 79.2 232.5 8 331.4 99 240 318.4 159.8 307.8 161.3 137.1 31.8 338.2 217
20	0.979	99.1 125.8 233.1 251.4 133.9 144 354.8 304.5 192.1 302.5 219.5 161.7 283.8 145.4 250.2 106.1 228.4 107

---

* Normalized form = The first two phase elements in each code are 0 and are excluded

22	0.995	23.8 53.7 82.1 74.5 349.3 265 314 247.2 147.2 74.6 285.7 160.2 335.4 78.5 317.2 148.4 248.6 344.3 87.8 208.7
23	0.912	7.4 276 286.4 253.9 256.7 351.7 58.4 60.2 226.3 353.1 100.5 168.6 41 208.5 347.8 219.2 125.9 349.7 315.3 182.1 56.3
24	0.997	5 316.4 257.1 216.5 202.4 319 311.1 356.9 296.8 111.2 36.1 280.8 136.9 10.1 115.7 259.2 134.3 268.0 28.0 142.3 208.4 333.8
25	0.936	81.9 65 316.3 273.1 326.3 339.8 62.7 18.8 270.5 198 98.8 126.6 206.5 350.7 105.9 270.8 295.4 162.3 334.2 155.5 339.8 147.7 4.4
26	0.879	51.3 117.1 138.2 265.4 267 175.4 117.8 260.2 200 136.1 154.2 179 75.8 341 187.4 307 194.4 92.5 190.2 17.2 110 250.3 38.7 199.7
27	0.985	10.6 21.9 28.7 324.7 308.4 280.6 118.4 99.2 112.2 284.5 200.6 313.8 116.3 326.7 184.8 53.4 8.8 193.9 97.1 240.9 335.3 103 228.6 332 93
28	0.950	46.9 84.3 166.3 145.7 199.8 105.1 116.6 58.7 109.7 325.9 24.3 189.9 21.4 196.2 58.8 326.5 129.2 259 306.7 123.5 111.2 312.7 298.5 173.8 97.9 327.8
29	0.871	6.9 318.2 239.9 264.7 239.2 160.4 301.5 327.5 18.7 319.7 84.9 108.6 224.1 6.3 31.4 184 167.8 89.9 325.2 227.5 145.4 329.9 91.6 263.7 94 252.9 59.6
30	0.998	33.1 34.6 33.7 11.9 300.1 281.5 26.5 54.2 155.6 211.9 231.6 134.4 76 317.7 275.8 67.6 299 184.6 72.6 153.8 6.6 262.6 94.1 242.8 359.1 149.7 306.4 71.5
31	0.935	28.4 117.7 165.1 236.5 308.7 305 236.5 216.4 327.4 279.5 211.3 247.2 192 95.4 17 273 52.8 331.1 224 303.7 147.2 21.7 245.6 29.3 145.5 297.1 62.4 190.8 7.8
32	0.996	13.5 16.5 90.5 110 95 60.5 333 307 289 281.5 85.5 164 248.5 335 171.5 76 64 221.5 298 110 37 272.5 179.5 19.5 179 288 82.5 292 133 329.5
33	0.990	143 153.5 339 332.5 180.5 133.5 19 108.5 166 216.5 225.5 227.5 318.5 238.5 184.5 226 141.5 113.5 75 36 185.5 327 226.5 108.5 302.5 116.5 273 350 188 356.5 164.5
34	0.997	11 1 307 245 200 184 231 293 300 348 45 227 247 57 335 1 127 249 68 91 315 221 57 116 238 58 287 127 273 127 5 216
35	0.999	93.2 65.4 166.4 132.4 344.1 279.4 337.6 301.3 197.6 56.2 36.8 9.2 325.8 334.3 24.4 157.8 291.1 301.1 148.4 112.9 141.3 296.6 128.7 125.4 341.4 129.9 244.6 73.8 321.5 157.6 300.7 107.5 254.4
36	0.969	82 118 228 228 58 60 154 108 20 234 212 262 236 196 220 116 12 226 178 122 126 76 266 114 256 108 320 100 266 30 124 246 60 186

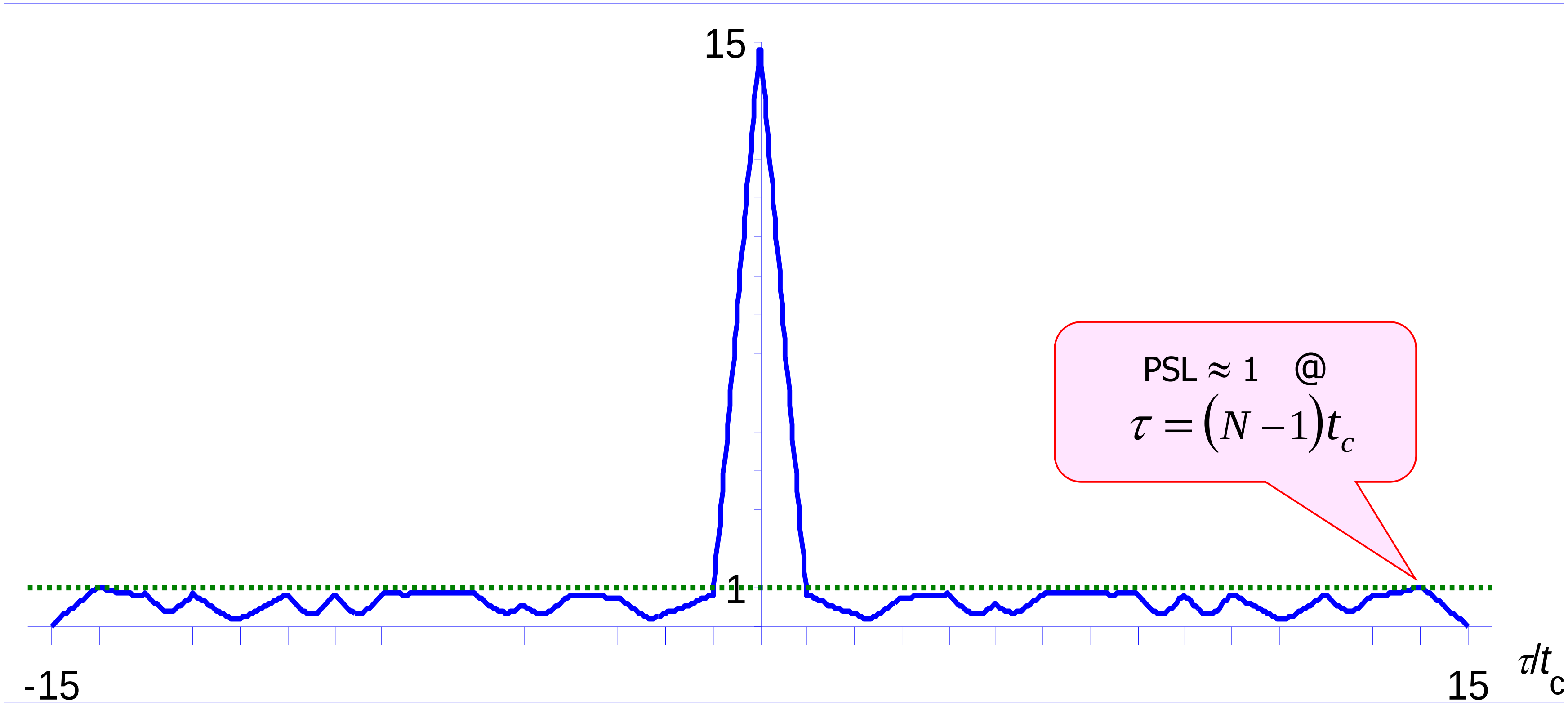

PSL ≈ 1 @
$$\tau = (N-1)t_c$$

The autocorrelation function of the 15-element polyphase Barker coded pulse

Polyphase Barker codes were found up to length 77 (Carroll J. Nunn and Gregory E. Coxson, private communication, 2008)

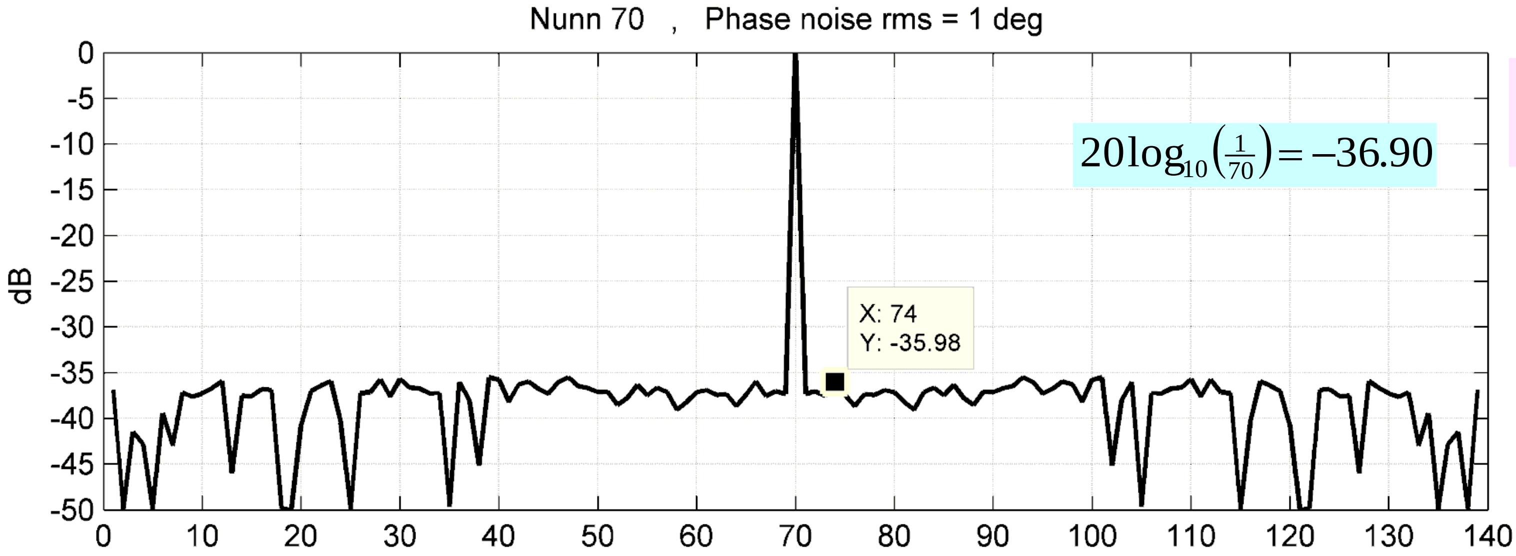

$$20\log_{10}\left(\frac{1}{70}\right)=-36.90$$

Polyphase Barker

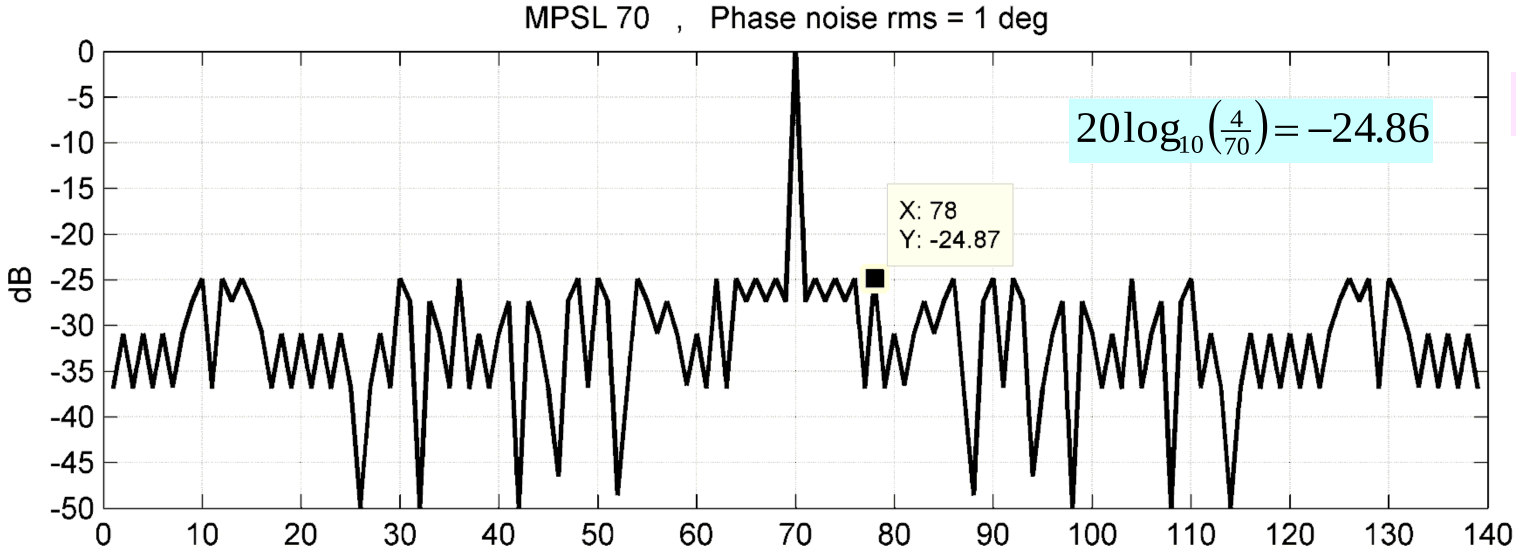

$$20\log_{10}\left(\frac{4}{70}\right)=-24.86$$

Binary MPSL

Nunn, C. J., and Coxson, G. E. :"**Polyphase pulse compression codes with optimal peak and integrated sidelobes**". *IEEE Trans. on AES.* **45**, 2, pp. 775-781, 2009.

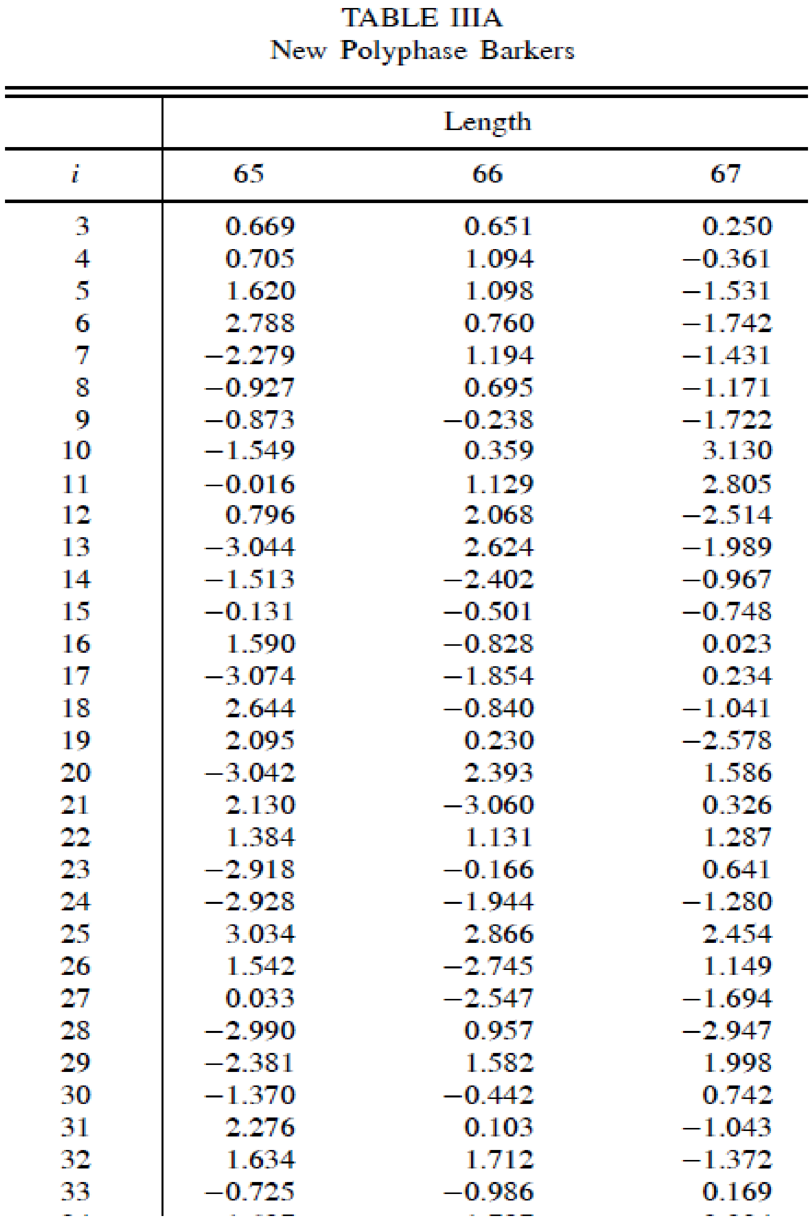

TABLE IIIA
New Polyphase Barkers

	Length		
i	65	66	67
3	0.669	0.651	0.250
4	0.705	1.094	−0.361
5	1.620	1.098	−1.531
6	2.788	0.760	−1.742
7	−2.279	1.194	−1.431
8	−0.927	0.695	−1.171
9	−0.873	−0.238	−1.722
10	−1.549	0.359	3.130
11	−0.016	1.129	2.805
12	0.796	2.068	−2.514
13	−3.044	2.624	−1.989
14	−1.513	−2.402	−0.967
15	−0.131	−0.501	−0.748
16	1.590	−0.828	0.023
17	−3.074	−1.854	0.234
18	2.644	−0.840	−1.041
19	2.095	0.230	−2.578
20	−3.042	2.393	1.586
21	2.130	−3.060	0.326
22	1.384	1.131	1.287
23	−2.918	−0.166	0.641
24	−2.928	−1.944	−1.280
25	3.034	2.866	2.454
26	1.542	−2.745	1.149
27	0.033	−2.547	−1.694
28	−2.990	0.957	−2.947
29	−2.381	1.582	1.998
30	−1.370	−0.442	0.742
31	2.276	0.103	−1.043
32	1.634	1.712	−1.372
33	−0.725	−0.986	0.169

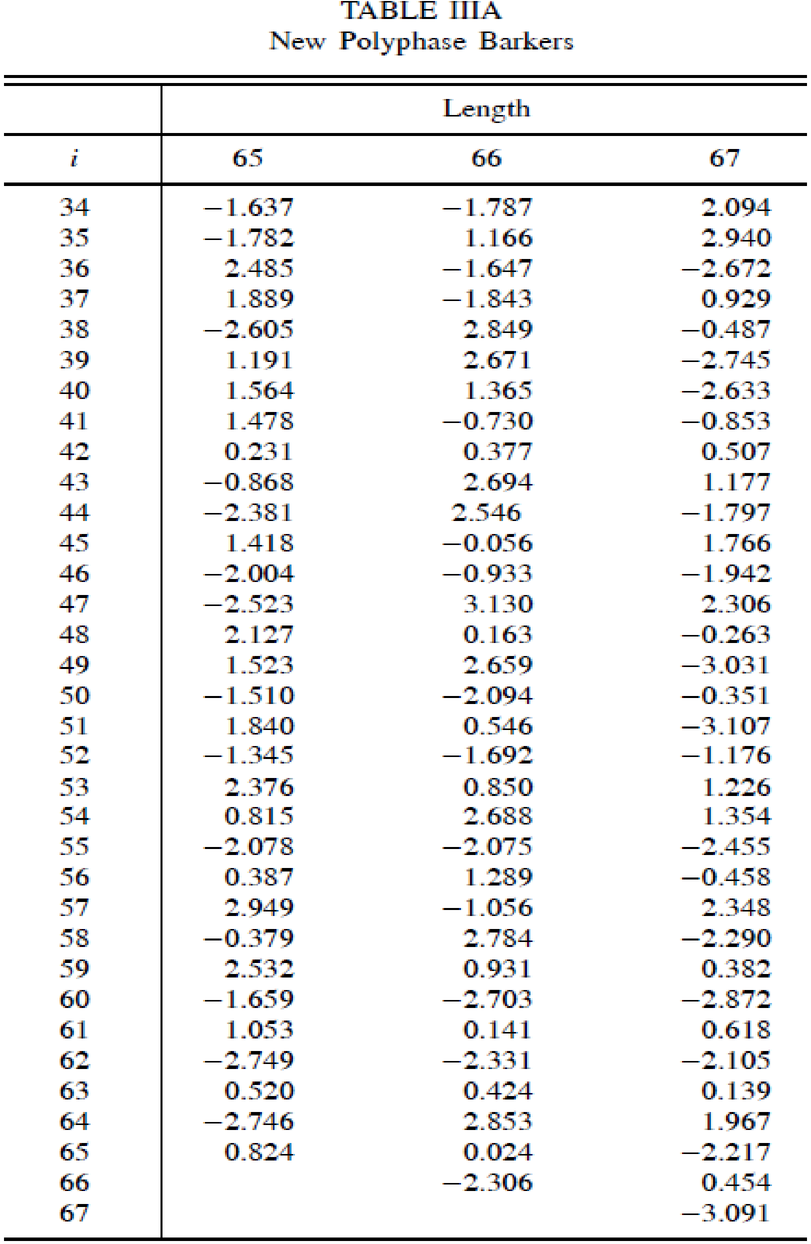

TABLE IIIA
New Polyphase Barkers

	Length		
i	65	66	67
34	−1.637	−1.787	2.094
35	−1.782	1.166	2.940
36	2.485	−1.647	−2.672
37	1.889	−1.843	0.929
38	−2.605	2.849	−0.487
39	1.191	2.671	−2.745
40	1.564	1.365	−2.633
41	1.478	−0.730	−0.853
42	0.231	0.377	0.507
43	−0.868	2.694	1.177
44	−2.381	2.546	−1.797
45	1.418	−0.056	1.766
46	−2.004	−0.933	−1.942
47	−2.523	3.130	2.306
48	2.127	0.163	−0.263
49	1.523	2.659	−3.031
50	−1.510	−2.094	−0.351
51	1.840	0.546	−3.107
52	−1.345	−1.692	−1.176
53	2.376	0.850	1.226
54	0.815	2.688	1.354
55	−2.078	−2.075	−2.455
56	0.387	1.289	−0.458
57	2.949	−1.056	2.348
58	−0.379	2.784	−2.290
59	2.532	0.931	0.382
60	−1.659	−2.703	−2.872
61	1.053	0.141	0.618
62	−2.749	−2.331	−2.105
63	0.520	0.424	0.139
64	−2.746	2.853	1.967
65	0.824	0.024	−2.217
66		−2.306	0.454
67			−3.091

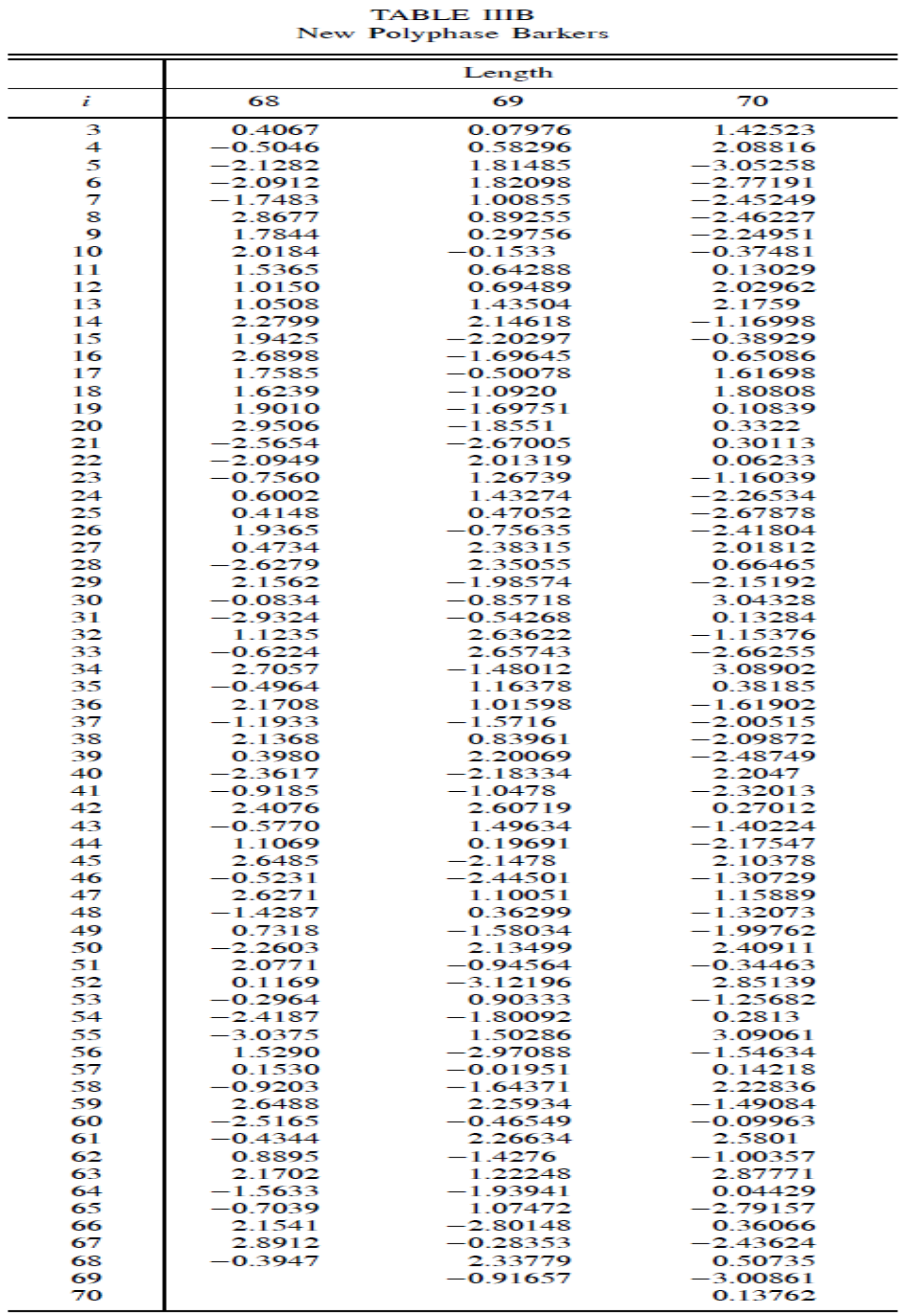

TABLE IIIB

New Polyphase Barkers

	Length		
i	68	69	70
3	0.4067	0.07976	1.42523
4	−0.5046	0.58296	2.08816
5	−2.1282	1.81485	−3.05258
6	−2.0912	1.82098	−2.77191
7	−1.7483	1.00855	−2.45249
8	2.8677	0.89255	−2.46227
9	1.7844	0.29756	−2.24951
10	2.0184	−0.1533	−0.37481
11	1.5365	0.64288	0.13029
12	1.0150	0.69489	2.02962
13	1.0508	1.43504	2.1759
14	2.2799	2.14618	−1.16998
15	1.9425	−2.20297	−0.38929
16	2.6898	−1.69645	0.65086
17	1.7585	−0.50078	1.61698
18	1.6239	−1.0920	1.80808
19	1.9010	−1.69751	0.10839
20	2.9506	−1.8551	0.3322
21	−2.5654	−2.67005	0.30113
22	−2.0949	2.01319	0.06233
23	−0.7560	1.26739	−1.16039
24	0.6002	1.43274	−2.26534
25	0.4148	0.47052	−2.67878
26	1.9365	−0.75635	−2.41804
27	0.4734	2.38315	2.01812
28	−2.6279	2.35055	0.66465
29	2.1562	−1.98574	−2.15192
30	−0.0834	−0.85718	3.04328
31	−2.9324	−0.54268	0.13284
32	1.1235	2.63622	−1.15376
33	−0.6224	2.65743	−2.66255
34	2.7057	−1.48012	3.08902
35	−0.4964	1.16378	0.38185
36	2.1708	1.01598	−1.61902
37	−1.1933	−1.5716	−2.00515
38	2.1368	0.83961	−2.09872
39	0.3980	2.20069	−2.48749
40	−2.3617	−2.18334	2.2047
41	−0.9185	−1.0478	−2.32013
42	2.4076	2.60719	0.27012
43	−0.5770	1.49634	−1.40224
44	1.1069	0.19691	−2.17547
45	2.6485	−2.1478	2.10378
46	−0.5231	−2.44501	−1.30729
47	2.6271	1.10051	1.15889
48	−1.4287	0.36299	−1.32073
49	0.7318	−1.58034	−1.99762
50	−2.2603	2.13499	2.40911
51	2.0771	−0.94564	−0.34463
52	0.1169	−3.12196	2.85139
53	−0.2964	0.90333	−1.25682
54	−2.4187	−1.80092	0.2813
55	−3.0375	1.50286	3.09061
56	1.5290	−2.97088	−1.54634
57	0.1530	−0.01951	0.14218
58	−0.9203	−1.64371	2.22836
59	2.6488	2.25934	−1.49084
60	−2.5165	−0.46549	−0.09963
61	−0.4344	2.26634	2.5801
62	0.8895	−1.4276	−1.00357
63	2.1702	1.22248	2.87771
64	−1.5633	−1.93941	0.04429
65	−0.7039	1.07472	−2.79157
66	2.1541	−2.80148	0.36066
67	2.8912	−0.28353	−2.43624
68	−0.3947	2.33779	0.50735
69		−0.91657	−3.00861
70			0.13762

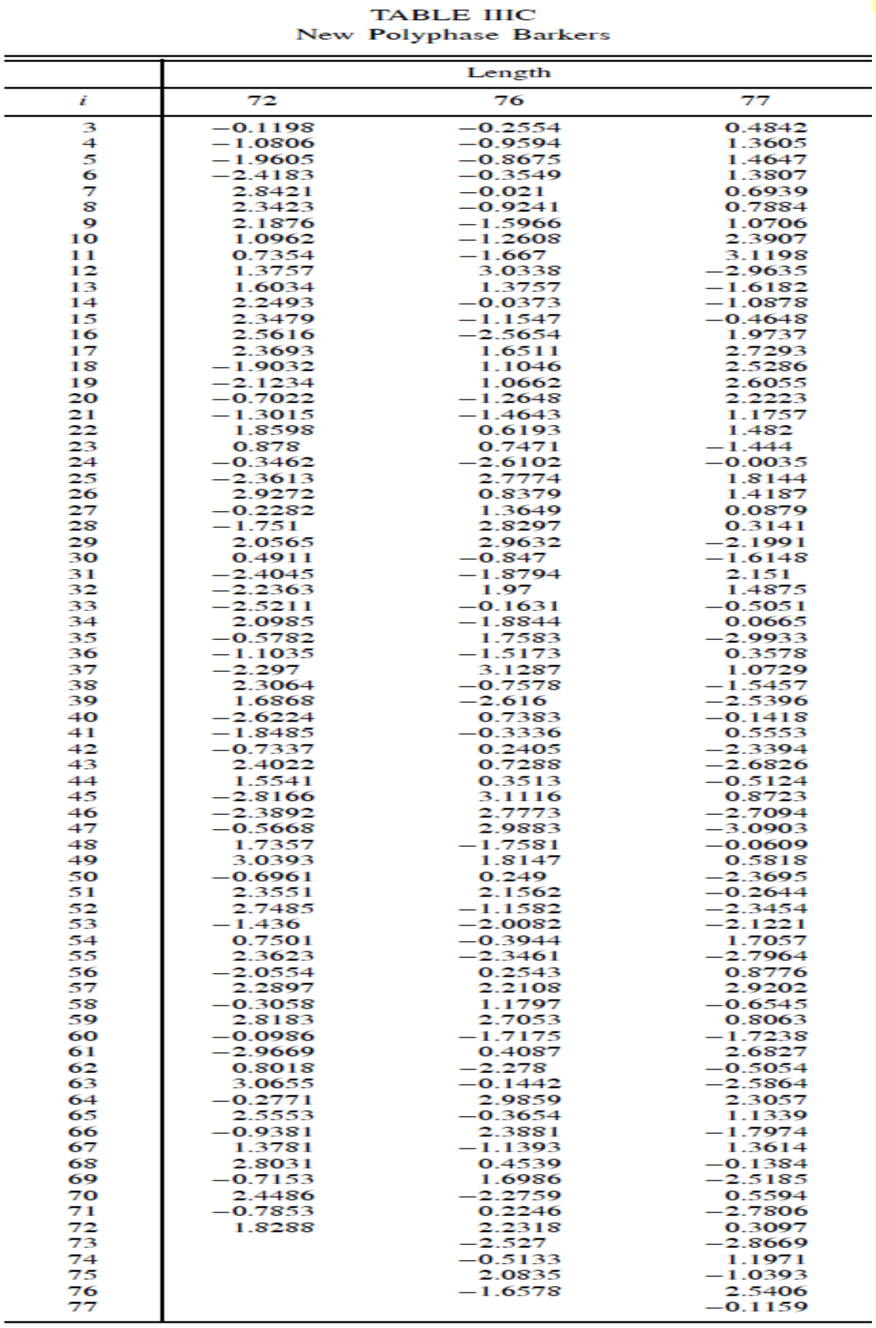

TABLE IIIC

New Polyphase Barkers

	Length		
i	72	76	77
3	−0.1198	−0.2554	0.4842
4	−1.0806	−0.9594	1.3605
5	−1.9605	−0.8675	1.4647
6	−2.4183	−0.3549	1.3807
7	2.8421	−0.021	0.6939
8	2.3423	−0.9241	0.7884
9	2.1876	−1.5966	1.0706
10	1.0962	−1.2608	2.3907
11	0.7354	−1.667	3.1198
12	1.3757	3.0338	−2.9635
13	1.6034	1.3757	−1.6182
14	2.2493	−0.0373	−1.0878
15	2.3479	−1.1547	−0.4648
16	2.5616	−2.5654	1.9737
17	2.3693	1.6511	2.7293
18	−1.9032	1.1046	2.5286
19	−2.1234	1.0662	2.6055
20	−0.7022	−1.2648	2.2223
21	−1.3015	−1.4643	1.1757
22	1.8598	0.6193	1.482
23	0.878	0.7471	−1.444
24	−0.3462	−2.6102	−0.0035
25	−2.3613	2.7774	1.8144
26	2.9272	0.8379	1.4187
27	−0.2282	1.3649	0.0879
28	−1.751	2.8297	0.3141
29	2.0565	2.9632	−2.1991
30	0.4911	−0.847	−1.6148
31	−2.4045	−1.8794	2.151
32	−2.2363	1.97	1.4875
33	−2.5211	−0.1631	−0.5051
34	2.0985	−1.8844	0.0665
35	−0.5782	1.7583	−2.9933
36	−1.1035	−1.5173	0.3578
37	−2.297	3.1287	1.0729
38	2.3064	−0.7578	−1.5457
39	1.6868	−2.616	−2.5396
40	−2.6224	0.7383	−0.1418
41	−1.8485	−0.3336	0.5553
42	−0.7337	0.2405	−2.3394
43	2.4022	0.7288	−2.6826
44	1.5541	0.3513	−0.5124
45	−2.8166	3.1116	0.8723
46	−2.3892	2.7773	−2.7094
47	−0.5668	2.9883	−3.0903
48	1.7357	−1.7581	−0.0609
49	3.0393	1.8147	0.5818
50	−0.6961	0.249	−2.3695
51	2.3551	2.1562	−0.2644
52	2.7485	−1.1582	−2.3454
53	−1.436	−2.0082	−2.1221
54	0.7501	−0.3944	1.7057
55	2.3623	−2.3461	−2.7964
56	−2.0554	0.2543	0.8776
57	2.2897	2.2108	2.9202
58	−0.3058	1.1797	−0.6545
59	2.8183	2.7053	0.8063
60	−0.0986	−1.7175	−1.7238
61	−2.9669	0.4087	2.6827
62	0.8018	−2.278	−0.5054
63	3.0655	−0.1442	−2.5864
64	−0.2771	2.9859	2.3057
65	2.5553	−0.3654	1.1339
66	−0.9381	2.3881	−1.7974
67	1.3781	−1.1393	1.3614
68	2.8031	0.4539	−0.1384
69	−0.7153	1.6986	−2.5185
70	2.4486	−2.2759	0.5594
71	−0.7853	0.2246	−2.7806
72	1.8288	2.2318	0.3097
73		−2.527	−2.8669
74		−0.5133	1.1971
75		2.0835	−1.0393
76		−1.6578	2.5406
77			−0.1159

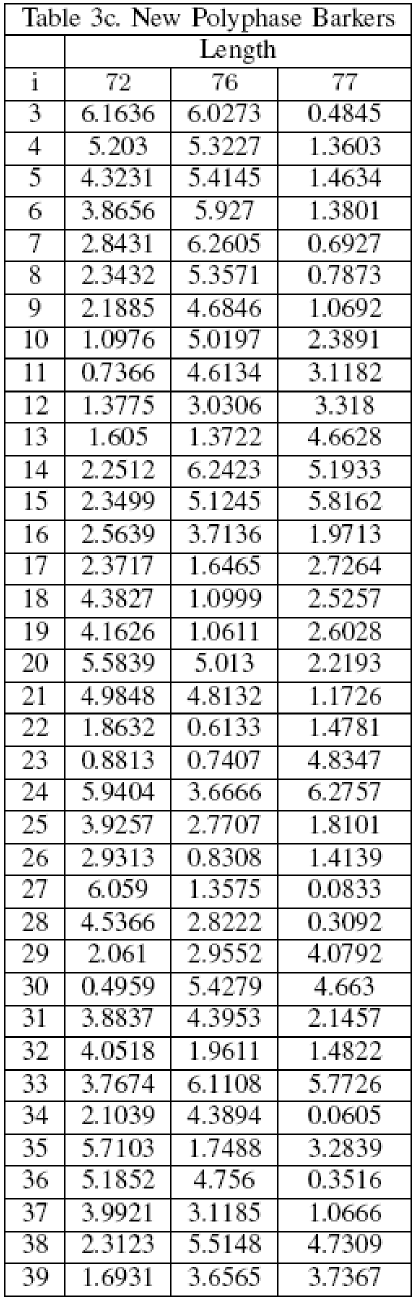

Table 3c. New Polyphase Barkers

	Length		
i	72	76	77
3	6.1636	6.0273	0.4845
4	5.203	5.3227	1.3603
5	4.3231	5.4145	1.4634
6	3.8656	5.927	1.3801
7	2.8431	6.2605	0.6927
8	2.3432	5.3571	0.7873
9	2.1885	4.6846	1.0692
10	1.0976	5.0197	2.3891
11	0.7366	4.6134	3.1182
12	1.3775	3.0306	3.318
13	1.605	1.3722	4.6628
14	2.2512	6.2423	5.1933
15	2.3499	5.1245	5.8162
16	2.5639	3.7136	1.9713
17	2.3717	1.6465	2.7264
18	4.3827	1.0999	2.5257
19	4.1626	1.0611	2.6028
20	5.5839	5.013	2.2193
21	4.9848	4.8132	1.1726
22	1.8632	0.6133	1.4781
23	0.8813	0.7407	4.8347
24	5.9404	3.6666	6.2757
25	3.9257	2.7707	1.8101
26	2.9313	0.8308	1.4139
27	6.059	1.3575	0.0833
28	4.5366	2.8222	0.3092
29	2.061	2.9552	4.0792
30	0.4959	5.4279	4.663
31	3.8837	4.3953	2.1457
32	4.0518	1.9611	1.4822
33	3.7674	6.1108	5.7726
34	2.1039	4.3894	0.0605
35	5.7103	1.7488	3.2839
36	5.1852	4.756	0.3516
37	3.9921	3.1185	1.0666
38	2.3123	5.5148	4.7309
39	1.6931	3.6565	3.7367

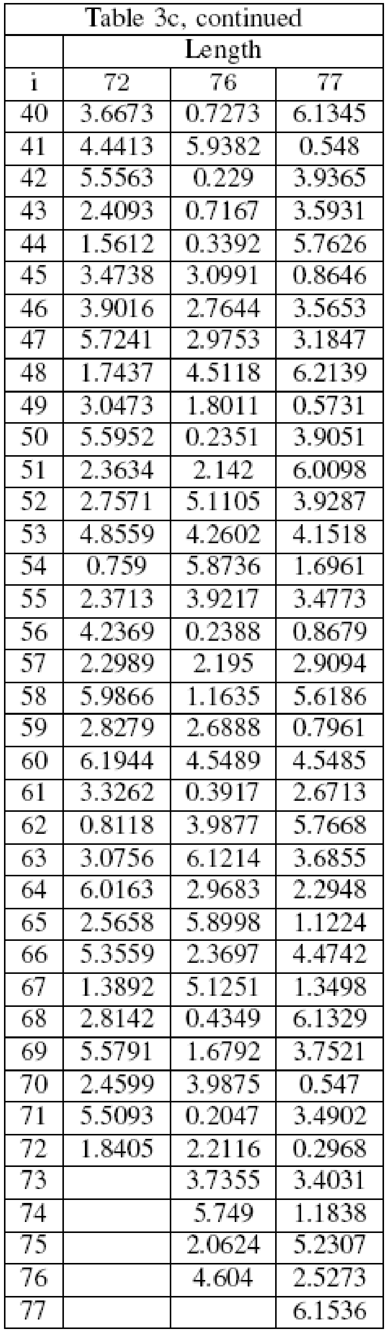

Table 3c, continued

	Length		
i	72	76	77
40	3.6673	0.7273	6.1345
41	4.4413	5.9382	0.548
42	5.5563	0.229	3.9365
43	2.4093	0.7167	3.5931
44	1.5612	0.3392	5.7626
45	3.4738	3.0991	0.8646
46	3.9016	2.7644	3.5653
47	5.7241	2.9753	3.1847
48	1.7437	4.5118	6.2139
49	3.0473	1.8011	0.5731
50	5.5952	0.2351	3.9051
51	2.3634	2.142	6.0098
52	2.7571	5.1105	3.9287
53	4.8559	4.2602	4.1518
54	0.759	5.8736	1.6961
55	2.3713	3.9217	3.4773
56	4.2369	0.2388	0.8679
57	2.2989	2.195	2.9094
58	5.9866	1.1635	5.6186
59	2.8279	2.6888	0.7961
60	6.1944	4.5489	4.5485
61	3.3262	0.3917	2.6713
62	0.8118	3.9877	5.7668
63	3.0756	6.1214	3.6855
64	6.0163	2.9683	2.2948
65	2.5658	5.8998	1.1224
66	5.3559	2.3697	4.4742
67	1.3892	5.1251	1.3498
68	2.8142	0.4349	6.1329
69	5.5791	1.6792	3.7521
70	2.4599	3.9875	0.547
71	5.5093	0.2047	3.4902
72	1.8405	2.2116	0.2968
73		3.7355	3.4031
74		5.749	1.1838
75		2.0624	5.2307
76		4.604	2.5273
77			6.1536

Nunn, C. J., and Coxson, G. E. :″**Polyphase pulse compression codes with optimal peak and integrated sidelobes**″. *IEEE Trans. on AES.* **45**, 2, pp. 775-781, 2009.

Different phase codes that yield identical a-periodic autocorrelation function magnitude are called *equivalent*. It is easy to see, using properties of the crosscorrelation function, that the following operations on a phase code u_m give equivalent phase codes:

-A reversal transformation: $\hat{u}_m=u_{M-m}$.

-A conjugate transformation: $\hat{u}_m=u^*_m$.

-A constant multiplication transformation: $\hat{u}_m=\eta u_m$ where $|\eta|=1$.

-A progressive multiplication transformation: $\hat{u}_m=\rho^m u_m$ where $|\rho|=1$.

It is easy to show that every polyphase code is equivalent to one which begins $\{\phi_1=0,\ \phi_2=0,\ \phi_3\ \ldots\}$ where $0\le\phi_3\le\pi$. This form of the polyphase code is known as the *normalized form*.

Constant multiplication transformation: The crosscorrelation of sequences multiplied by a constant is the multiplied crosscorrelation of the original sequences

$$R_{\hat{u}\hat{v}}[k]=\sum_m \hat{u}_m \hat{v}^*_{m+k}=\sum_m \eta_u u_m \eta^*_v v^*_{m+k}=\eta_u\eta^*_v\sum_m u_m v^*_{m+k}=\eta_u\eta^*_v R_{uv}[k]$$

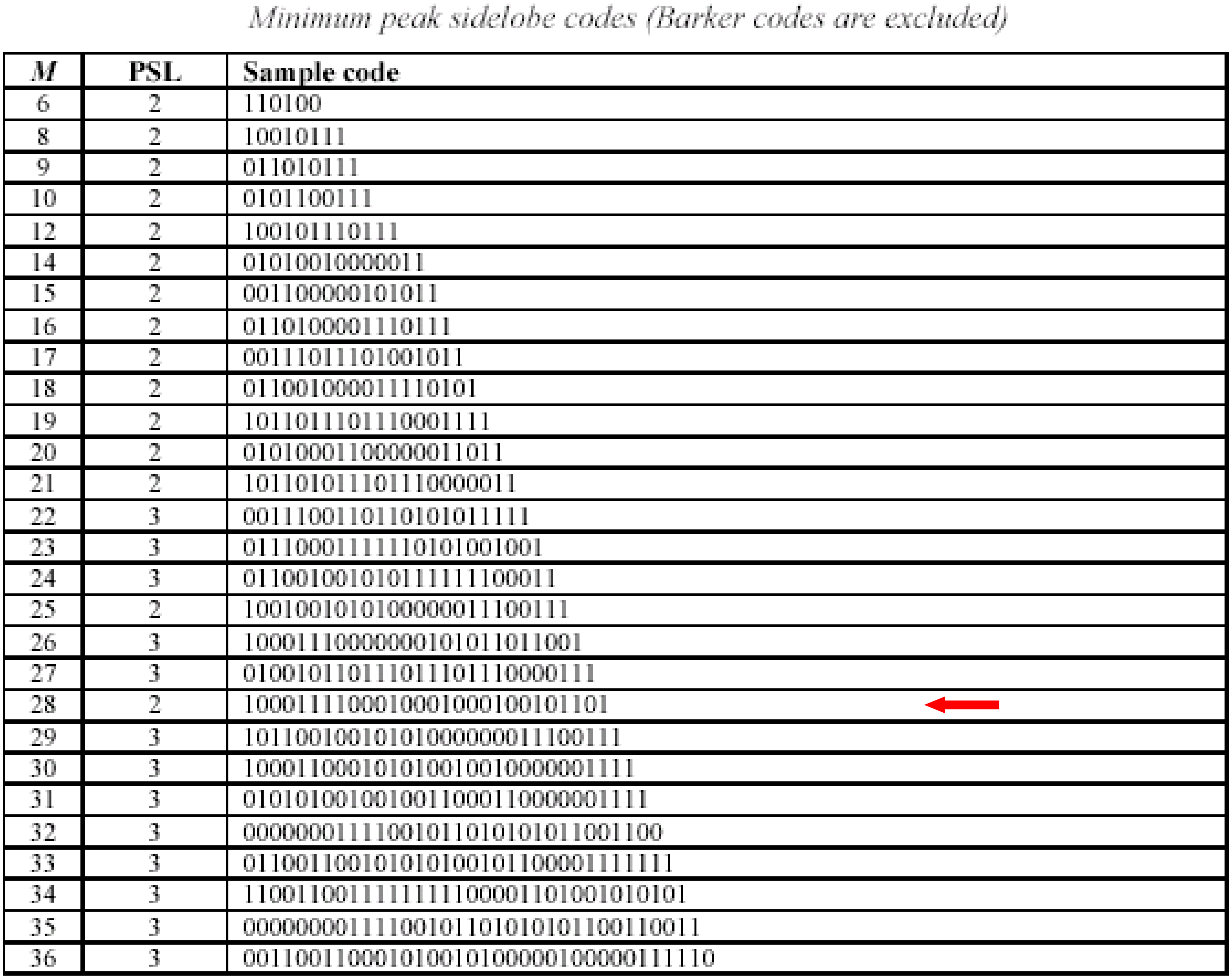

Minimum peak sidelobe codes (Barker codes are excluded)

M	PSL	Sample code
6	2	110100
8	2	10010111
9	2	011010111
10	2	0101100111
12	2	100101110111
14	2	01010010000011
15	2	001100000101011
16	2	0110100001110111
17	2	00111011101001011
18	2	011001000011110101
19	2	1011011101110001111
20	2	01010001100000011011
21	2	101101011101110000011
22	3	0011100110110101011111
23	3	01110001111110101001001
24	3	011001001010111111100011
25	2	1001001010100000011100111
26	3	10001110000000101011011001
27	3	010010110111011101110000111
28	2	1000111100010001000100101101
29	3	10110010010101000000011100111
30	3	100011000101010010010000001111
31	3	0101010010010011000110000001111
32	3	00000001111001011010101011001100
33	3	011001100101010100101100001111111
34	3	1100110011111111100001101001010101
35	3	00000000111100101101010101100110011
36	3	001100110001010010100000100000111110

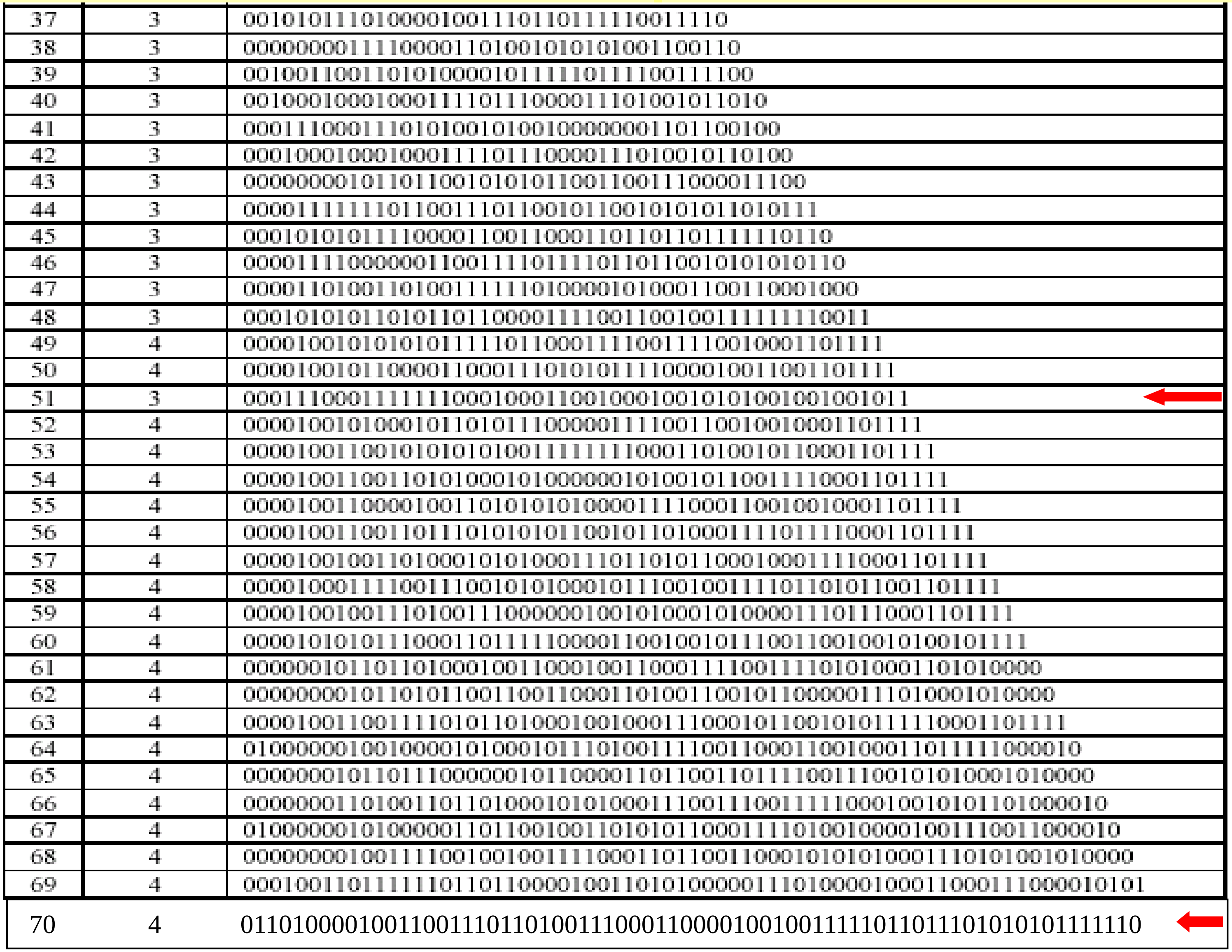

37	3	0010101110100001001110110111110011110	
38	3	00000000111100001101001010101001100110	
39	3	001001100110101000010111110111100111100	
40	3	0010001000100011110111000011101001011010	
41	3	00011100011101010010100100000001101100100	
42	3	000100010001000111101110000111010010110100	
43	3	0000000010110110010101011001100111000011100	
44	3	00001111111011001110110010110010101011010111	
45	3	000101010111100001100110001101101101111110110	
46	3	0000111100000011001111011110110110010101010110	
47	3	00001101001101001111110100001010001100110001000	
48	3	000101010110101101100001111001100100111111110011	
49	4	0000100101010101111101100011110011110010001101111	
50	4	00001001011000011000111010101111000010011001101111	
51	3	000111000111111100010001100100010010101001001001011	←
52	4	0000100101000101101011100000111100110010010001101111	
53	4	00001001100101010101001111111100011010010110001101111	
54	4	000010011001101010001010000001010010110011110001101111	
55	4	0000100110000100110101010100001111000110010010001101111	
56	4	00001001100110111010101011001011010001111011110001101111	
57	4	000010010011010001010100011101101011000100011110001101111	
58	4	0000100011110011100101010001011100100111101101011001101111	
59	4	00001001001110100111000000100101000101000011101110001101111	
60	4	000010101011100011011111000011001001011100110010010100101111	
61	4	0000001011011010001001100010011000111100111101010001101010000	
62	4	00000000101101011001100110001101001100101100000111010001010000	
63	4	000010011001111010110100010010001110001011001010111110001101111	
64	4	0100000010010000101000101110100111100110001100100011011111000010	
65	4	00000001011011100000010110000110110011011110011100101010001010000	
66	4	000000011010011011010001010100011100111001111100010010101101000010	
67	4	0100000010100000110110010011010101100011110100100001001110011000010	
68	4	00000000100111100100100111100011011001100010101010001110101001010000	
69	4	000100110111111011011000010011010100000111010000100011000111000010101	
70	4	0110100001001100111011010011100011000010010011111011011101010101111110	←

Coxson G. and Russo J. "Efficient exhaustive search for optimal-peak-sidelobe binary codes", IEEE 2004 Radar Conf., Philadelphia, pp. 438-443. Also *IEEE Trans. on AES*, **41**,1, (Jan. 2005), pp. 302-308.

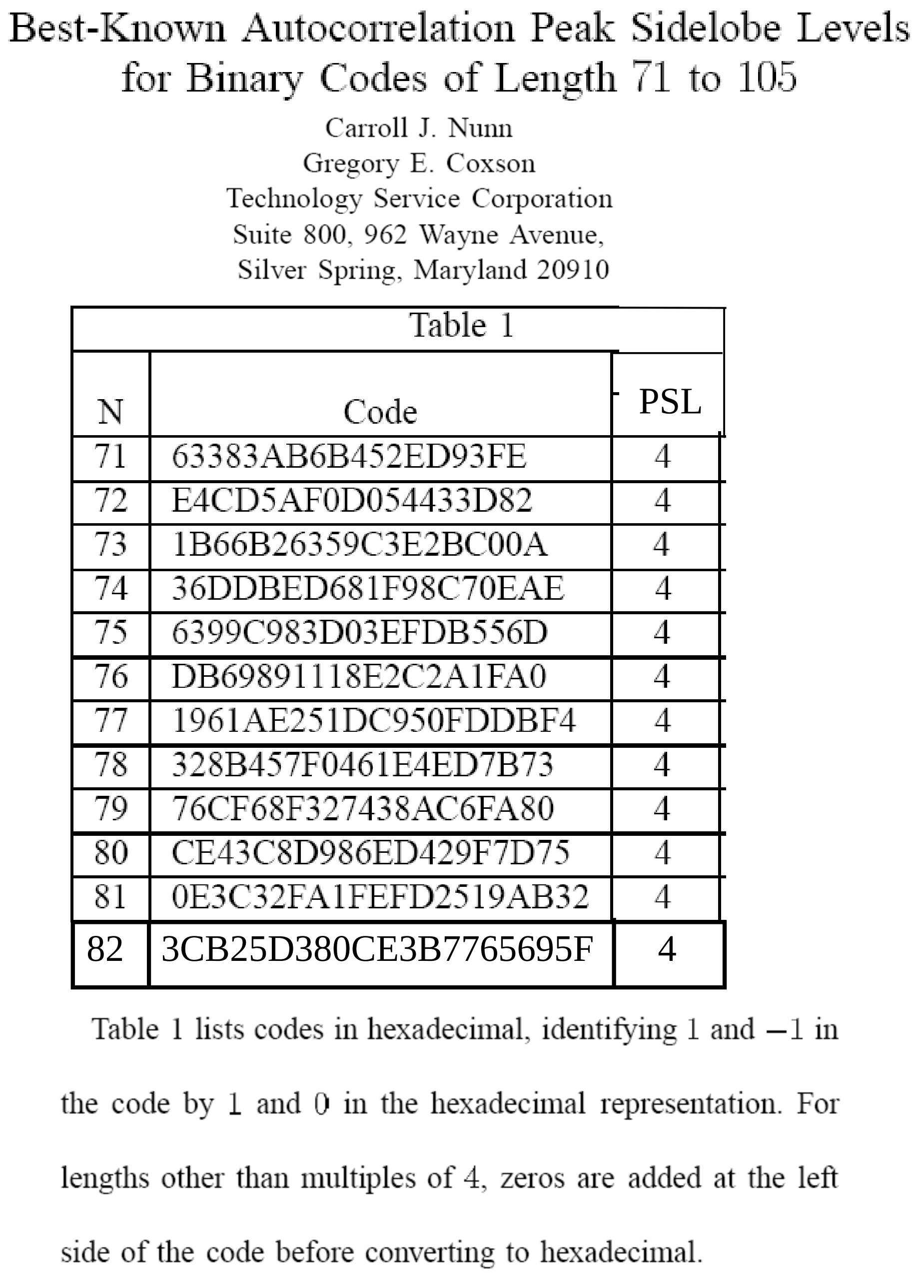

Best-Known Autocorrelation Peak Sidelobe Levels for Binary Codes of Length 71 to 105

Carroll J. Nunn
Gregory E. Coxson
Technology Service Corporation
Suite 800, 962 Wayne Avenue,
Silver Spring, Maryland 20910

Table 1

N	Code	PSL
71	63383AB6B452ED93FE	4
72	E4CD5AF0D054433D82	4
73	1B66B26359C3E2BC00A	4
74	36DDBED681F98C70EAE	4
75	6399C983D03EFDB556D	4
76	DB69891118E2C2A1FA0	4
77	1961AE251DC950FDDBF4	4
78	328B457F0461E4ED7B73	4
79	76CF68F327438AC6FA80	4
80	CE43C8D986ED429F7D75	4
81	0E3C32FA1FEFD2519AB32	4
82	3CB25D380CE3B7765695F	4

Table 1 lists codes in hexadecimal, identifying 1 and −1 in the code by 1 and 0 in the hexadecimal representation. For lengths other than multiples of 4, zeros are added at the left side of the code before converting to hexadecimal.

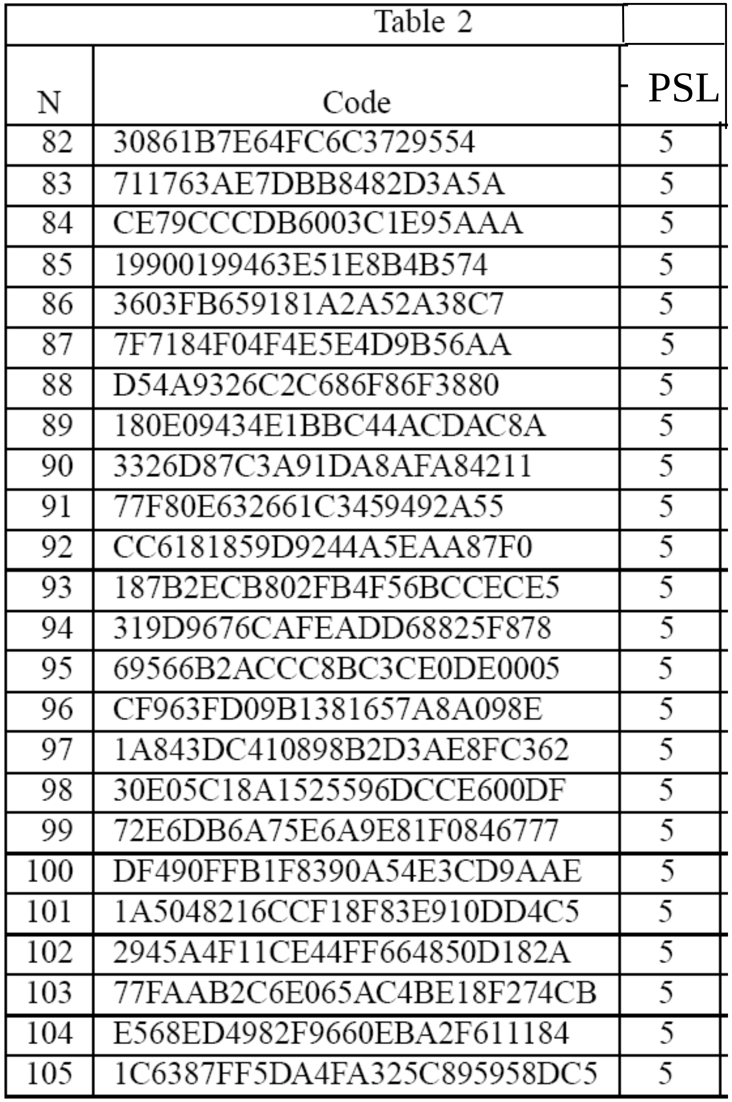

Table 2

N	Code	PSL
82	30861B7E64FC6C3729554	5
83	711763AE7DBB8482D3A5A	5
84	CE79CCCDB6003C1E95AAA	5
85	19900199463E51E8B4B574	5
86	3603FB659181A2A52A38C7	5
87	7F7184F04F4E5E4D9B56AA	5
88	D54A9326C2C686F86F3880	5
89	180E09434E1BBC44ACDAC8A	5
90	3326D87C3A91DA8AFA84211	5
91	77F80E632661C3459492A55	5
92	CC6181859D9244A5EAA87F0	5
93	187B2ECB802FB4F56BCCECE5	5
94	319D9676CAFEADD68825F878	5
95	69566B2ACCC8BC3CE0DE0005	5
96	CF963FD09B1381657A8A098E	5
97	1A843DC410898B2D3AE8FC362	5
98	30E05C18A1525596DCCE600DF	5
99	72E6DB6A75E6A9E81F0846777	5
100	DF490FFB1F8390A54E3CD9AAE	5
101	1A5048216CCF18F83E910DD4C5	5
102	2945A4F11CE44FF664850D182A	5
103	77FAAB2C6E065AC4BE18F274CB	5
104	E568ED4982F9660EBA2F611184	5
105	1C6387FF5DA4FA325C895958DC5	5

Ron Ferguson and Peter Borwein

Simon Fraser University, Canada

`ronf@irmacs.sfu.ca ,pborwein@cecm.sfu.ca`

PSL=5:

N = 106
345D52C1A9412871027F6CE6133
38034442C45CBE68943D2CE6B21
3B9D66D12077DEA98F9E96D08F8

N = 107
7B6A20356519F937CC7A753AC7C
6EAE32EB0537FCBEC4F1D8B12D4
F4947B5A3756777EBB3488E1F70
679C606EDE06A551BD836505049

N = 108
CC267AC7245F5C1E0481592B656
FDBB76F94097C56718CBCD49E8F
F4947B5A3756777EBB3488E1F70

N = 113
1E90FC54B4E259765D3FF7628CDCE

PSL = 24:

N = 1112
FFEB761F4F18B489C76E27ACE89E7486183DA96FEFBA4FC9DA8D1A
A1D638386EA2BBAD77515D87071AE1562C56E4FC977DFDA56F061
84B9E45CD791DB8E44B463CBE1BB5FAC020CCB61D151800C4DB69
4428B56599A837F5988BF5265F84AF80BE0D0DCF9CC4958C635246
73E76160FA03EA43F4C95FA2335FD82B334D5A28452DB646003151
70DA660802

EFF5BB0FA78C5A44E3B713D6744F3A430C1ED4B7F7DD27E4ED468
D50EB1C1C37515DD6BBA8AEC3838D70AB162B727E4BBEFED2B783
0C25CF22E6BC8EDC7225A31E5F0DDAFD6010665B0E8A8C00626DB
4A2145AB2CCD41BFACC45FA932FC257C05F0686E7CE624AC631A92
339F3B0B07D01F521FA64AFD119AFEC1599A6AD142296DB230018A
8B86D330401

N = 113, PSL=5: 1E90FC54B4E259765D3FF7628CDCE

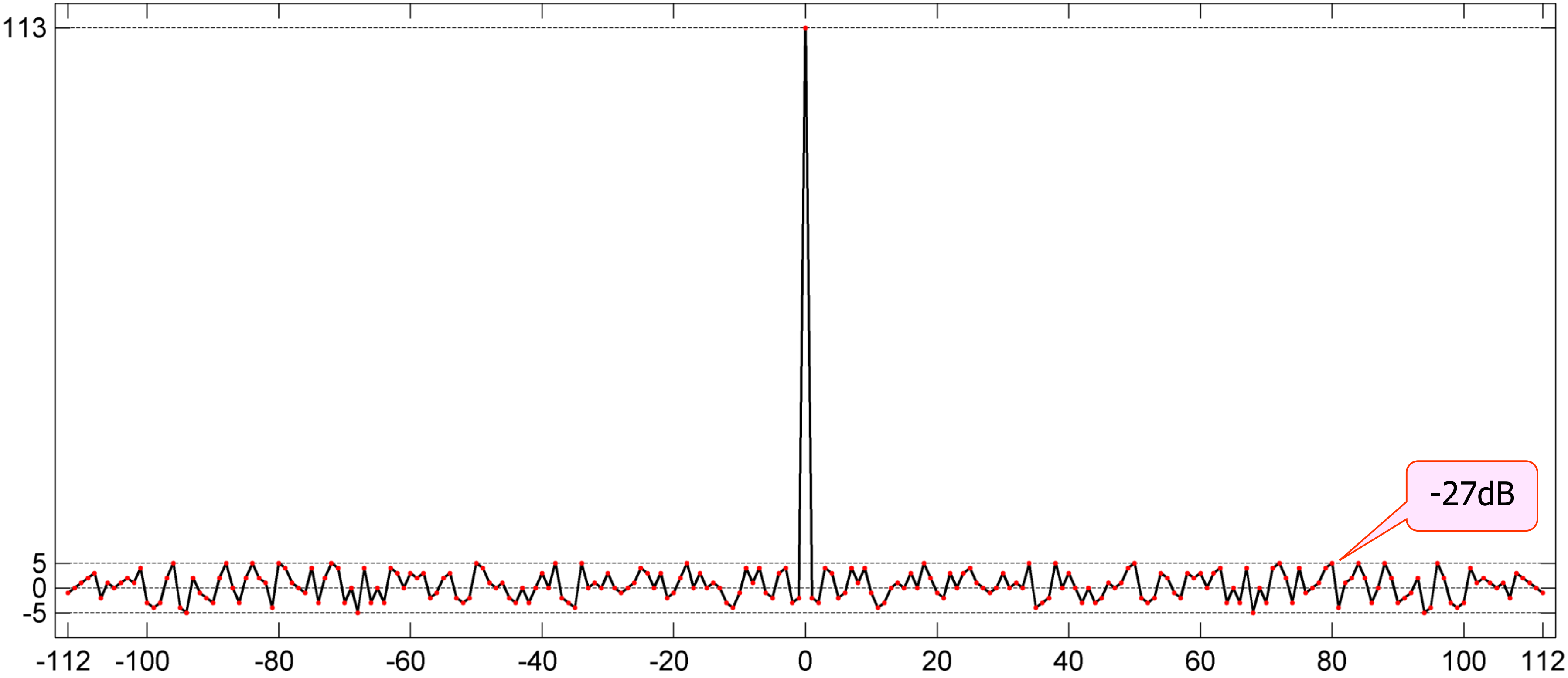

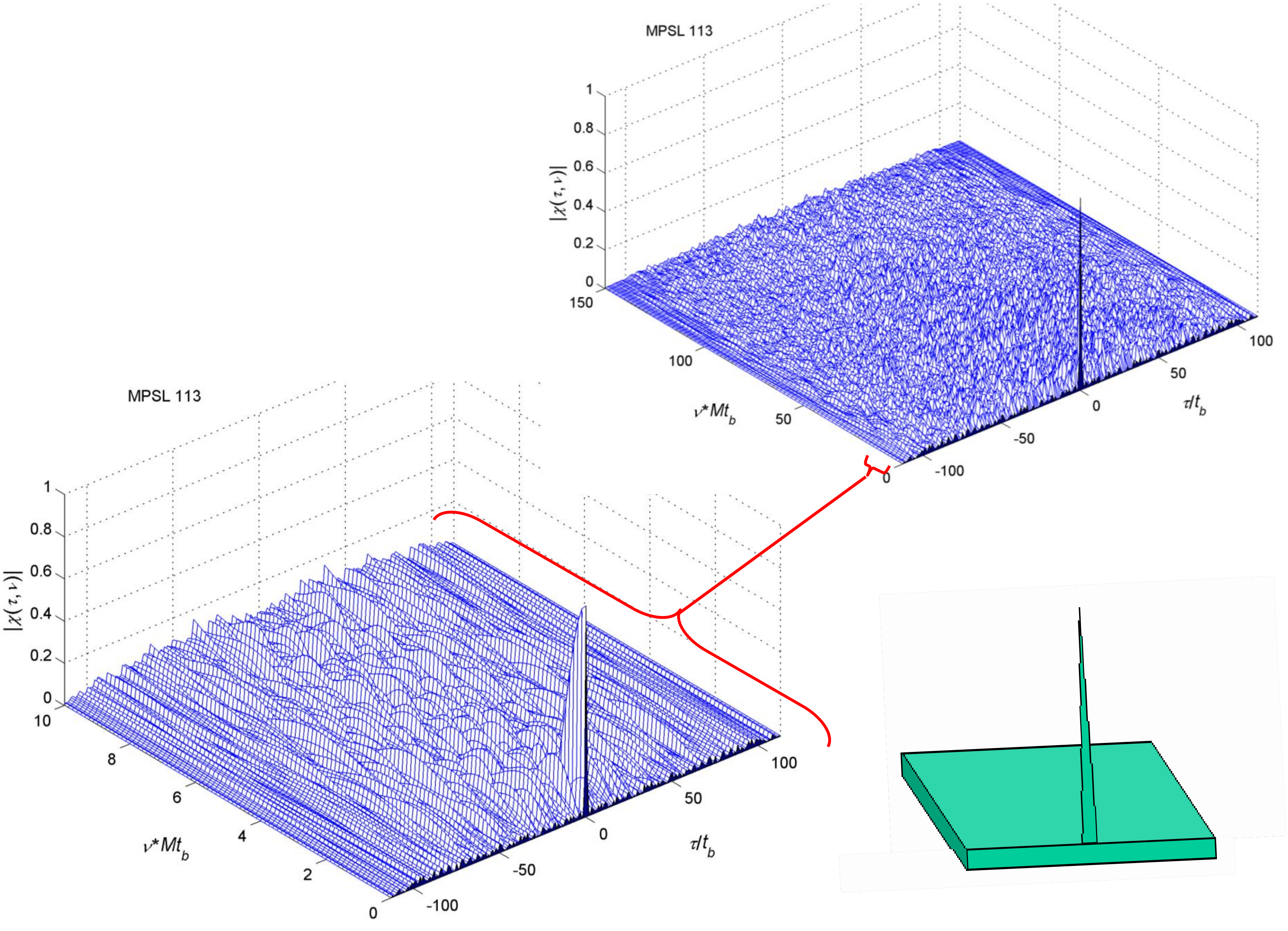
MPSL 113
$|\chi(\tau,\nu)|$
1
0.8
0.6
0.4
0.2
0
150
100
50
0
ν*Mt_b
-100
-50
0
50
100
τ/t_b
MPSL 113
$|\chi(\tau,\nu)|$
1
0.8
0.6
0.4
0.2
0
10
8
6
4
2
0
ν*Mt_b
-100
-50
0
50
100
τ/t_b

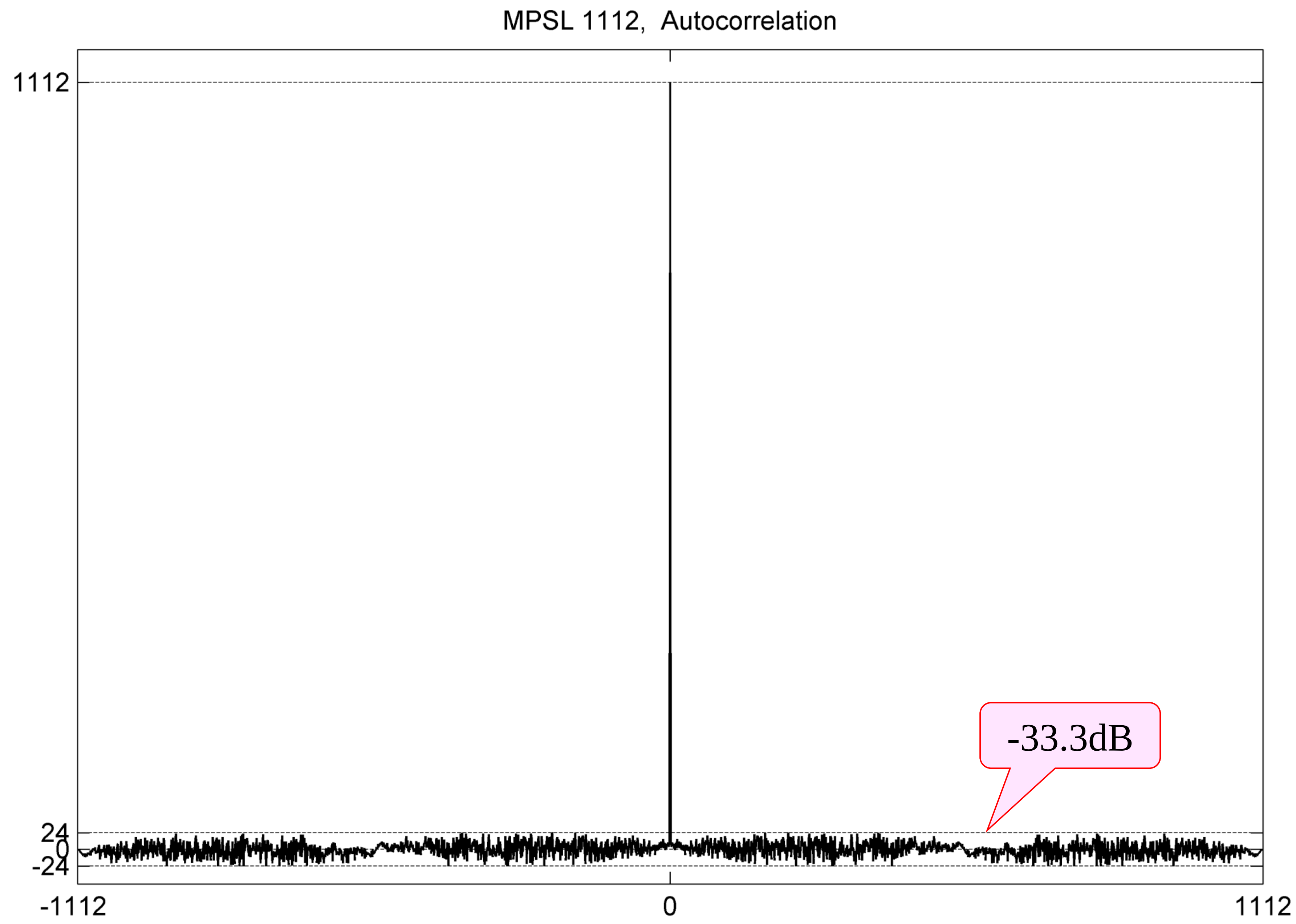

-33.3dB

State of the art of the search for binary codes with good ACF

PSL	Length of longest known code, N_{max}	N_{max}/PSL	PSL+16
1	13	13	
2	28	14	
3	51	17	19
4	82	20.5	20
5	113	22.6	21
6	140	23.3	22
7	167	23.9	23
8	202	25.2	24
10	259	25.9	26
24	1112	46.3	40
28	1559	55.7	44

Date: 29 Oct 2008 , From: "Ronald Ferguson" <ronf@univlora.edu.al>

For PSL=5, we have examples at lengths 106-109 and at 112, 113.
For PSL=6, we have examples at lengths to 132 and at 134-137, 140.
For PSL=7, we have examples at lengths to 161 and at 163-165, 167.
For PSL=8, we have examples at lengths to 192, and at 194, 196, 198-200, 202.

Courtesy of Dr. Ronald Ferguson, University of Vlora, Albania
(Previously with Simon Frazer University, Canada.)

Status of the search for long binary MPSL codes (Oct. 2008)

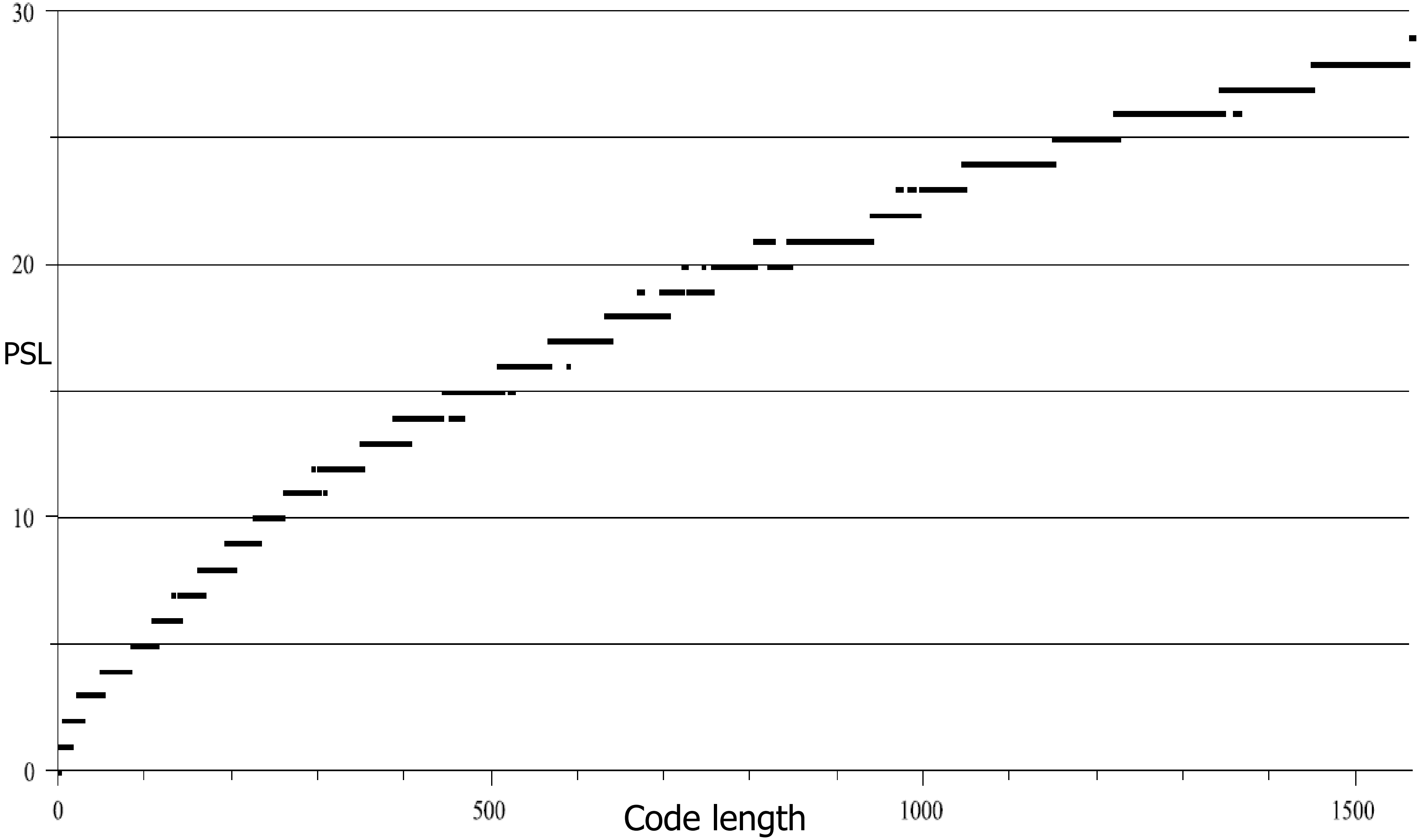

BEST QUADRIPHASE CODES UP TO LENGTH 24

W. H. Mow

Indexing terms: Codes, Information theory

Quadriphase codes with minimum peak sidelobe magnitudes up to length 24 are found by the exhaustive search method. In particular, of these best quadriphase codes, all those achieving the maximum factor of merit are listed.

18th March 1993

W. H. Mow (*Department of Information Engineering, Chinese University of Hong Kong, Shatin, Hong Kong*)

ELECTRONICS LETTERS 13th May 1993 Vol. 29 No. 10

$$
\begin{aligned}
0 &= 1\\
1 &= j\\
2 &= -1\\
3 &= -j
\end{aligned}
$$

N	PSL	Optimal-PSL Code
2	1	00
3	1	002
4	1	0002; 0013
5	1	00020
6	$\sqrt{2}$	000132; 000201 ; 001023; 001203 001303; 002010; 002121
7	1	0002202
8	$\sqrt{2}$	00103120
9	$\sqrt{2}$	000021302
10	$\sqrt{2}$	0001023113
11	1	00022202202
12	$\sqrt{2}$	000120032021
13	1	0000022002020
14	$\sqrt{2}$	00000220020201
15	1	000110331231020
16	$\sqrt{2}$	0000110331231020
17	$\sqrt{2}$	00000123020203210; 00221330131011010
18	2	000001230131310321; 000002022020002200; 000022220202200220; 001220320033323130; 002200221210101212
19	2	0000120003231321020; 0001121003203231202; 0013330231320333100
20	2	00000200220202002220; 00010202122100201200; 00102021222012022100
21	2	001012132012310221100
22	2	0001113311030232131131
23	2	00123023121212132032100
24	2	001023303213312303320100
25	**2**	**0220220202022222200022000**
26	$\sqrt{5}$	**00001013121033102133022311**

Table II. Optimal PSL and representative optimal-PSL quadphase codes for lengths $2 \leq N \leq 26$.

2016 results by G.E. Coxson and J. C. Ruso

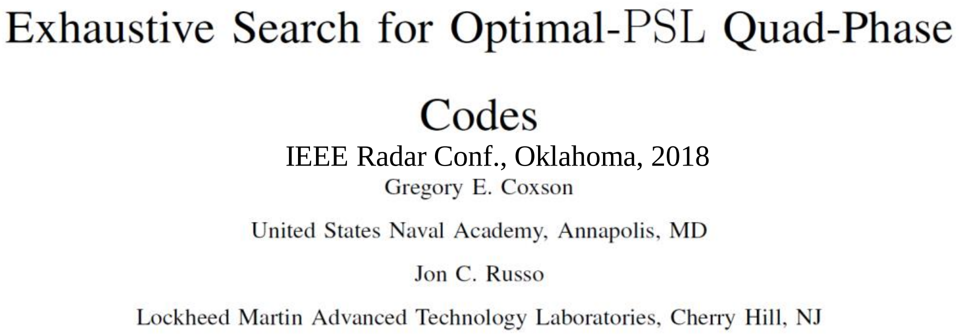

Exhaustive Search for Optimal-PSL Quad-Phase Codes

IEEE Radar Conf., Oklahoma, 2018

Gregory E. Coxson

United States Naval Academy, Annapolis, MD

Jon C. Russo

Lockheed Martin Advanced Technology Laboratories, Cherry Hill, NJ

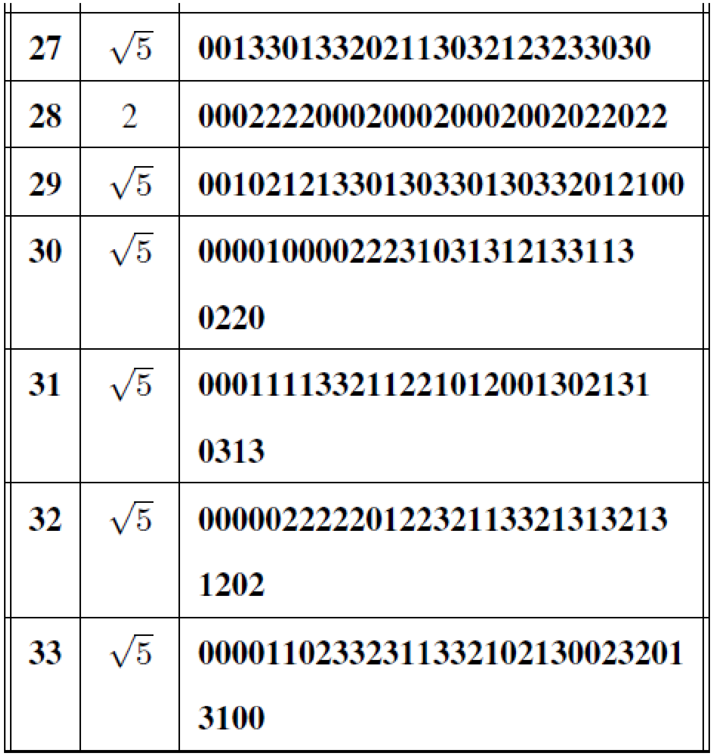

27	$\sqrt{5}$	**001330133202113032123233030**
28	2	**0002222000200020002002022022**
29	$\sqrt{5}$	**00102121330130330130332012100**
30	$\sqrt{5}$	**000010000222310313121331130220**
31	$\sqrt{5}$	**0001111332112210120013021310313**
32	$\sqrt{5}$	**00000222220122321133213132131202**
33	$\sqrt{5}$	**000011023323113321021300232013100**

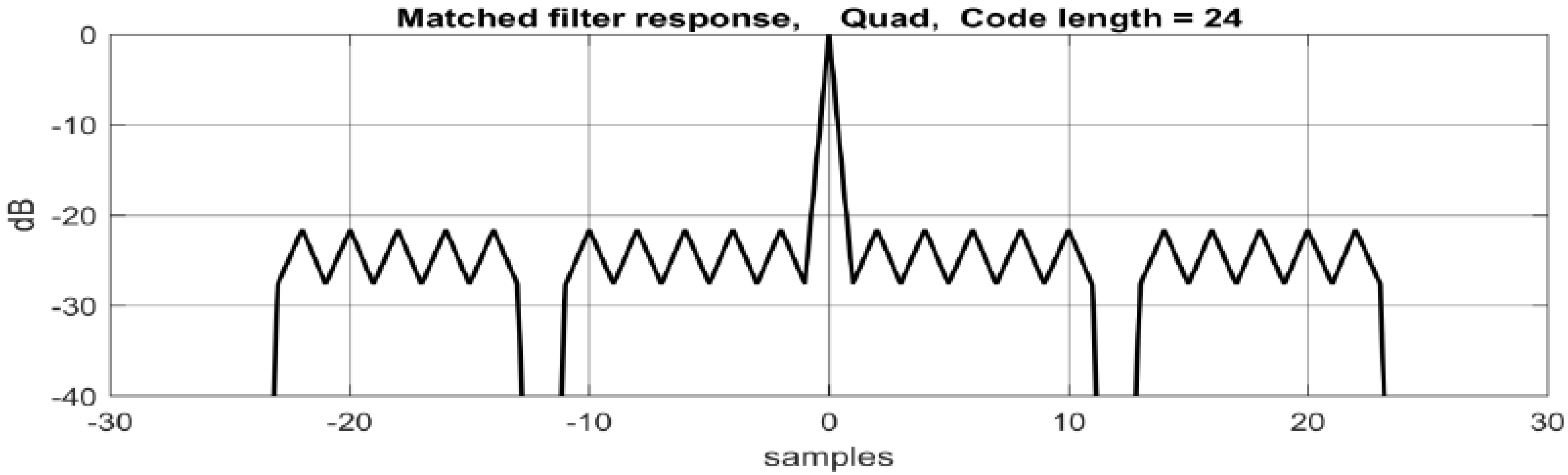
Matched filter response, Quad, Code length = 24
0
-10
-20
-30
-40
dB
-30
-20
-10
0
10
20
30
samples

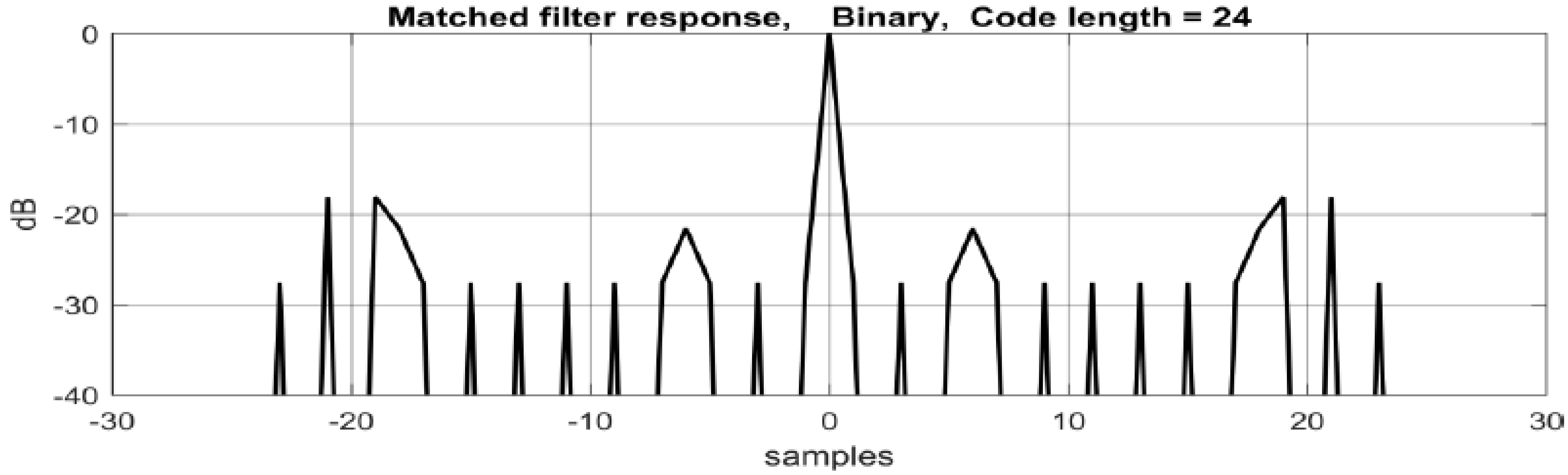
Matched filter response, Binary, Code length = 24
0
-10
-20
-30
-40
dB
-30
-20
-10
0
10
20
30
samples

Improving spectrum efficiency
(Spectrum sidelobe reduction)

Example: **Barker 13**

Approaches:

- Derivative phase
- Biphase to qudriphase transformation
- Replacing the rectangular bit with a “Gaussian windowed sinc” bit

Conventional Barker 13

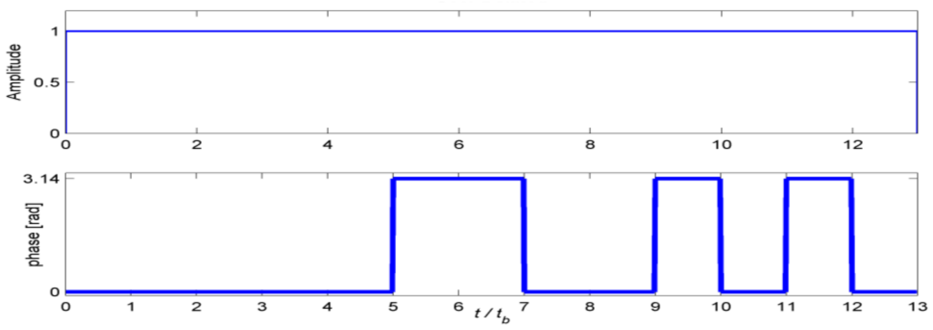

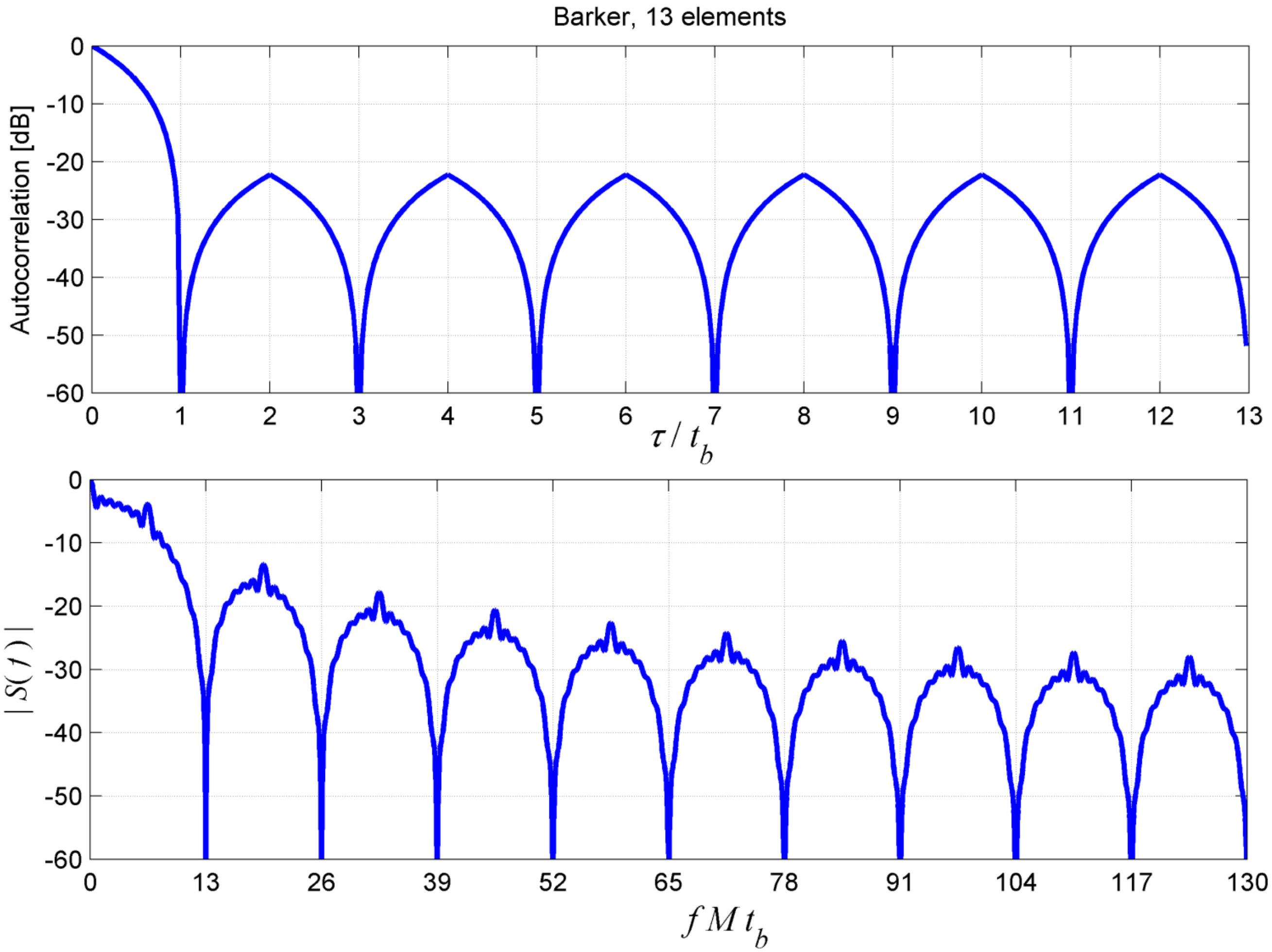

Derivative phase

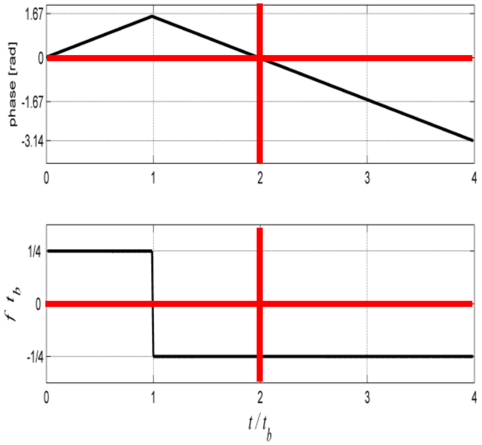

$$f\,t_b = 0.5$$

$$\therefore\ f\,\frac{t_b}{2} = 0.25$$

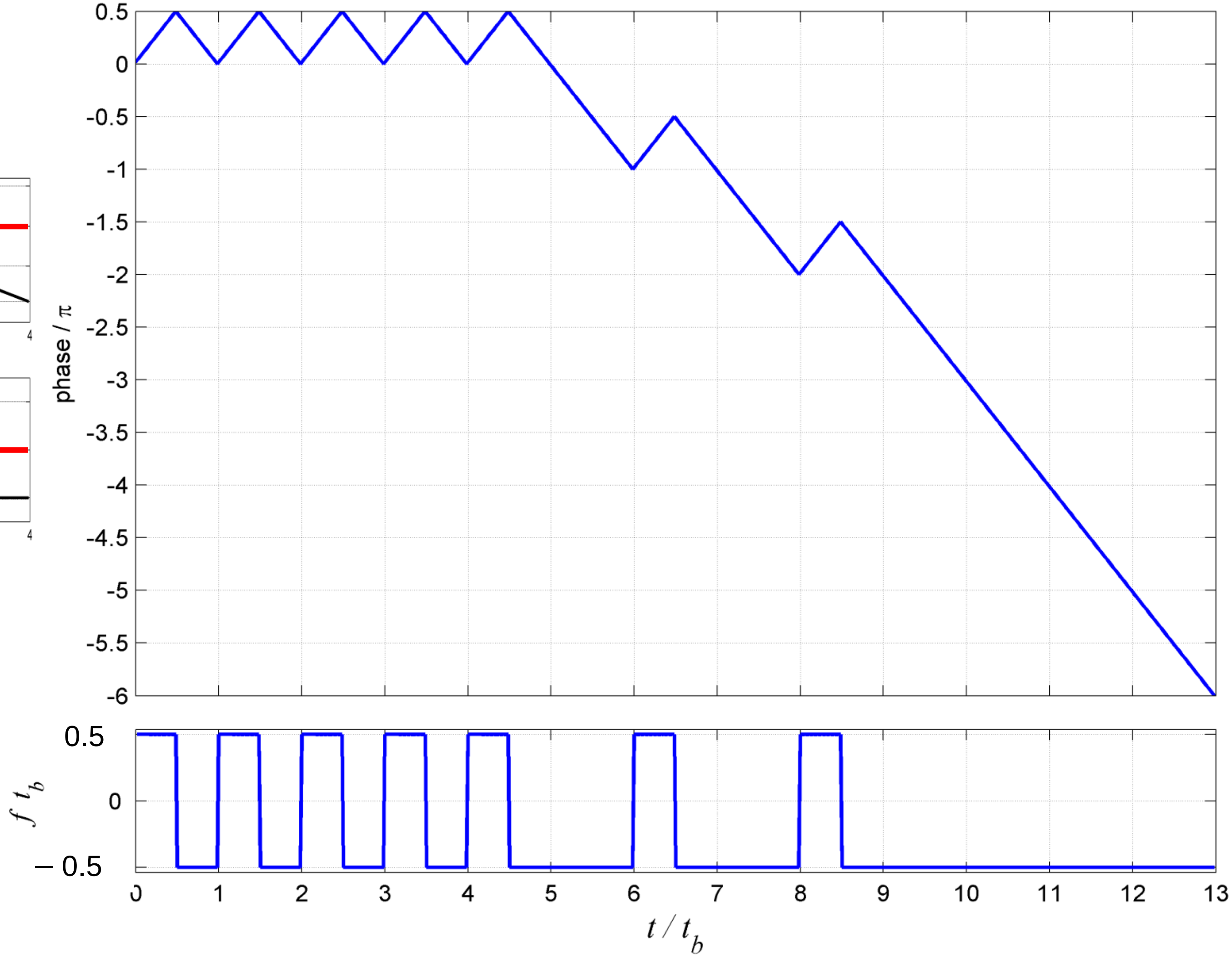

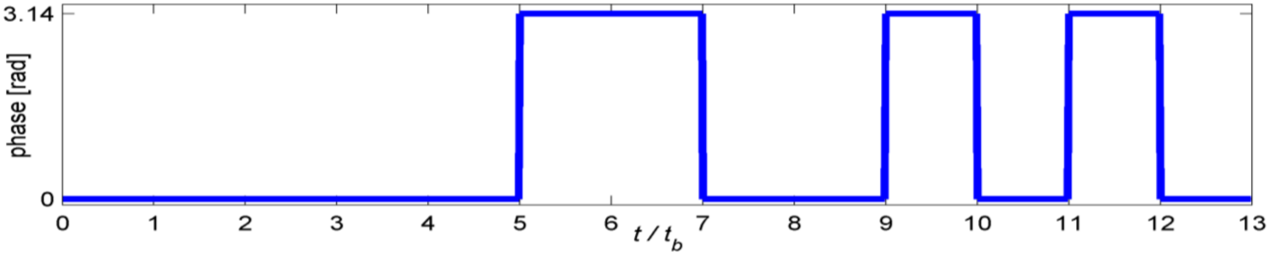

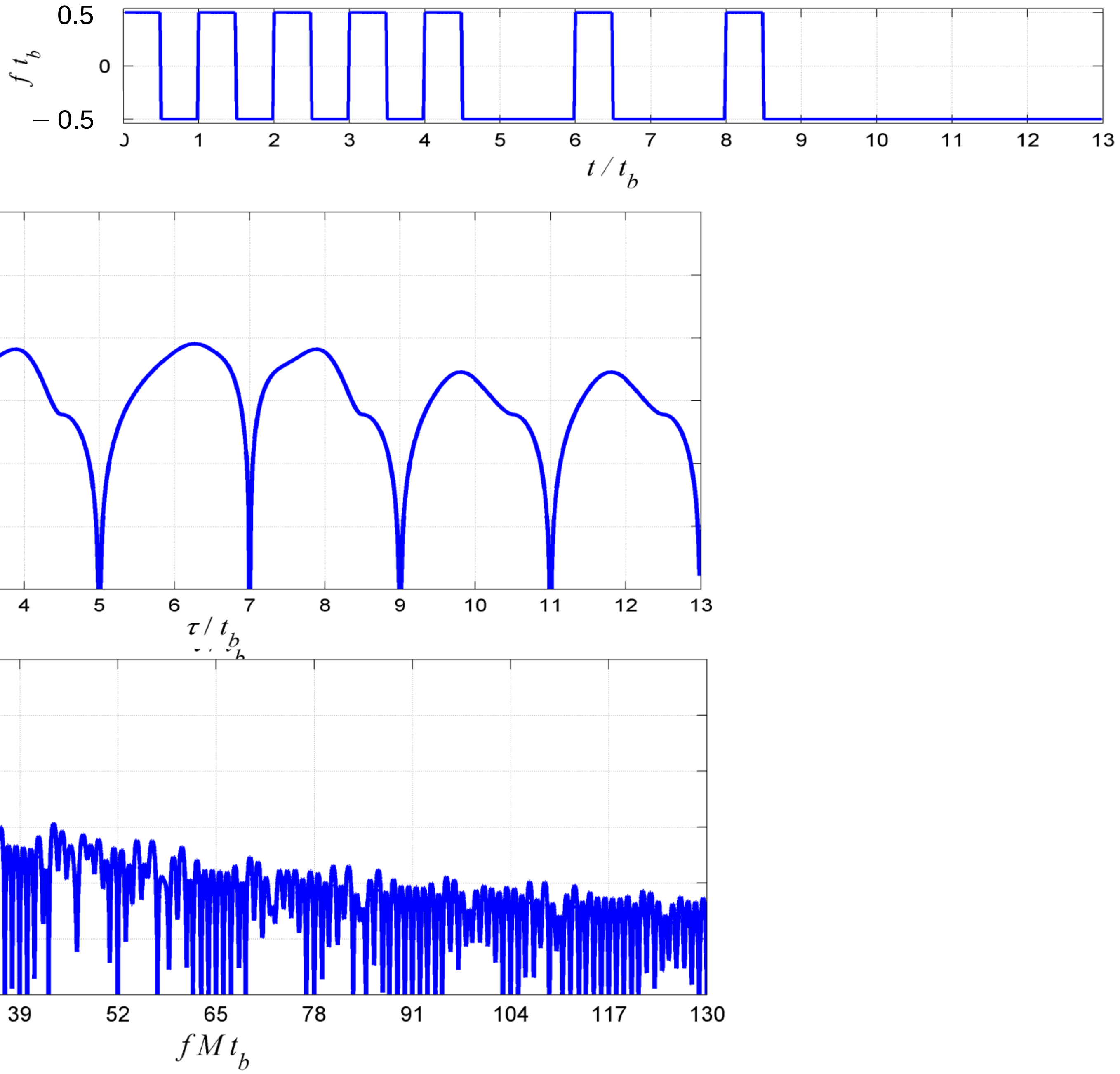
0.5
0
– 0.5
$f\, t_b$
0
1
2
3
4
5
6
7
8
9
10
11
12
13
$t\, /\, t_b$
Autocorrelation [dB]
0
-10
-20
-30
-40
-50
-60
$\tau\, /\, t_b$
$|\, S(f)\, |$
0
13
26
39
52
65
78
91
104
117
130
$f\, M\, t_b$

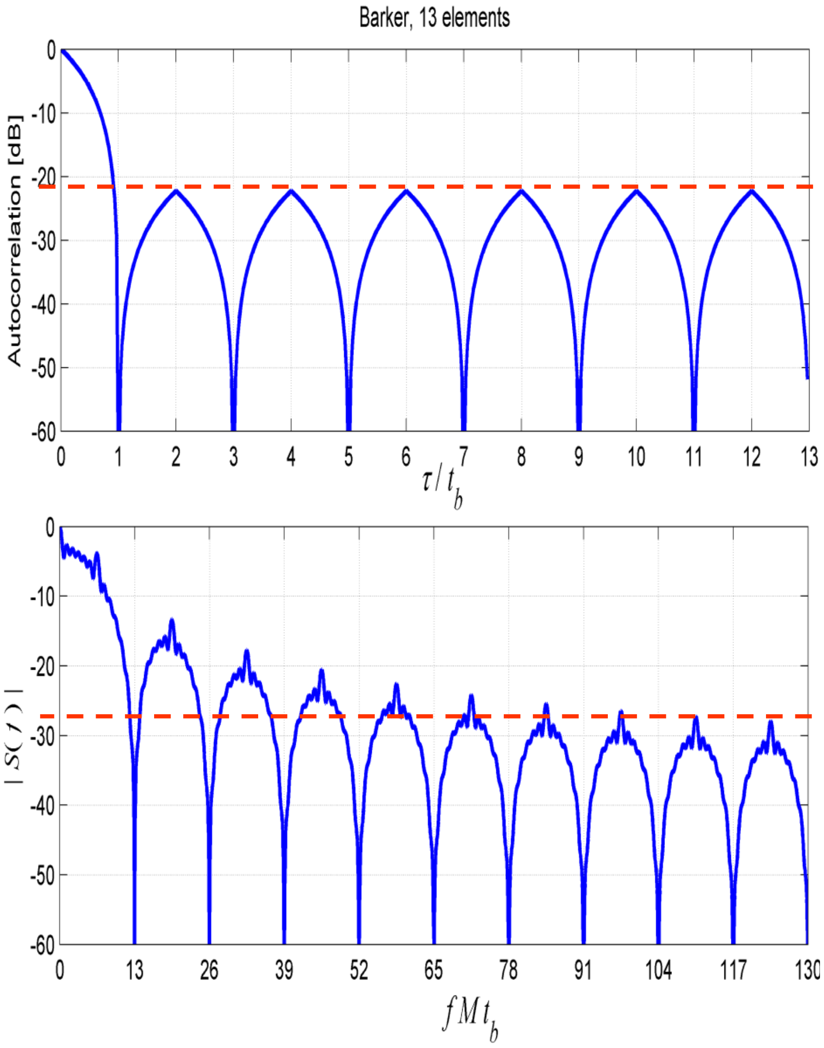

Derivative phase – Barker 13

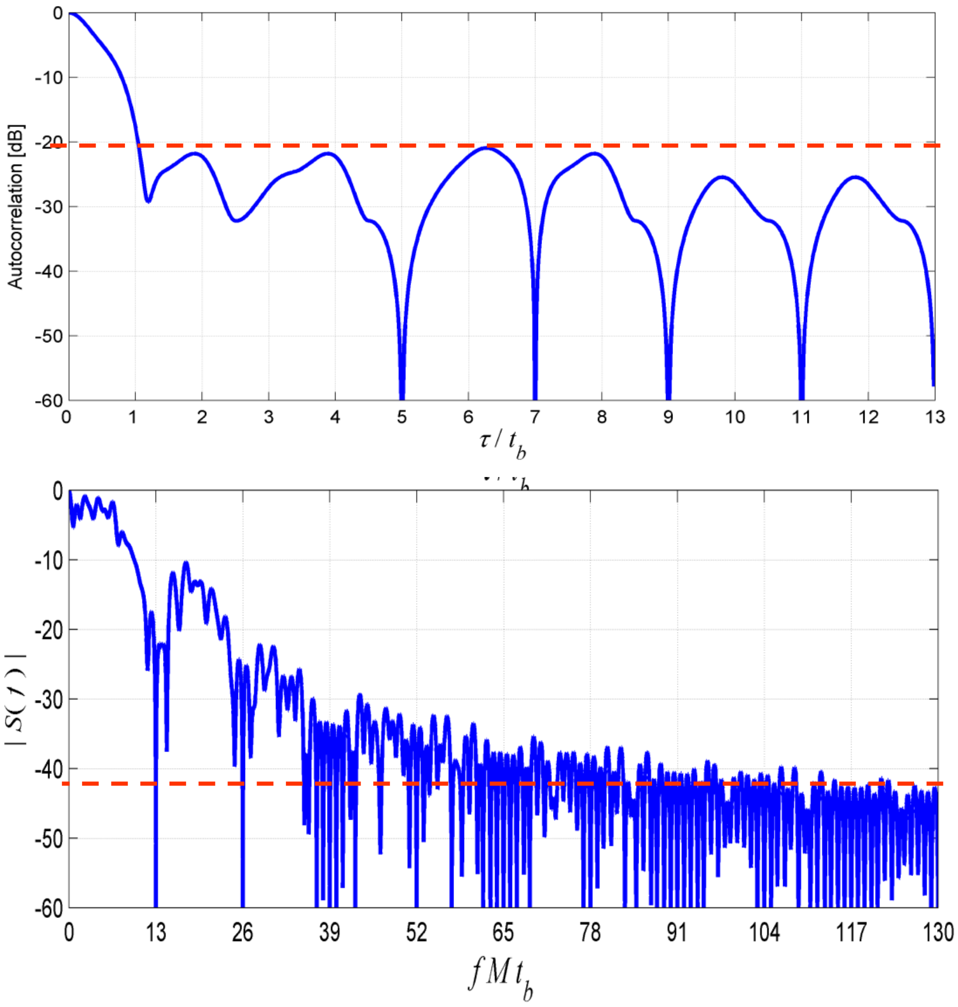

Biphase to qudriphase transformation

$$u(t)=a(t)\exp[j\phi(t)]$$

$$\phi(kt_\mathrm{b})=\begin{cases} 0 & , \quad k=0 \\ s(k-1)\pi/2+\theta_k & , \quad k=1,\dots,M \\ 0 & , \quad k=M+1 \end{cases}$$

$$a(t)=\begin{cases} A\sin(2\pi t/4t_\mathrm{b}) & , \quad 0\le t\le t_\mathrm{b} \\ A & , \quad t_\mathrm{b}\le t\le Mt_\mathrm{b} \\ A\cos[2\pi(t-Mt_\mathrm{b})/4t_\mathrm{b}] & , \quad Mt_\mathrm{b}\le t\le (M+1)t_\mathrm{b} \end{cases}$$

Biphase-to-qudriphase transformation (s=+1) of Barker 13 sequence

k	0	1	2	3	4	5	6	7	8	9	10	11	12	13	14
θ_k		0	0	0	0	0	π	π	0	0	π	0	π	0	
ϕ_k mod 2π	0	0	π/2	π	3π/2	2π	3π/2	2π	3π/2	2π	3π/2	π	π/2	0	0

Taylor, J.W., and Blinchikoff, H.J. "Quadriphase code: a radar pulse compression signal with unique characteristics", *IEEE Trans. on Aerospace and Electronic Systems*, 24, (2), March 1988, pp. 156-170

Qudriphase transformation of Barker 13

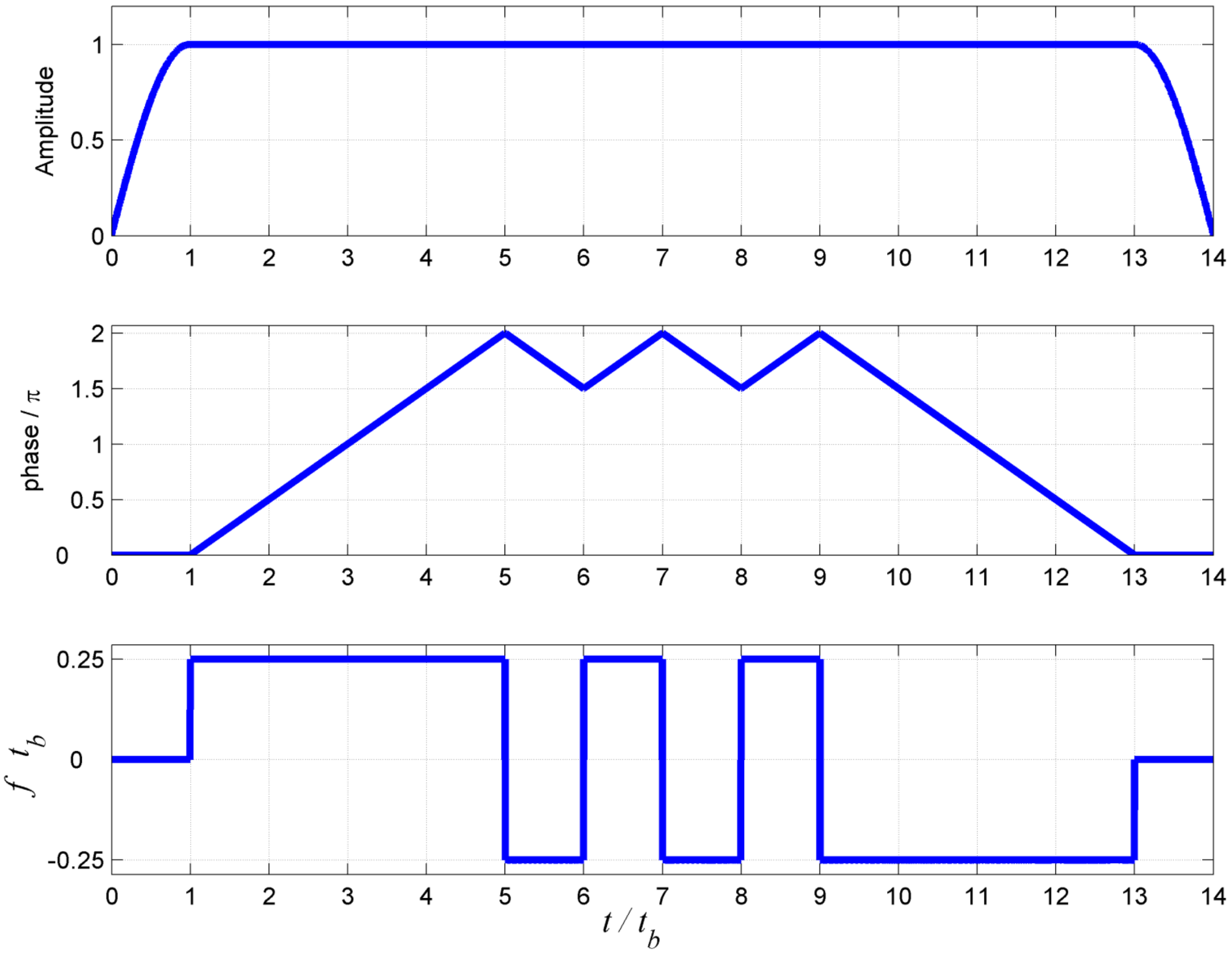

Qudriphase transformation of Barker 13

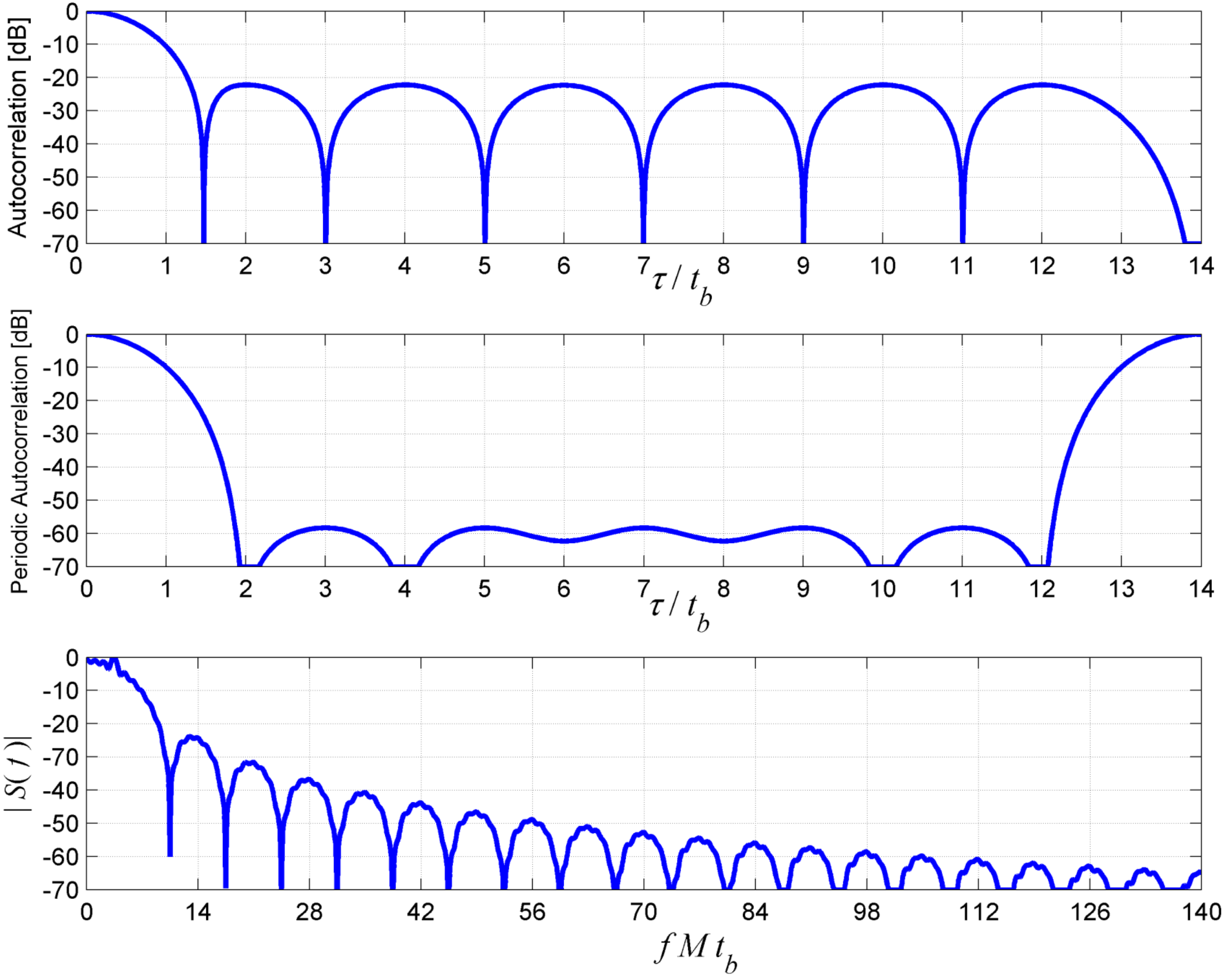

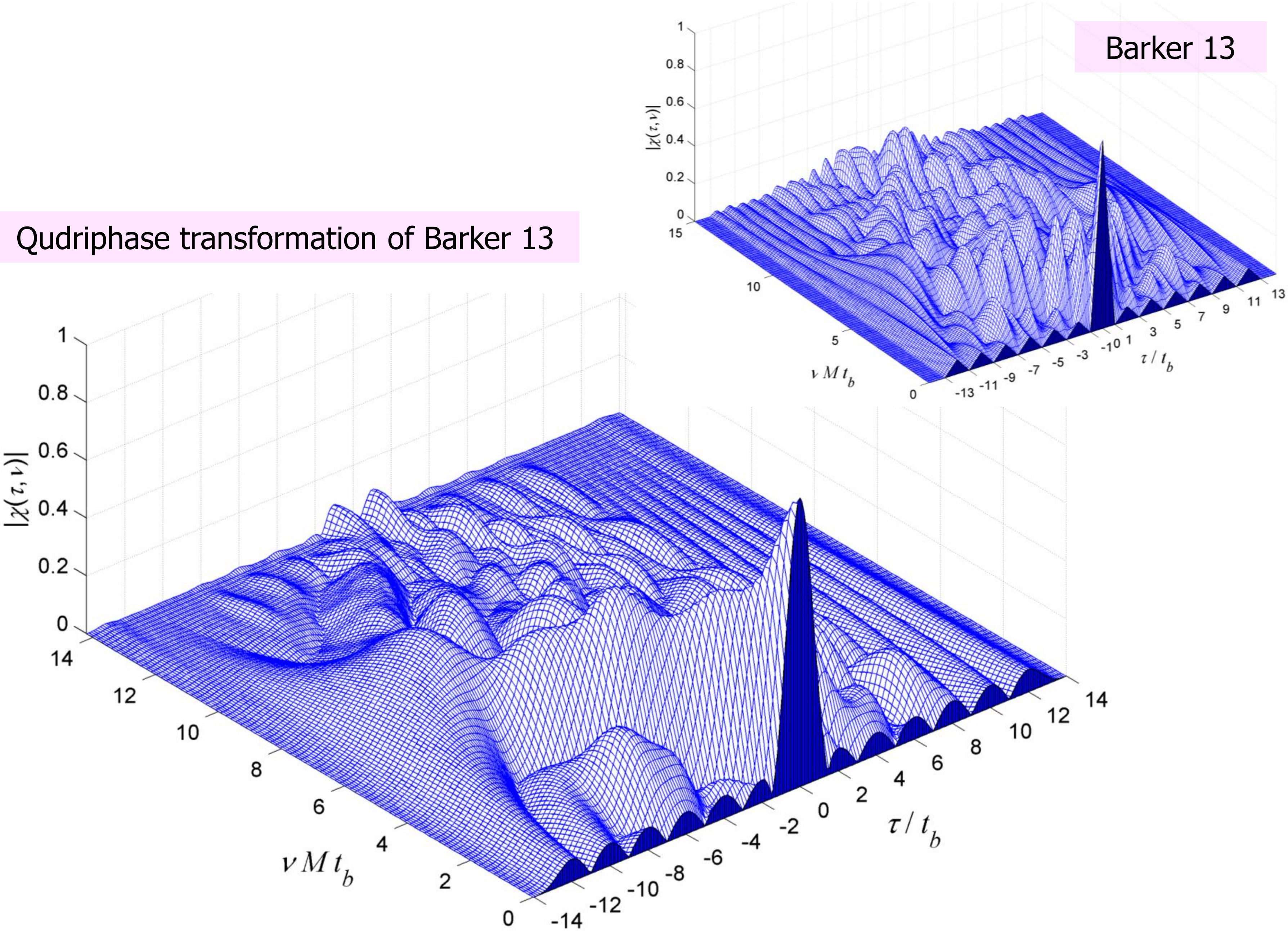

Barker 13

Qudriphase transformation of Barker 13

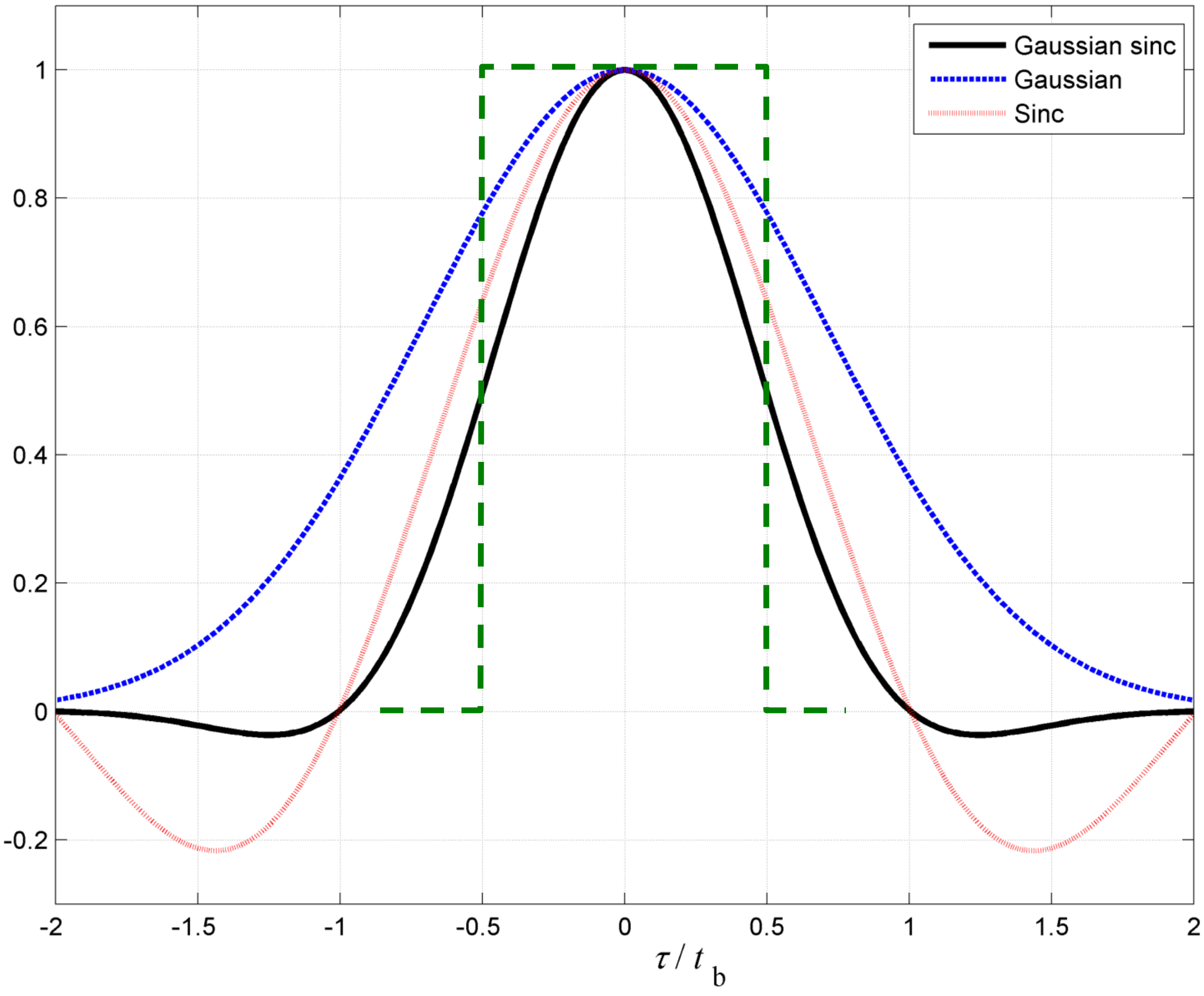

Chen, R., and Cantrell, B., “Highly bandlimited radar signals”, 2002 IEEE Radar Conf., Long Beach CA, April 2002, pp. 220-226.

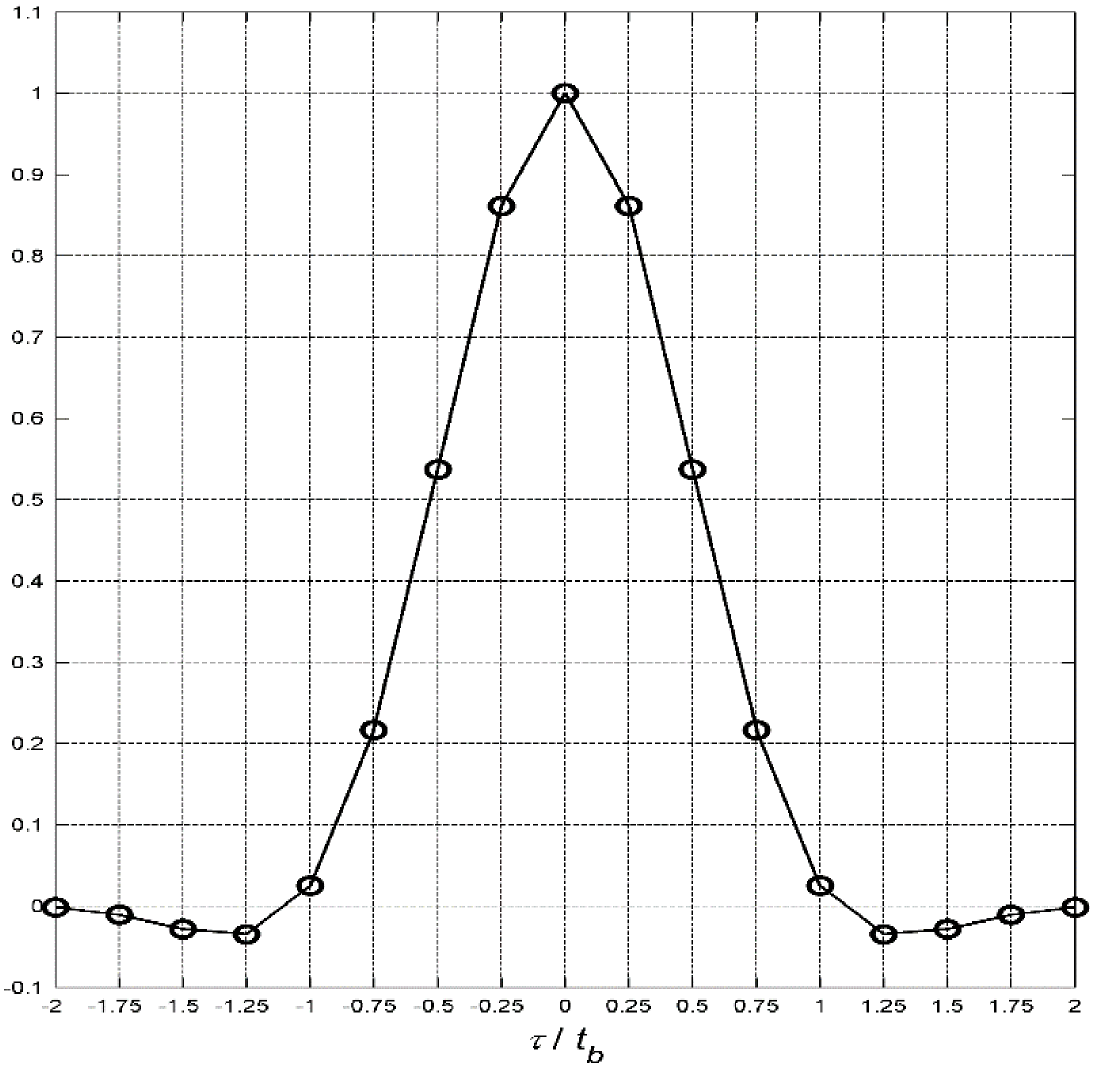

$M = 4$

M is the number of samples per code element (bit).

σ is a parameter chosen as 0.7.

$$GWS_m = \exp\left[-\frac{1}{2}\left(\frac{4m}{\sigma\left(4M+1\right)}\right)^2\right]\frac{\sin\alpha_m}{\alpha_m},\ \alpha_m = \frac{4\pi m}{4M+1},\ m = -2M, -2M+1, \ldots, 2M$$

Barker 13 – using Gaussian windowed sinc

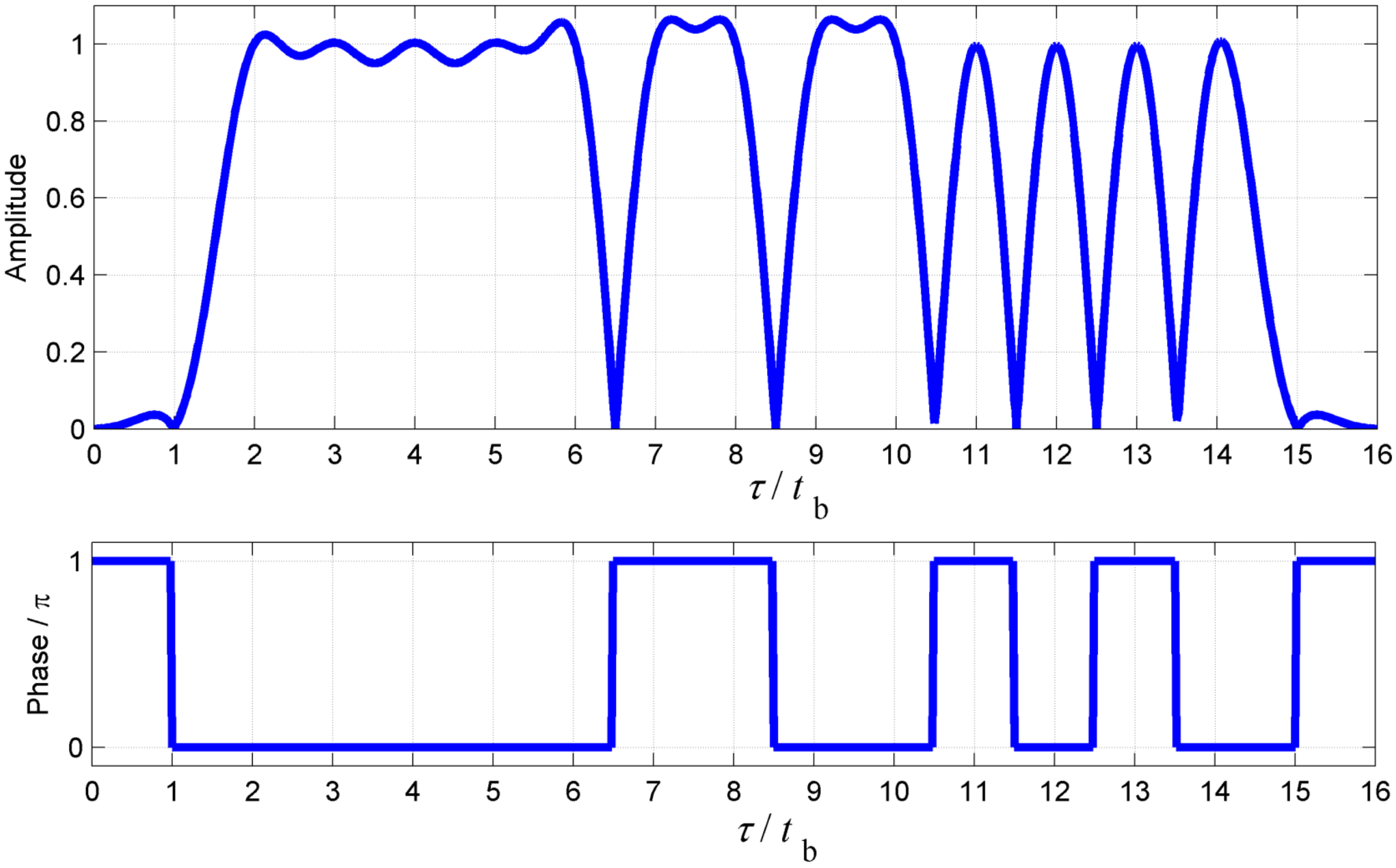

Barker 13 – using Gaussian windowed sinc

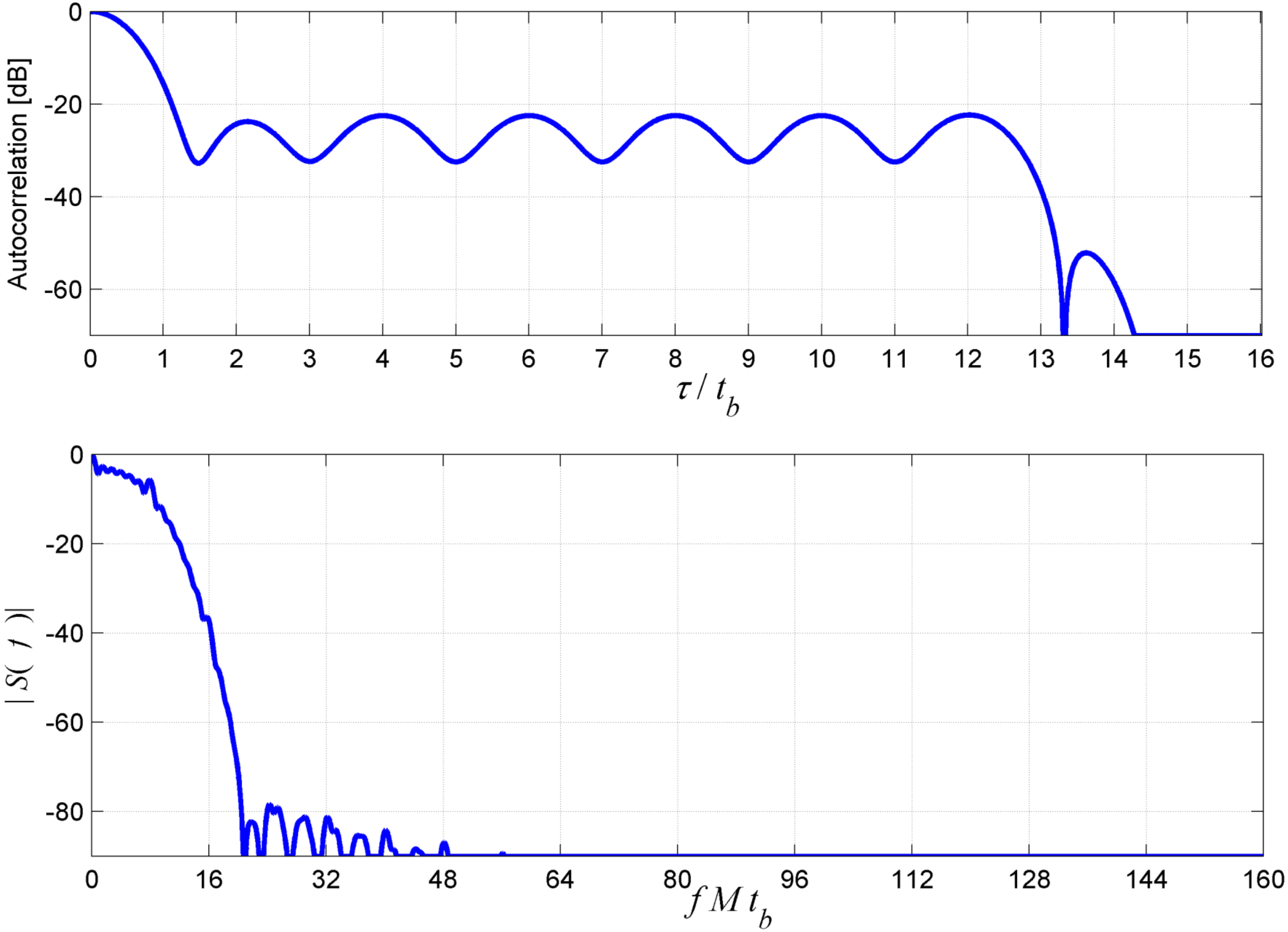

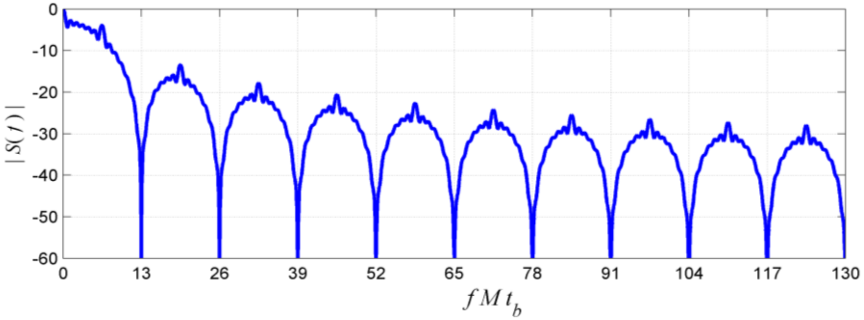

Barker 13 – rectangular bit

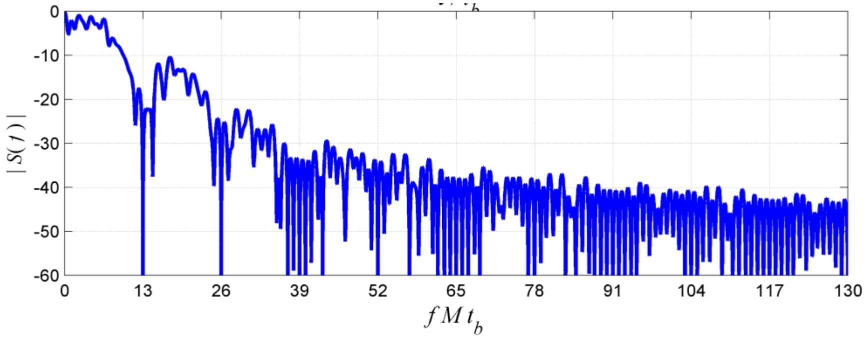

Barker 13 - Derivative phase

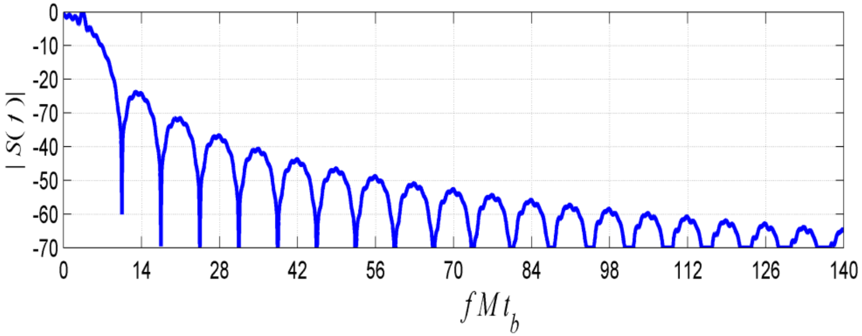

Barker 13 - Quadriphase

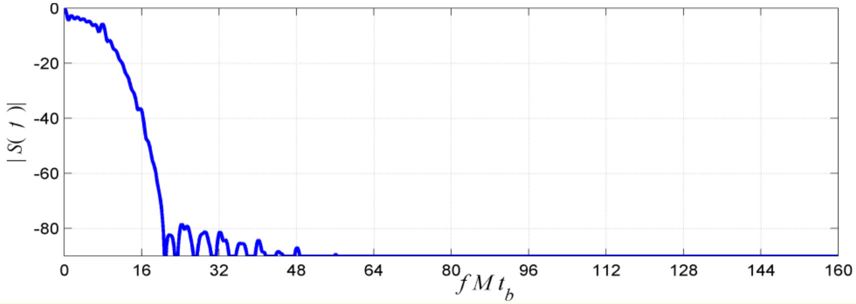

Barker 13 – Gaussian windowed sinc bit

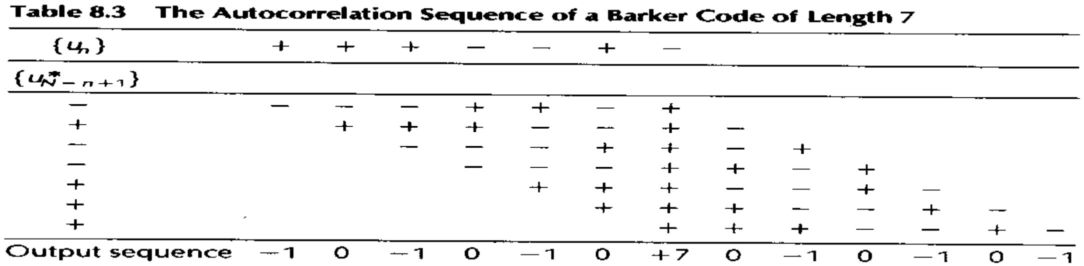

Table 8.3 The Autocorrelation Sequence of a Barker Code of Length 7

$\{u_n\}$	+	+	+	−	−	+	−						
$\{u^*_{N-n+1}\}$													
−	−	−	−	+	+	−	+						
+		+	+	+	−	−	+	−					
−			−	−	−	+	+	−	+				
−				−	−	−	+	+	−	+			
+					+	+	+	−	−	+	−		
+						+	+	+	−	−	+	−	
+							+	+	+	−	−	+	−
Output sequence	−1	0	−1	0	−1	0	+7	0	−1	0	−1	0	−1

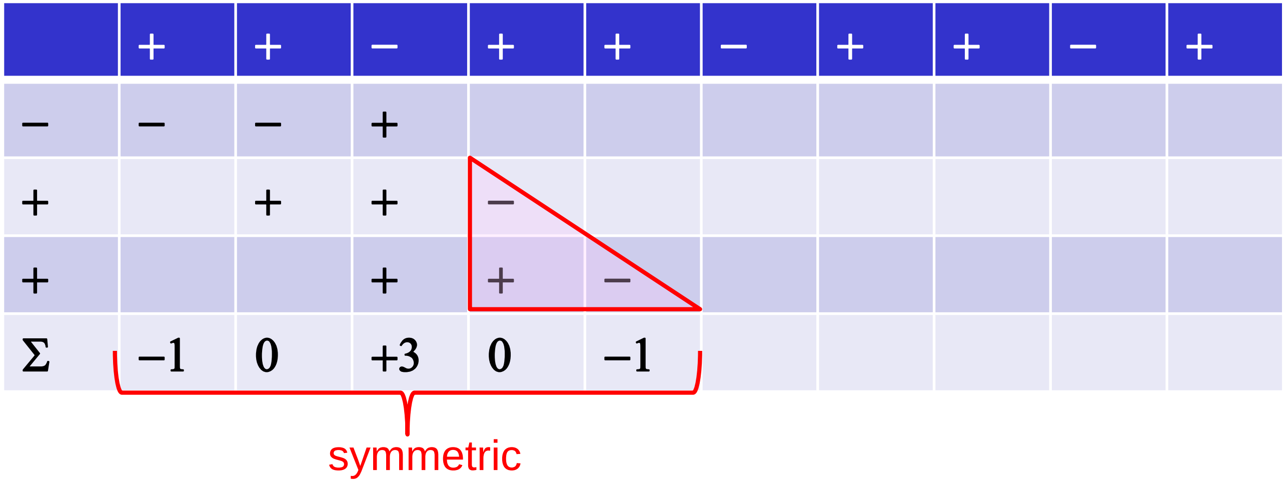

	+	+	−	+	+	−	+	+	−	+
−	−	−	+							
+		+	+	−						
+			+	+	−					
Σ	−1	0	+3	0	−1					

symmetric

a-periodic autocorrelation

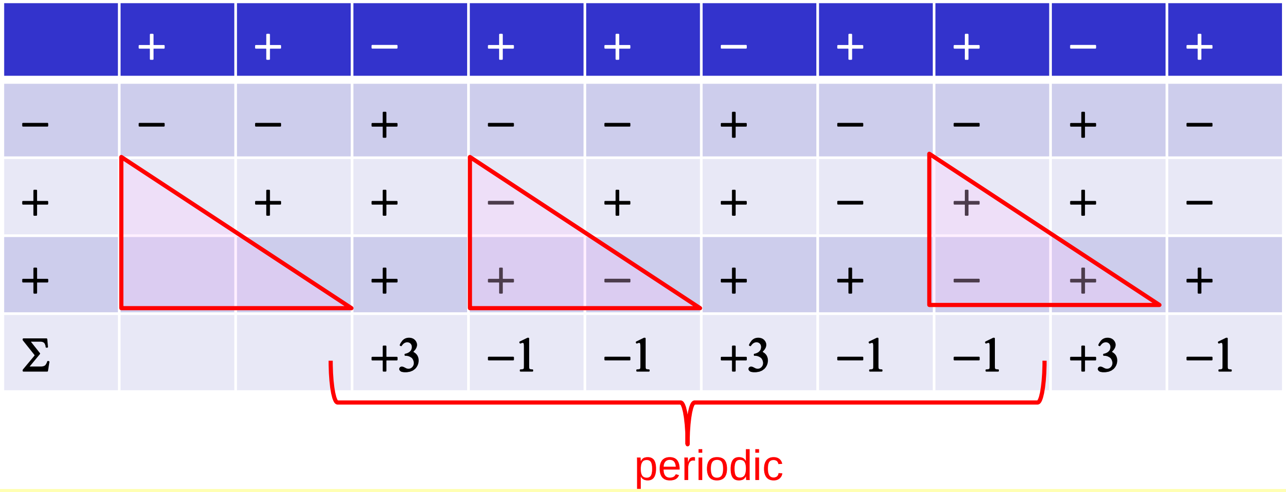

	+	+	−	+	+	−	+	+	−	+
−	−	−	+	−	−	+	−	−	+	−
+		+	+	−	+	+	−	+	+	−
+			+	+	−	+	+	−	+	+
Σ			+3	−1	−1	+3	−1	−1	+3	−1

periodic

periodic autocorrelation

periodic autocorrelation

	+	+	−	+	+	−	+	+	−	+
−	−	−	+	−	−	+	−	−	+	−
+		+	+	−	+	+	−	+	+	−
+			+	+	−	+	+	−	+	+
Σ			+3	−1	−1	+3	−1	−1	+3	−1

Ideal correlation

periodic cross-correlation

	+	+	−	+	+	−	+	+	−	+
0	0	0	0	0	0	0	0	0	0	0
+		+	+	−	+	+	−	+	+	−
+			+	+	−	+	+	−	+	+
Σ			+2	0	0	+2	0	0	+2	0

Perfect correlation

Switching the roles of signal and reference

	+	+	0	+	+	0	+	+	0	+
−	−	−	0	−	−	0	−	−	0	−
+		+	+	0	+	+	0	+	+	0
+			+	+	0	+	+	0	+	+
Σ			+2	0	0	+2	0	0	+2	0

Perfect correlation